Lattice gauge theory calculations of hadron phenomenology.

Craig McNeile

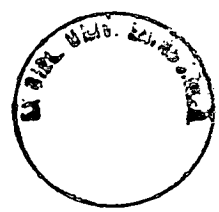

Submitted for the degree of **Doctor of Philosophy** 1992

Declaration

This thesis has been composed by me, and contains my own research, carried out independently or as a member of the UKQCD collaboration. The work in chapter 2 on reflection positivity, I did independently, following encouragement to work on the project by Simon Hands. The strong coupling study of the clover action in chapter 3 is my own work; the original project was suggested by Brian Pendleton. The motivation for the calculation of the O(a) corrections to the vacuum polarisation diagram in chapter 4 came from Richard Kenway. The actual calculation is my own work.

The results in chapter 5 I obtained as a member of the UKQCD collaboration. I played a substantial role in all the work reported. Some of the work on the P-wave meson analysis was checked by Chris Alton. In the work on finite momentum correlators I was guided and motivated by David Richards. The project to look at the convergence of hadron correlators was suggested by David Richards; I also collaborated in that work with David Henty. The development of the Maxwell spectrum code was carried out with: Rob Baxter, Steve Booth, David Richards, Alan Simpson, and Hugh Shanahan. In the analysis of the data from the simulations, I was helped by Alan Simpson and David Richards. Jim Simone provided valuable help in the correct use of his analysis program.

The only parts of this thesis which has been published are sections of chapter 5 which occur in the following papers:

- UKQCD Collaboration. Quenched Hadrons using Wilson and O(a)-Improved Fermion Actions at $\beta = 6.2$. *Phys. Lett.*B284(1992)377
- UKQCD Collaboration. Latest results from the UKQCD collaboration. *Nucl.Phys.B(Proc. Suppl.)*, to be published.

Abstract

In this thesis I study Quantum Chromodynamics on the lattice. A central theme will be the concept of improvement; this is choosing the lattice Lagrangian to minimise the effects of the lattice spacing on the results from numerical simulation.

The first chapter reviews lattice gauge theory and introduces the idea of improvement. The techniques used in numerical simulations are briefly described.

The second chapter will discuss whether an improved fermion lattice action called the clover action, obeys the reflection positivity condition. This is related to the existence of a transfer matrix. In the third chapter I will study the clover action in the strong coupling limit. Results for the pion and rho masses will be reported. A calculation of the O(a) lattice artifact correction to the gluon vacuum polarisation diagram for the clover action is described in chapter 4

The penultimate chapter contains results from various numerical simulations of lattice QCD using the clover action. The masses of some P-wave mesons will be reported, and used in a calculation of the QCD coupling. Results from a simulation of particles at finite momentum will be discussed.

Acknowledgements

First of all I would like to thank my Mother and Sister for their constant love and support. Special thanks goto my two supervisors Ken Bowler and Brian Pendleton for looking after me during these last three years, and for a careful reading of my thesis. I appreciate the large amount of help that David Richards has given me through out my PhD at Edinburgh. I thank Richard Kenway for his help on various physics problems. I have enjoyed sharing an office with Barry Wilkes for three years, and sharing an office with Rob Baxter and Sara Collins for two. I gratefully acknowledge the help of the Edinburgh postdoc team: Steve Booth, David Henty, Alan Simpson and Jim Simone. For help with physics and computer problems, and for answering all my dumb questions.

Contents

1

Introduction.

To test a theory its predictions must be compared with experiment. If the theory cannot be solved, we are stuck. Quantum Chromodynamics (QCD) was first suggested as the theory of the strong interactions in 1973 [82]. It is everything a good theory should be: elegant, with a lot of predictive power. Although no one seriously doubts that QCD is one of the key theories describing low energy physics, it is frustrating that after nearly twenty years of struggle, the hadron mass spectrum has not been satisfactorily extracted from it.

One of the most promising approaches for solving QCD is to use lattice gauge theory techniques to solve the theory numerically. Computer simulations of lattice QCD offer the real prospect of deriving the phenomenology of the strong interactions, from first principles in a controlled way. The one caveat to this is that it is going to require a lot of supercomputer time to complete this grand challenge.

The central aim of the work in this thesis is to use lattice gauge theory techniques to predict experimental numbers. However I will only really start doing this in chapter 5. The main reason for this is that, numerical simulations of lattice QCD push computational resources to their limit and anything which can be done to squeeze more physics out of the computer should be investigated.

One of the current hot topics in lattice gauge theory is the use of improved lattice actions in numerical simulations. These actions are specially chosen to produce better continuum behaviour on smaller lattices. The actions traditionally used for lattice QCD have been around for nearly twenty years and during that time, a lot of valuable knowledge has been accumulated from both analytic and numerical studies. Much less work has been done on improved actions. In the

first three chapters after the introduction, I will try to rectify this, by presenting calculations that provide some insight into a particular improved fermion action known as the clover action.

I will first discuss the definition of a transfer matrix for the clover action, this is complicated because it stretches over more than one time slice. In the third chapter I will study the meson spectrum of the clover action using strong coupling techniques. In the next chapter, I will present the results of a calculation of the one loop fermion contribution to the vacuum polarisation on the lattice, this will test whether the clover action is improved for dynamical fermion simulations

The penultimate chapter will contain the results of various numerical simulations of QCD. The mass spectrum for some of the charmonium P-wave mesons will be reported and used to calculate the QCD coupling constant. Results from a study of particles at finite momentum will be discused.

In the rest of this chapter, I will first briefly review lattice gauge theory and introduce my notation. After that I will review the concept of improvement of lattice QCD actions. The final part of this chapter will briefly describe numerical simulations of lattice QCD, and the analysis of data from them.

1.1 A brief review of lattice gauge theory.

I will now quickly review lattice gauge theory and introduce the notation used throughout this thesis. Two recent general reviews of lattice gauge theory are [66] [65]

1.1.1 Quantum field theory on the lattice.

At the most basic level, the solution of quantum field theory requires the calculation of the vacuum expectation values of operators $\langle A \rangle$, where A is some function of the fundamental fields. In general, for arbitrary fields ϕ, the vacuum expectation values can be calculated from the following functional integral:

$$\langle \mathcal{A} \rangle = \frac{\int \mathcal{D}\phi \mathcal{A} e^{-S}}{\int \mathcal{D}\phi e^{-S}} \tag{1.1}$$

where S is the action for the theory.

The rest of this introduction will deal with the correct choices of the operators A, fields ϕ, and the action S, required for the nonperturbative solution of QCD.

As an important technical point, I will always work in Euclidean space.

1.1.2 Lattice gauge theory.

In this section I will introduce lattice gauge theory and motivate the pure Yang Mills lattice action. The Lagrangian for quarks on the lattice is complicated enough to merit its own section.

Lattice gauge theories are an elegant example of how a powerful symmetry constrains the Lagrangian of a theory. Consider a hypercubic lattice with quark fields $\psi(x)$ and $\overline{\psi}(x)$ at every site on the lattice. The quark fields carry flavour and colour indices and belong to a grassmann algebra (they anticommute). Between the lattice sites there are gauge fields U. The convention is that the SU(N) matrix $U_\mu(x)$ sits on the link between x and $x+\mu$.

Gauge symmetry is the freedom to "rotate" in colour space, the quark field at every point on the lattice independently of all the other quarks on the lattice. This means that under the transformation:

$$\begin{aligned} \psi(x) &\rightarrow V(x)\psi(x) \\ \overline{\psi}(x) &\rightarrow \overline{\psi}(x)V(x)^\dagger \\ U_\mu(x) &\rightarrow V(x)U_\mu(x)V(x+\mu)^\dagger \end{aligned} \tag{1.2}$$

where $V(x) \in SU(N)$, no physical predictions of the theory should change.

The building blocks of the lattice Yang Mills theory must be gauge invariant objects constructed from the links $U_\mu(x)$, the most obvious candidate being the traces of the closed paths of gauge fields. This implies that the local gauge invariance has constrained the pure gauge Lagrangian to be the sum of the closed paths of gauge links. To proc eed further we need to investigate the classical continuum limit of the action.

The connection between the lattice gauge fields, and the Lie algebra valued continuum field A_μ is made by using:

$$U_\mu(x) = e^{igaA_\mu(x+\frac{a\mu}{2})} \tag{1.3}$$

where g is the coupling constant. I will use the convention for the continuum gauge fields where they are hermitian and can be written as $A_\mu = A^a_\mu \lambda^a$ The λ^a matrices are the generators of the$\mathcal{SU}$(N) algebra (Gell Mann matrices for QCD)

and I will use the normalisation:

$$\text{trace}\lambda^a\lambda^b = \frac{1}{2}\delta^{ab} \tag{1.4}$$

The traditional choice of lattice pure gauge action was made by Ken Wilson [8]:

$$S_G = \frac{-\beta}{2N}\sum_{\square}(traceU_{\square} + traceU_{\square}^{\dagger}) \tag{1.5}$$

where $U_{\square}$ is the product of four links around a square in the $\mu\nu$ plane:

$$U_{\square} = U_{\mu}(x)U_{\nu}(x+\mu)U_{\mu}^{\dagger}(x+\nu)U_{\nu}^{\dagger}(x) \tag{1.6}$$

The definition of β is $\frac{2N}{g^2}$. The motivation for this choice comes from expanding it in terms of the lattice spacing a:

$$S_G = \int d^4x \frac{(F_{\mu\nu}^a)^2}{4} + O(a^2) \tag{1.7}$$

where $F_{\mu\nu}$ is defined as:

$$F_{\mu\nu} = \partial_\mu A_\nu - \partial_\nu A_\mu + ig[A_\mu, A_\nu] \tag{1.8}$$

and is simply the Lagrangian for a continuum gauge theory. Extra terms can be added to the lattice Lagrangian comprised of bigger loops of link variables. This leads to the idea of improvement which I will discuss later on.

The measure for the gauge fields is the Haar measure so the measure in the functional integral is:

$$\mathcal{D}U = \prod_{x,\mu}\mathcal{D}U_\mu(x) \tag{1.9}$$

The Haar measure has the following property:

$$\begin{aligned}\int \mathcal{D}U f(U) &= \int D(UV)f(U) = \int \mathcal{D}'U f(UV^{-1}) \\ &= \int D(VU)f(U) = \int \mathcal{D}(U) f(V^{-1}U)\end{aligned} \tag{1.10}$$

required to make the functional integral gauge invariant.

1.1.3 Fermions on the lattice.

I will now briefly discuss the problem of obtaining a lattice Lagrangian for fermions. While the lattice Yang Mills theory can be described as elegant, fermions on the lattice can only be described as bizarre.

A possible choice of the lattice Dirac Lagrangian is:

$$\mathcal{L}_{NF} = \frac{1}{2a}\sum_{\mu}(\overline{\psi}(x)\gamma_\mu U_\mu(x)\psi(x+\mu) - \overline{\psi}(x+\mu)\gamma_\mu U_\mu^\dagger(x)\psi(x)) + m\overline{\psi}(x)\psi(x) \quad (1.11)$$

which describes naive lattice fermions; the name hints at considerable subtlety.

If the naive lattice Lagrangian is Taylor expanded in the lattice spacing, the following continuum result is obtained:

$$\mathcal{L}_{NF} = \overline{\psi}(x)(\not{D} + m)\psi(x) + O(a^2) \quad (1.12)$$

where the continuum covariant derivative is defined as:

$$\mathrm{D}_\mu = \partial_\mu + \mathrm{igA}_\mu \quad (1.13)$$

The naive lattice fermion action is equal to the continuum Dirac action, up to $O(a^2)$ corrections. But a more detailed investigation reveals extra problems. Consider the naive lattice free fermion propagator in momentum space:

$$S(p) = \frac{1}{\sum_\mu i\sin(p_\mu a)\gamma_\mu + m} \quad (1.14)$$

from which the energy dispersion relation:

$$\sinh(Ea)^2 = (ma)^2 + \sum_i \sin^2(p_i a) \quad (1.15)$$

can be derived by looking for poles in the propagator. When the $a \to 0$ limit is taken the continuum dispersion relation is obtained, however the energy also equals the rest mass when the momenta has components with magnitude $\frac{\pi}{a}$. It is instructive to look at the naive lattice propagator with a momenta at the edge of the brillouin zone : $\hat{q}_\mu = p_\mu - \frac{\pi}{a}$, in the small lattice spacing limit the fermion propagator becomes:

$$S(p) = \frac{1}{\sum_\mu -i\gamma_\mu \hat{q}_\mu + m} \quad (1.16)$$

which up to the minus sign, which can be absorbed into a redefinition of the gamma matrices, is the propagator for a free fermion.

This free field argument has shown the phenomena of species doubling, the theory in four dimensions based on the naive action has produced sixteen fermion species. There are a number of topological arguments that show that for an action with all the properties that are normally considered inviolate, species doubling will occur [79].

The pragmatic way to produce a fermion action, which does not have the doublers is to add a term to the naive lattice Lagrangian so that they are given a large mass and decouple from the theory, this is the approach suggested by Ken Wilson [9]. The result is Wilson's fermion action:

$$\begin{aligned} S_F^W &= \sum_x - \sum_\mu \frac{1}{2}[\overline{\psi}(x)(r-\gamma_\mu)U_\mu(x)\psi(x+\mu) + \overline{\psi}(x+\mu)(r+\gamma_\mu)U_\mu^\dagger(x)\psi(x)] \\ &+ \sum_x \overline{\psi}(x)\psi(x)(m+4r) \end{aligned} \tag{1.17}$$

Wilson's r parameter can in principle take any nonzero value. The value of r used in the numerical simulations was 1.

If the action in equation 1.17 is Taylor expanded in the lattice spacing, the following continuum action is obtained:

$$S_F^W = \int d^4x \overline{\psi}(x)(\not{D} + m - \frac{arD^2}{2})\psi(x) + O(a^2) \tag{1.18}$$

From the continuum action it can be seen that a price has been paid for the removal of the species doublers, the addition of an O(a) correction to the action. Although in the continuum limit this correction should not matter, from current numerical simulations there is some evidence that it affects the results. Attempting to remove this correction leads to the idea of improvement. The fermion matrix for a given action is implicitly defined by:

$$S = \overline{\psi}(x)M\psi(x) \tag{1.19}$$

where S is one of the multitude of possible fermion actions.

Throughout this thesis I will use a Euclidean representation of gamma matrices, with the following properties:

$$\begin{aligned} \{\gamma_\mu, \gamma_\nu\} &= 2\delta_{\mu\nu} \\ \gamma_\mu^\dagger &= \gamma_\mu \end{aligned} \tag{1.20}$$

The only explicit representation I will use is explicitly written out in [1]. My definition for $\sigma_{\mu\nu}$ is:

$$\sigma_{\mu\nu} = \frac{\gamma_\mu\gamma_\nu - \gamma_\nu\gamma_\mu}{2} \tag{1.21}$$

The rules for integration of a single Grassmann variable ψ are:

$$\begin{aligned} \int \mathcal{D}\psi\psi &= 1 \\ \int \mathcal{D}\psi &= 0 \end{aligned} \tag{1.22}$$

with a similar definition for $\overline{\psi}$. The total measure for all the spinor fields in the space is:

$$\mathcal{D}\overline{\psi}\mathcal{D}\psi = \prod_x \mathcal{D}\overline{\psi}(x)\mathcal{D}\psi(x) \tag{1.23}$$

1.2 Improvement in lattice QCD.

1.2.1 Symanzik improvement.

Because the lattice is only the scaffolding which enables the continuum field theory to be solved nonperturbatively, it seems sensible to chose the lattice action in such a way that its predictions are minimally affected by unphysical lattice artifacts. One way of doing this is to try and reduce the discretisation effects in the lattice action. One naive example of this would to be use $\frac{f(x+a)+f(x-a)}{2}$ as the lattice approximation of a one dimensional derivative, rather than f(x+a)−f(a), because the difference between the continuum and the lattice result is smaller for the first expression than in the second expression. The removal of discretisation errors from a fully interacting quantum field theory is more complicated.

The field theory method of trying to remove discretisation errors is to add irrelevant operators, multiplied by arbitrary coefficients to the lattice Lagrangian. Irrelevant operators are operators of typically high engineering dimension (in units of energy), whose effects on the dynamics of the theory decrease as the continuum limit is approached. Because lattice QCD cannot (as yet) be solved analytically in the low energy region, it is not obvious how to choose the coefficients, in such a way as to reduce the amount of discretisation error in a mass or decay constant.

Symanzik's improvement [20] uses weak coupling lattice perturbation theory to make sensible choices for the coefficients. His improvement program is based on the analysis of the asymptotic behaviour of lattice Feynman diagrams, he noted that certain terms in asymptotic expansion would stubbornly resist the onslaught of the continuum limit, and he developed a formalism to remove them. Although its not obvious that the improved convergence of lattice Feynman diagrams will be converted into improved behaviour of nonperturbative quantities, it is a sensible method, in the low energy regime where there is a dearth of analytical tools.

I will now briefly explain Symanzik's formalism, a more detailed rendition of his ideas is in chapter 4, where I will use them in a lattice Feynman diagram

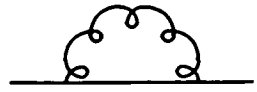

Figure 1.1: The fermion self energy.

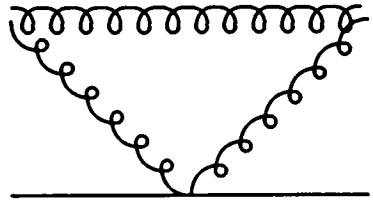

Figure 1.2: The tadpole self energy.

calculation. Symanzik's improvement program is based on the existence of a local effective Lagrangian (LEL). If A_0 is the bare lattice Lagrangian, then abstractly the LEL can be written down as:

$$A_0 = L_0 + aL_1 + a^2L_2 + \cdots \tag{1.24}$$

where L_i consists of the sum of all possible continuum operators with dimension 4+i and a is the lattice spacing. The coefficients of the operators in each L_i are series in the coupling constant g_0; in Symanzik's original paper he gives methods for their calculation using a suitable regularisation method.

If (fairly unbelievably) the L_1 term has been calculated to all orders in perturbation theory, then if A_1 is the lattice version of the continuum expression L_1 the improved action is now $A_0 - A_1$, which has a new LEL without an O(a) term. At the classical level the above procedure corresponds to adding extra terms to the initial Lagrangian so that when Taylor expanded it agrees with the continuum expression up to an error, which will typically be the lattice spacing to some power.

To flesh out the above discussion I will consider the mundane world of one loop improvement. I will review a calculation to remove the one loop $O(a^2)$ and $O(a)$ corrections from a two-link lattice fermion action. Although the improvement program has been carried out for Pure Yang-Mills theory [83], the pure gauge ac-

tion has no O(a) corrections at tree level. However the Wilson fermion Lagrangian does, so I will concentrate on fermion Lagrangians. Eguchi and Kawamoto [17] applied Symanzik's improvement program to the following lattice fermion action:

$$\begin{aligned} S &= \sum_x \sum_\mu \frac{4\kappa}{3}[\overline{\psi}(x)(r-\gamma_\mu)U_\mu(x)\psi(x+\mu) + \overline{\psi}(x+\mu)(r+\gamma_\mu)U_\mu^\dagger(x)\psi(x)] \\ &- \sum_x \sum_\mu \frac{\kappa}{6}[\overline{\psi}(x)(2r-\gamma_\mu)U_\mu(x)U_\mu(x+\mu)\psi(x+2\mu) \\ &+ \overline{\psi}(x+2\mu)(2r+\gamma_\mu)U_\mu^\dagger(x+\mu)U_\mu^\dagger(x)\psi(x)] \\ &- \sum_x \overline{\psi}(x)\psi(x) \end{aligned} \tag{1.25}$$

If the weak coupling Feynman rules are derived for the above action, there are no O(a) or $O(a^2)$ corrections to the quark propagator, and no O(a) corrections to the quark gluon vertex.

To remove the one loop $O(a)$ and $O(a^2)$ terms they Taylor expanded the standard quark self energy graphs (regularising à la Symanzik) to look at the following terms: $\sum_\nu p_\mu^2$, $m\sum_\nu p_\mu^2$, $\sum_\mu i\gamma_\mu p_\mu \sum_\rho p_\rho^2$, and $\sum_\mu i\gamma_\mu p_\mu^3$. These are the lowest order lattice artifacts in the local effective Lagrangian.

One of the results of their calculation was that the coefficient of the $\sum_\mu i\gamma_\mu p_\mu \sum_\rho p_\rho^2$ ter turned out to be:

$$- c_3 C(N)\kappa g^2 \tag{1.26}$$

where c_3 is a number which varies between $\pm 10^{-3}$ as r changes from $-\frac{1}{2}$ to $\frac{1}{2}$ and C(N) is $\frac{N^2-1}{2N}$ group theory factor for the diagram.

The lattice term which is perturbatively equivalent to $\sum_\mu i\gamma_\mu p_\mu \sum_\rho p_\rho^2$ is:

$$\begin{aligned} &- \frac{1}{2}\sum_{\mu\nu}[\overline{\psi}(x)\gamma_\mu U_\mu(x)U_\nu(x+\mu)\psi(x+\mu+\nu) \\ &+ \overline{\psi}(x)\gamma_\mu U_\mu(x)U_\nu^\dagger(x+\mu-\nu)\psi(x+\mu-\nu) \\ &- \overline{\psi}(x+\mu+\nu)\gamma_\mu U_\nu^\dagger(x+\mu)U_\mu^\dagger(x)\psi(x) \\ &- \overline{\psi}(x+\mu-\nu)\gamma_\mu U_\nu(x+\mu-\nu)U_\mu^\dagger(x)\psi(x) \\ &-2\ \{\overline{\psi}(x)\gamma_\mu U_\mu(x)\psi(x+\mu) - \overline{\psi}(x+\mu)\gamma_\mu U_\mu^\dagger(x)\psi(x)\}] \end{aligned} \tag{1.27}$$

To remove the $\sum_\mu i\gamma_\mu p_\mu \sum_\rho p_\rho^2$ correction from the local effective Lagrangian the lattice expression 1.27 multiplied by the coefficient 1.26 must be subtracted from the original lattice expression 1.25; by carrying out the same procedure for all the aforementioned lattice artifacts, Eguchi and Kawamoto produced an improved action which had no one loop $O(a^2)$ or $O(a)$ corrections.

1.2.2 On-shell improvement.

There are a number of problems with Symanzik's original improvement program. One practical difficulty is that the numerical inversion of terms like equation 1.27 will be difficult to implement on parallel computers. There is also a theoretical problem associated with gauge invariance of terms like mp^2 and the uniqueness of their reconstruction into terms in the lattice Lagrangians.

In an attempt to address the above issues, Lüscher and Weisz introduced [67] the idea of on-shell improvement in their studies of lattice Yang-Mills theory. To construct an on-shell improved action, only the minimal set of irrelevant operators are added to the naive lattice action so that only spectral quantities such as masses or decay constants are improved.

Their methods do have some surprising features for example the tree level actions have O(a) terms (for an on-shell improved fermion action), yet they claim the physical predictions obtained from solving such a theory do not contain O(a) corrections. The starting point of their analysis is the existence of a whole family of lattice actions which predict physical amplitudes with the same error. Consider two actions S and S' which lead to physical amplitudes m and m', then the actions are similarly improved if the relation:

$$m - m' = O(a^k) \tag{1.28}$$

for some integer k, holds for all possible physical predictions of the two theories

Lüscher and Weisz assumed the existence of families of equivalent lattice actions and by constructing transformations in the functional integral between these actions, they were able to obtain constraints on the improvement coefficients. Perhaps the most useful result of their method was that certain irrelevant operators would not introduce $O(a^k)$ effects in spectral quantities, so their coefficients could be set to any convenient value.

The crucial assumption in the above arguments is that at least one of the actions out of the family of equivalent actions, does produce the correct continuum value for a spectral quantity up to some lattice spacing error. Proving this assumption is tantamount to solving the theory. The only attempt at a justification I will offer is that for a class of fermion improved actions, numerical simulations seem to show that improvement is beneficial (see section 1.2.4).

Sheikholeslami and Wohlert produced on shell improved fermion actions based on the Wilson action [19]. I will use their work to explain the nature of on-

shell improvement. As continuum manipulations mirror the lattice ones for this derivation, for simplicity I will work in the continuum, see the original paper for the lattice arguments. Consider the following lattice action which contains all independent gauge invariant terms up to O(a):

$$S_F = \frac{a^4}{g^2} \int d^4x \sum_{i=0}^{3} a^{dimO_i - 4} b_i(g^2, ma) O_i \tag{1.29}$$

The $b_i(g^2, ma)$ coefficients have to be computed order by order in perturbation theory and do not show any pathological behaviour as $g \to 0$. The four operators O^i are:

$$\begin{aligned} O_0 &= \overline{\psi}(x)\psi(x) \\ O_1 &= \overline{\psi}(x)\not{D}\psi(x) \\ O_2 &= \overline{\psi}(x)(D^2 + \frac{1}{2}\sigma_{\mu\nu}F_{\mu\nu})\psi(x) \\ O_3 &= -\frac{1}{2}\overline{\psi}(x)\sigma_{\mu\nu}F_{\mu\nu}\psi(x) \end{aligned} \tag{1.30}$$

To try to gain some information about the coefficients b_i, consider the following gauge covariant transformation on the fermion functional integral:

$$\psi \to \psi + a\epsilon_1 \not{D}\psi + O(a^2) \tag{1.31}$$

$$\overline{\psi} \to \overline{\psi} + a\epsilon_1^{'}\overline{\psi}\not{D} + O(a^2) \tag{1.32}$$

governed by the parameters ϵ_1 and $\epsilon_1^{'}$ Although it will change the value of correlators, it should not effect the values of spectral quantities. Using the standard identity $\det M = e^{\mathrm{trace}\log M}$ and $\mathrm{trace}\not{D} = 0$, the determinant of the transformation can easily be shown to have no O(a) term.

The change produced in the action is:

$$\Delta S = a^4 \int d^4x [(\epsilon_1 - \epsilon_1^{'})b_0(0, ma)O_1 + a(\epsilon_1 - \epsilon_1^{'})b_1(0, ma)O_2] \tag{1.33}$$

The change in the O_1 term is not interesting, because it can be absorbed by rescaling the fields, what is interesting is that the coefficient of the O_2 term can be changed by the transformation. If the action has no O(a) affect on the mass spectrum and the general action with appropriate coefficients b_i is on-shell improved through O(a), then the variation of the O_2 term's coefficient under the transformation must mean that it has no effect on the mass spectrum of the theory to order a. By adding appropriate factors of g^{2l} to the ϵ factors, the argument

can be generalised to all orders in perturbation theory. The b_3 coefficient has to be fixed in perturbation theory, at tree level this means $b_3 = 0$. Because of the problems with species doubling, the most convenient value of b_2 is 1.

Reverting back to the lattice, the final action is the Wilson action plus the following term:

$$\Delta S^I = -i\frac{cg_o\kappa}{2}\sum_{x,\mu,\nu}\overline{\psi}(x)P_{\mu\nu}\sigma_{\mu\nu}\psi(x) \tag{1.34}$$

where I have introduced a coefficient c, multiplying the clover term. The tree level value of c is one (this was the value used in the numerical work), but its value can be changed to try to remove the radiative corrections. The lattice field strength is defined to be:

$$P_{\mu\nu} = \frac{1}{4}\sum_{i=1}^{4}\frac{1}{2ig_o}(U_i - U_i^\dagger) \tag{1.35}$$

The sum is over the 4 plaquettes in the $\mu\nu$ plane stemming from the point x and taken in an anticlockwise sense, see figure 1.3.

The clover lattice action considered is:

$$\begin{aligned} S_F^I &= \sum_x - \sum_\mu \kappa[\overline{\psi}(x)(1-\gamma_\mu)U_\mu(x)\psi(x+\mu) + \overline{\psi}(x+\mu)(1+\gamma_\mu)U_\mu^\dagger(x)\psi(x)] \\ &+ \sum_x \overline{\psi}(x)\psi(x) - i\frac{cg_o\kappa}{2}\sum_{x,\mu,\nu}\overline{\psi}(x)P_{\mu\nu}\sigma_{\mu\nu}\psi(x) \end{aligned} \tag{1.36}$$

where I have rescaled the fields and introduced the kappa value:

$$\kappa = \frac{1}{2(4+m)} \tag{1.37}$$

If on-shell improvement is correct, all loop O(a) effects can be eliminated by a suitable choice of c, which is a series in the coupling constant with the lowest order term of 1. It is amusing to see our classical intuition go wrong, because at tree level, the clover action has O(a) terms when it is expanded in the lattice spacing.

The calculation of the coefficient c in perturbation theory is more complicated than for the equivalent calculation for the two link action, because the effect of the clover term is difficult to identify in the fermion self energy. However two calculations have been done, one using weak coupling perturbation theory, and the other using mean field theory.

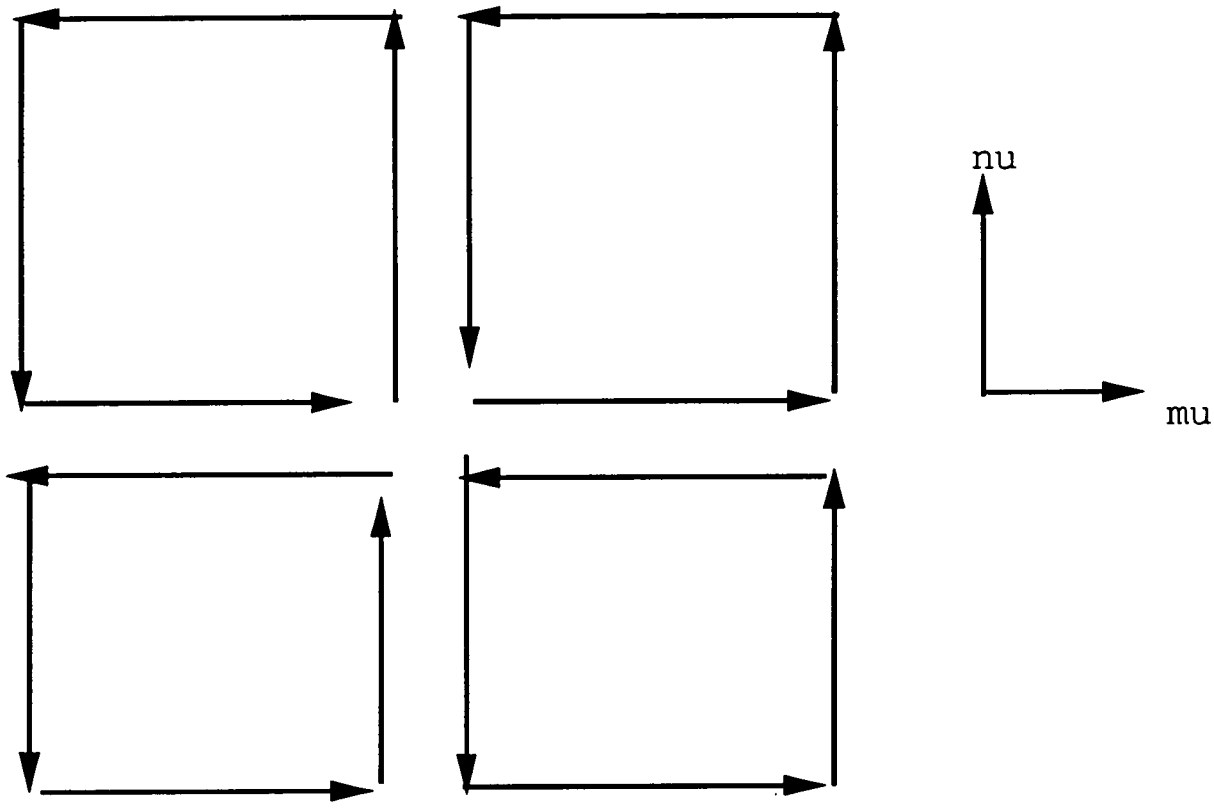

Figure 1.3: The field strength tensor on the lattice $P_{\mu,\nu}$.

Wohlert calculated the value of c to one loop in perturbation theory using twisted boundary conditions [32]. In an extremely lengthy calculation he found the value of c by calculating diagrams relevant to quark-quark scattering. The final result was:

$$c = 1 + 0.26590(7)g^2 \tag{1.38}$$

The Fermilab group in their numerical simulations of the clover action used c = 1.4 to try to remove radiative corrections [48]. They obtained this estimate of c by using mean field theory; although their exact method is not disclosed. Lepage and Mackenzie [84] have a formalism to improve the convergence of lattice perturbation theory; which also allows an estimate of the c coefficient.

I will try to explain Lepage and Mackenzie's ideas. If u_0 is defined as:

$$u_0 = (\frac{1}{3}\langle U_{\square}\rangle)^{\frac{1}{4}} \tag{1.39}$$

where $U_{\square}$ is the plaquette operator, the value of u_0 can be obtained from the results of simulation, or by using weak coupling estimates. The resulting value of c is:

$$c = \frac{1}{u_0^4} \tag{1.40}$$

which is obtained by rescaling the field strength tensor by the mean plaquette:

$$P_{\mu\nu} \rightarrow \frac{P_{\mu\nu}}{\frac{1}{3}\langle U_{\square}\rangle} \tag{1.41}$$

Lepage and Mackenzie argue that the effect of this rescaling is to remove tadpole graphs from lattice perturbation theory. The motivation for the rescaling in equation 1.41 comes from the expansion of the lattice gauge field:

$$U_\mu \longrightarrow u_0(1 + igA_\mu) \tag{1.42}$$

which could be thought of as expanding about the average "background" field configuration, rather than around the free field unit gauge configuration. Intuitively this might improve the convergence of lattice perturbation theory because it is a better starting point in the expansion.

The results from numerical simulation in this thesis were obtained by using a slight variation on the above action, which I will describe in the next section.

1.2.3 The rotated clover theory.

The authors of reference [18] suggested a better solution to the removal of O(a) effects, which recognised the importance of the evolution of the coupling constant with lattice spacing. They considered the lattice action comprising the sum of the Wilson action and the following term [6] [85]:

$$\begin{aligned}\Delta S_F^{II} &= a^4 \sum_{x,\mu} \frac{r}{8a}(\overline{\psi}(x)U_\mu(x)U_\mu(x+\mu)\psi(x+2\mu) + \overline{\psi}(x+2\mu)U_\mu^\dagger(x+\mu)U_\mu^\dagger(x)\psi(x)) \\ &- \sum_x \overline{\psi}(x)\psi(x) \end{aligned} \tag{1.43}$$

The total two link fermion action is:

$$S_F^{II} = S_F^W + \Delta S_F^{II} \tag{1.44}$$

By expanding S_F^{II} in the lattice spacing a, it can easily be seen that it has no O(a) terms.

Consider a possible term in a diagram with l loops of the form $(\log a)^l (g^2)^l a$ Recall that the coupling constant depends on the lattice spacing via $g^2 \sim \frac{1}{\log a}$, hence this term is effectively an O(a) correction and could spoil the improvement program. By an explicit perturbative calculation of the quark self energy and some of the graphs contributing to the quark-gluon vertex, they verified that these diagrams had no $g^2 a \log a$ terms for the action in equation 1.44.

All the above work suggested that S^{II} was a good theoretical candidate for an O(a) improved action, but because ΔS^{II} stretches over two time slices it is more complicated to invert than an action with only nearest neighbour terms, so a transformation was used to obtain a more convenient action, namely the clover action.

The following transformations on the spinor fields:

$$\begin{aligned}\psi &\rightarrow (1 + \frac{ar}{4}(m - \not{D}))\psi \\ \overline{\psi} &\rightarrow \overline{\psi}(1 + \frac{ar}{4}(m + \overleftarrow{\not{D}}) \end{aligned} \tag{1.45}$$

where the covariant lattice derivatives are defined by:

$$\begin{aligned} D_\mu \psi(x) &= \frac{1}{2}[U_\mu(x)\psi(x+\mu) - U_\mu^\dagger(x-\mu)\psi(x-\mu)] \\ \overline{\psi}(x)\overleftarrow{D}_\mu &= \frac{1}{2}[\overline{\psi}(x+\mu)U_\mu^\dagger(x) - \overline{\psi}(x-\mu)U_\mu(x-\mu)] \end{aligned} \tag{1.46}$$

converts the action S^{II} into the action S^{I} via:

$$S_F^{II}(\psi,\overline{\psi},m) \rightarrow S_F^{I}(\psi,\overline{\psi},m+\frac{arm}{2}) + O(a^2) \tag{1.47}$$

Contrary to the claim of the authors of [18], the jacobian of the above transformation contains O(a) terms because of the m factors (this is easy to see by ignoring the $\not{D}$ terms), although this could have no effect because it is just a constant factor (depending on the definition of m) and could be absorbed in the normalisation.

The relation between the quark masses in the two actions is not significant. Because of the breaking of the chiral symmetry on the lattice, the quark masses have to be tuned empirically to their physical values. The only slight subtlety is due to the quark masses in the rotations being different to the ones in the action, however the $\frac{m^2ar}{2}$ term in the rotation is an $O(a^2)$ correction and thus can be neglected; the result of this is that a consistent quark mass can be used in the rotated clover action. Another way of avoiding the problems in the definition of the quark mass in the rotations is to use the following on-shell condition in the rotations:

$$-m \longrightarrow \not{D} \tag{1.48}$$

to produce the fermion field rotations:

$$\begin{aligned} \psi &\rightarrow (1-\frac{ar}{2}\not{D})\psi \\ \overline{\psi} &\rightarrow \overline{\psi}(1+\frac{ar}{2}\overleftarrow{\not{D}}) \end{aligned} \tag{1.49}$$

The final prescription for the action used in the numerical work in this thesis was the clover action and the on-shell fermion rotations 1.49, which combine the theoretical advantages of S_F^{II} with the numerical advantages of S_F^{I}. The authors of [18] checked the above argument in perturbation theory by calculating the quark self energy and some of the graphs contributing to the renormalisation of the quark-gluon vertex for the clover action, where they found explicit $g^2 a \log a$ terms. After the rotations were performed, the $g^2 a \log a$ terms were found to vanish, but only if an on-shell condition was imposed.

1.2.4 Numerical tests of improvement.

Throughout the previous introduction to improvement, I have emphasised that the correct choice of improvement coefficients requires the full solution of the

theory. Although sensible choices can be made in perturbation theory. In this section I will discuss in very broad terms the current status of the numerical tests of improvement from Monte Carlo simulations. The number of results from simulations of improved actions is increasingly rapidly, so I will only concentrate on results of direct relevance to the rest of this thesis.

There is one obvious test of improvement, that is to do simulations at different β values to look at the violations of scaling. Numerical results from different fermion actions should be compared on the same set of gauge configurations (in the quenched approximation). From dimensional arguments O(a) effects are likely to come from the effect of quark masses, so the change of the measured quantities with kappa would be expected to be sensitive to discretisation errors.

Quantities such as the difference in the square of the pseudo-scalar and vector meson masses, which experimentally are roughly independent of quark masses, provide good tests of improvement. The explicit magnetic moment term in the clover action coupled with ideas from nonrelativistic quark models suggest that the mass splittings due to spin effects, such as the nucleon-delta splitting should be closer to experiment for the clover action than the Wilson action.

The UKQCD collaboration has studied the Wilson and clover actions on the same set of eighteen gauge configurations on a $24^3 \times 48$ lattice at $\beta = 6.2$. For the range of pseudoscalar meson masses 350 MeV to 800 MeV they found no statistically significant differences between the results from the two actions [16]. In a similar comparative simulation with kappa values appropriate to the charm quark mass [46], the UKQCD collaboration found significant differences between the two actions. The $m_{J/\psi} - m_{\eta_c}$ splitting predicted by the rotated clover action was $52 \pm \frac{3}{4}$ MeV, which is closer to the experimental value of 117(2) MeV, than the Wilson action prediction of $28 \pm \frac{2}{2}$ MeV.

The Fermilab group [48] found, in a number of simulations using their mean field improved clover action with β values between 5.7 and 6.1, that the $m_{J/\psi} - m_{\eta_c}$ splitting was sensitive to the lattice spacing. Their final result (after extrapolation in a^2) was:

$$m_{J/\psi} - m_{\eta_c} = 73 \pm 12$$

Comparing this to the equivalent UKQCD number gives some indication of the effect of $O(\alpha_s a)$ corrections.

Perhaps the most tantalising numerical results in favour of improved actions is a study of the renormalisations constants by Martinelli and collaborators [81]. By taking the ratio of a lattice current with a conserved current, the renormalisation factor between the continuum and the lattice scheme for the nonconserved current can be measured from a simulation. At $\beta = 6.0$ on a $10^3 \times 20$ lattice, Martinelli and collaborators found that consistent values for the renormalisation factors could be obtained using the clover action, and suitably improved currents. However the renormalisation constants obtained from the Wilson action using the same methods were inconsistent with each other. This was thought to be due to O(a) effects.

1.3 The Quenched approximation.

I have now motivated all the details to set up full QCD on the lattice. All that is required is the evaluation of:

$$\frac{\int \mathcal{D}\overline{\psi}\mathcal{D}\psi e^{-S_c - S_G}\mathcal{A}}{\int \mathcal{D}\overline{\psi}\mathcal{D}\psi e^{-S_c - S_G}} \tag{1.50}$$

where $\mathcal{A}$ is some combination of quark and gluon fields, which I will discuss in section 1.5 . Although, in principle, the fermion part of the functional integral can be solved explicitly, by using:

$$\int \mathcal{D}\overline{\psi}\mathcal{D}\psi e^{-\overline{\psi}M\psi} = \det M \tag{1.51}$$

the resulting fermion determinant is a highly nonlocal object and is therefore very computationally expensive to simulate numerically. To save computer time the fermion determinant is set equal to a constant [56]. This is called the quenched approximation to QCD.

There are various physical arguments that can be used to suggest that the main features of full QCD will be reproduced by the quenched approximation. The effect of the fermion determinant on the dynamics is from closed quark loops. Physically the existence of quark loops requires the creation of quark antiquark pairs from a gluon, however the phenomenological success of the OZI rule, suggests that this process is suppressed.

1.4 Numerical simulations of lattice QCD.

The following sections are a brief review of numerical simulations of quenched lattice QCD, and a description of the production code used by the UKQCD collaboration in their simulations. In chapter 5 I will present analysis of some of UKQCD's numerical investigations of QCD, and the following pages are background material to that work.

1.4.1 Generation of gauge fields.

The solution of quenched QCD requires the evaluation of:

$$\langle f(M^{-1}(U))\rangle = \frac{1}{Z}\int \mathcal{D}U f(M^{-1}(U))e^{-S_{YM}} \tag{1.52}$$

Typically the $f(M^{-1}(U))$ function will be products of quark propagators, tied together to form the appropriate hadron propagator.

Currently the only competitive method to evaluate an expression like 1.52 and obtain nonperturbative information about the continuum, is by numerical simulation. The underlying method for solving equation 1.52 used in the computational work in this thesis is Monte Carlo importance sampling . The basic idea is to sample gauge configurations from the probability distribution $\mathcal{D}Ue^{-S_{YM}}$, an estimate of the required observable is then obtained from:

$$\overline{f(M^{-1}(U))} = \frac{1}{N}\sum_{i=1}^{N} f(M^{-1}(U^i)) \tag{1.53}$$

where N is the number of gauge configurations generated

I will now briefly discuss the way in which the gauge configurations, used in the numerical work in this thesis were generated. A more detailed study of the reasons for the choice of algorithm and its parameters can be found in [51]. The numerical work in this thesis used gauge configurations generated on the 64 i860 node Meiko Computing Surface at Edinburgh. The SU(3) fields were generated by using a cycle of one Cabbibo-Marinari heat bath sweep followed by 5 overrelaxed sweeps. The first configuration started at sweep 16800 and there after each configuration was separated by 2400 sweeps.

1.4.2 Quark propagator inversion.

To construct hadron operators from gauge configurations, quark propagators must be computed. In principle all that is required is the inversion of the fermion matrix

M. The large order of the matrix M, means that an iterative algorithm must be used. At the start of the project an extensive series of tests were carried out to find the computationally cheapest algorithm [51]. The final choice used in the production runs was the overrelaxed minimal residual algorithm [53] which solves:

$$M\chi = \phi \tag{1.54}$$

where χ is the quark propagator and ϕ is the source, by iterating the following steps:

$$\begin{aligned} \alpha_n &= \frac{(Mr_n, r_n)}{\mid Mr_n \mid^2} \\ \chi_{n+1} &= \chi_n + \omega\alpha_n r_n \\ r_{n+1} &= r_n - \omega\alpha_n M r_n \end{aligned} \tag{1.55}$$

the optimum choice of the free parameter ω was found to be 1.1. For a more detailed discussion of the various possible inversion algorithms and numerical comparisons between them see [51]. All the quark propagators used in the numerical work in this thesis were calculated using the above algorithm with red black preconditioning on the 64 i860-node Meiko computer at Edinburgh.

1.4.3 The extraction of physics from the simulation.

One of the basic processes in lattice gauge QCD calculations is the creation of a particle and its subsequent annihilation after a time t, the amplitude for this process is computed using the vacuum expectation values of operators. To project out the states with definite momenta, the operators are weighted with the required phase factors and summed up over the lattice to produce the time sliced propagator:

$$G_M(\underline{p}, t) = \sum_{\underline{x}} e^{-i\underline{p}\cdot\underline{x}} \langle 0 \mid \chi_M(\underline{x}, t)\chi_M^{\dagger}(\underline{0}, 0) \mid 0 \rangle \tag{1.56}$$

for the particle M. Using translational invariance and after inserting a complete set of states, the following formula for the time sliced propagator can be derived:

$$G_M(\underline{p}, t) = \sum_n \frac{\mid \langle \chi_n \mid \chi_n \rangle \mid^2}{2E_n} e^{-E_n t} \tag{1.57}$$

where E_n is the energy of the nth particle with the same quantum numbers as the original operators. The above formula is only valid on an infinite lattice; on a finite lattice its exponential decay with time gets modified into a hyperbolic function.

In numerical simulations, it is usually assumed that by going far enough in time, only one term will contribute to the sum in equation 1.57, the mass and amplitude can then be extracted by fitting a function to the results of the simulation.

I will describe the correct choices of operators to create given particles in section 1.5. There is another important point in chosing the operator χ_M. Empirically a better signal is found by making the annihilation and creation operators nonlocal in space, this is known as smearing. For details of how this is done by the UKQCD collaboration see [73].

The amplitude extracted from the time sliced propagator on the lattice is in the lattice regularisation scheme. To compare with experiment this must be converted into a continuum regularisation scheme, such as $\overline{MS}$. This can be done by multiplying the result with a suitable renormalisation factor [62].

1.4.4 The analysis of data from simulation.

The final result of a lattice QCD simulation described above is a table of numbers for each configuration as a function of time. These numbers must be combined in a sensible way to form an estimate of the correlator in the functional integral. The masses and decay constants are extracted by a suitable fit procedure. The existence of excited states in equation 1.57, makes this procedure complicated. In this section I will describe the fit procedure I used in the data analysis in chapter 5.

In this section I will use the notation $\langle x(t) \rangle$ for $G_M(\underline{p}, t)$ in equation 1.56. To obtain an estimate of the correlator in equation 1.56 from N samples $x_n(t)$, the sample mean is used:

$$\overline{x} = \frac{1}{N} \sum_{n=1}^{N} x_n(t) \tag{1.58}$$

To extract the masses and decay constants from the x(t), the traditional gaussian motivated χ^2 fit method has to be modified, because adjacent time slices in an individual correlator are not statistically independent of each other. The covariance matrix:

$$V(t,t') = \frac{1}{N(N-1)} \sum_{n=1}^{N} [x_n(t) - \langle x(t) \rangle][x_n(t') - \langle x(t') \rangle] \tag{1.59}$$

takes into account the correlation between timeslices. The V matrix is rescaled

by dividing out its diagonal elements $\sigma(t)^2$ producing:

$$A(t,t') = \frac{V(t,t')}{\sigma(t)\sigma(t')} \tag{1.60}$$

The function which provides the goodness of fit of the model function, and whose minimisation gives the fit parameters, is the correlated χ^2 function:

$$\chi^2 = \sum_{t \in FITREGION} \frac{[\overline{x}(t) - f(t;\{\alpha\})]}{\sigma(t)} A^{-1}(t,t') \frac{[\overline{x}(t') - f(t';\{\alpha\})]}{\sigma(t')} \tag{1.61}$$

where $f(t,\{\alpha\})$ is the model fit function depending on the fit parameters α. The matrix A is introduced because the original covariance matrix V has eigenvalues with many orders of magnitude, which makes it difficult to invert. The matrix A is inverted using the singular value decomposition algorithm.

The χ^2 value obtained from the fit procedure gives an indication of whether the single exponential models for the correlators are a good description of the data. The rule of thumb is that the $\frac{\chi^2}{dof}$ per degree of freedom should be of the order one. The number of degrees of freedom (dof) is defined as the number of time slices fitted minus the number of model parameters. Small $\frac{\chi^2}{dof}$ indicate that the signal is very noisy or that the errors have been overestimated.

For the mesons the fit model used was:

$$f(t) = a_m(e^{-E_m t} + e^{-E_m(T-t)}) \tag{1.62}$$

and for the nucleon the model used was:

$$\begin{aligned} f(t) &= a_N(e^{-E_N t}) \;\; t \leq \frac{T}{2} \\ f(t) &= a_N(e^{-E_N(T-t)}) \;\; t > \frac{T}{2} \end{aligned} \tag{1.63}$$

where T was the length of the lattice in the time direction, and a_m, a_N, E_m, and E_N are the fit parameters for the two classes of particles. The nucleon correlator in equation 1.63 is constructed from the forward moving nucleon in the positive parity channel (upper two components) for $t < \frac{T}{2}$ and the backward moving nucleon in the corresponding negative parity channel (lower two components) (multiplied by -1) for $t > \frac{T}{2}$.

The errors on the final fit parameters were estimated by using the bootstrap method. A thousand bootstrap samples were used to estimate the 68% confidence interval.

All the above error analysis is standard UKQCD procedure for extracting physics from time sliced propagators and has been implemented in a computer

program. One of the crucial aspects of extracting sensible results from the data is the fit region used. For small times the ground state signal is contaminated by excited states. To find a fit region where the correlator is dominated by the ground state only, I looked for plateaux in the effective mass:

$$m_{eff} = -\log(\frac{G(t+1)}{G(t)}) \tag{1.64}$$

1.5 Transformation properties of lattice hadron operators.

In this section I will consider the problem of the construction of hadron operators which couple to particles of a definite spin and momentum. The introduction of a lattice destroys the Poincare invariance of the theory and thus naively makes the choice of creation and annihilation operators for particles of a given spin and momentum more difficult.

The problem of the construction of operators which create particles with a given momentum has never been satisfactorily treated. The effect of the lattice is seen immediately because a particle's spatial momentum is quantised. Producing good operators for particles at finite momentum is important because they are used in the calculation of the pion form factor, and the calculation of the Isgur-Wise function. I will end this chapter with a discussion about operators for particles outside their rest frame.

1.5.1 Spin on the lattice.

The spin of a particle is intrinsically connected to the symmetries of space time. Wigner showed [80] how the particles of nature could be classified using the representation theory of the Poincare group. The introduction of a lattice mutilates the precious spacetime symmetries of the theory. This makes the construction of operators on the lattice which couple to a particle with a given spin more complicated.

The symmetry group relevant to spin in Euclidean space is $SU(2)\otimes SU(2)$, the theory and relevance to physics of this group is covered in a number of textbooks [69] [70] A representation of $SU(2)\otimes SU(2)$ can be obtained from the set of linear transformations that leave:

$$x_1^2 + x_2^2 + x_3^2 + x_4^2 \tag{1.65}$$

invariant, where (x_1, x_2, x_3, x_4) labels a point in spacetime. There are also spinor representations.

Another important group for the theory of spin is the little group, which is the set of transformations which leave the four momentum invariant. For a massive particle the little group is SU(2), which is the connection between Euclidean invariance and the theory of angular momentum.

The notation for a representation of $SU(2) \otimes SU(2)$ is (j_1, j_2) where j_1 and j_2 are any multiples of a $\frac{1}{2}$. All the standard particles in the particle physics zoo can be labelled using one of these representations; for example a scalar particle is labelled by (0,0) and a Dirac spinor by $(\frac{1}{2}, 0) \oplus (0, \frac{1}{2})$. The spin of a particle which transforms like (j_1, j_2) is $j_1 + j_2$. The rule for how a representation of $SU(2) \otimes SU(2)$ decomposes in the rest frame into representations of the little group SU(2) labelled by j_i (the angular momentum) is [86]:

$$(j_1, j_2) \longrightarrow (j_1 + j_2) \oplus (j_1 + j_2 - 1) \cdots \mid j_1 - j_2 \mid \tag{1.66}$$

The symmetry group of lattice Lagrangians is the hypercubic group, which is a subgroup of $SU(2) \otimes SU(2)$. The hypercubic group is defined as the set of transformations which leave the hypercubic lattice unchanged. The required theory, such as character tables, has been worked out in [40][68]; I will use the notation used by Mandula and collaborators in [40]. When spinors are considered the relevant group is the covering group of the hypercubic group, details about which can be found in the paper by Mandula and Shpiz [3].

It turns out that all the SU(2)⊗SU(2) representations describing particles with spin less than two remain irreducible under transformations of the hypercubic group. However as Johnson pointed out [2], there is a subtlely due to higher spin representations of the continuum group. For example the (2,0) representation of SU(2)⊗SU(2) when decomposed into irreducible representations contains the (1,0) representation. As the continuum limit is taken, the SU(2)⊗SU(2) symmetry must be restored, so an operator transforming like (1,0) must be contaminated by a particle transforming like (2,0), even though it transforms irreducibly under the hypercubic group. In physical language there could be a spin two excited states for an operator whose ground state is a particle of spin one.

1.5.2 Point meson operators.

The operators used to create and annihilate mesons can be shown, using the standard character theory of finite groups, to be the same as the fermion bilinears in the theory of the Dirac equation [4]. Table 1.1 shows the classification of the quark-antiquark operators under the hypercubic group. The decomposition of the meson operators in the rest frame and the expected particles with the lowest mass in that channel are shown in table 1.2. Light particles are made out of the

Field	Representation	C
$\bar{\psi}\psi$	$(0,0)^+$	+
$\bar{\psi}\gamma_5\psi$	$(0,0)^-$	+
$\bar{\psi}\gamma_\mu\psi$	$(\frac{1}{2},\frac{1}{2})^+$	−
$\bar{\psi}\gamma_\mu\gamma_5\psi$	$(\frac{1}{2},\frac{1}{2})^-$	+
$\bar{\psi}\sigma_{\mu\nu}\psi$	$(1,0)\oplus(0,1)$	−

Table 1.1: Irreducible two quark operators under the hypercubic group.

Operator	Light Particle	Heavy particle	J^{PC}
$\bar{\psi}\gamma_5\psi$	π	η_c	0^{-+}
$\bar{\psi}\gamma_4\gamma_5\psi$	π	η_c	0^{-+}
$\bar{\psi}\gamma_i\psi$	ρ	J/ψ	1^{--}
$\bar{\psi}\gamma_i\gamma_4\psi$	ρ	J/ψ	1^{--}
$\bar{\psi}\gamma_i\gamma_5\psi$	$a1$	χ_{c_1}	1^{++}
$\bar{\psi}\psi$	a_0	χ_{c0}	0^{++}
$\epsilon^{ijk}\bar{\psi}\gamma_j\gamma_k\psi$	$b1$	h_c	1^{+-}

Table 1.2: Rest frame meson operators, together with the particle assignments.

up or down quarks and heavy particles constructed from charm quarks. The eigenvalues of the standard parity and charge conjugation operators in the theory of the Dirac equation are also shown in the tables.

1.5.3 Nonlocal meson operators.

Meson operators constructed from two quark operators connected by a string of gauge links, typically in the form of covariant derivatives, might prove useful in the simulation of particles on the lattice.One advantage of using extended operators is that is that group theoretically, it is like taking the kronecker product of the local meson operators with the gauge invariant translation operators. The decomposition of these representations can produce irreducible representations which couple to particles of spin 2, which are inaccessible using only local operators.

The use of extended operators could be crucial to the calculation of masses of the P-wave mesons. In the standard nonrelativistic quark model, the wave function of a meson is split into the product of a spin and spatial wavefunction. The spin part of the total wavefunction is constructed from two component Pauli spinors, combined to from spin singlets (S=0) or spin triplets (S=1). The spatial part of the wavefunction is obtained by solving the Schrödinger equation in a suitable central potential, the resulting wavefunctions are labelled by the energy and the orbital angular momentum L. The boundary conditions for a P-wave (L=1) state require that the wavefunction is zero at the origin. If this intuition gained from the quark model model can be directly applied to lattice gauge theory, then this suggests that the best operators for P-wave mesons would be the ones which are zero at the origin.

If the above nonrelativistic considerations are applicable, then purely local operators should not produce any signal for P-wave mesons. However in table 1.2 I have identified three sets of P-wave mesons (a1, a0, b1), with purely local lattice operators. The reason for this is that these operators have the correct parity and charge conjugation quantum numbers. The quark model predicts the charge conjugation and parity of a $\bar{q}q$ state to be:

$$C = (-1)^{L+S} \tag{1.67}$$

$$P = (-1)^{L+1} \tag{1.68}$$

The resulting spectrum of discrete quantum numbers is shown in table 1.3.

I will now briefly review the various operators that have been used in lattice gauge theory to attempt to simulate P-wave mesons. DeGrand and Hecht used quark model ideas in a lattice gauge theory simulation of P-wave mesons and baryons, using Wilson fermions at β =6.0. They combined nonrelativistic spinors with quark wavefunctions which by analogy with the quark model, should couple strongly to P-wave states. Although they were successful in extracting masses it is not clear that better operators could not be constructed using relativistic methods on the lattice. The APE collaboration used the operators in table 1.2 to project onto the P-wave meson states. They used cube smearing for their quark propagators, which made their mesons nonlocal. However no attempt was made to ensure that their operators were zero at the origin. In practice their operators were not very successful, at $\beta = 6.0$ for Wilson fermions they had no signal for the a0 and a1 particles, and only a poor signal for the b1. Lepage and Thacker in a

Orbital angular momentum	J^{PC}	
	S = 0	S = 1
L = 0	0^{-+}	1^{--}
L = 1	1^{+-}	0^{++}
L = 1		1^{++}
L = 1		2^{++}
L = 2	2^{-+}	1^{--}
L = 2		2^{--}
L = 2		3^{--}

Table 1.3: J^{PC} for mesons from the quark model.

paper on nonrelativistic lattice QCD used various covariant derivatives in between their nonrelativistic spinors to obtain operators for P and D wave mesons. They successfully simulated P-wave and S-wave mesons using their operators.

The use of fermion bilinears extended by covariant derivatives seems an ideal way of constructing operators for Wilson fermion calculations of P-wave states on the lattice, because the operator would be in a definite representation of the hypercubic group. The operator would also be zero at the origin, in accordance with the intuition gained from the quark model. In practice there is a problem. Because of the computational cost of computing quark propagators; they are normally only calculated from one fixed origin to any other point on the lattice. A nonlocal operator made out of covariant derivatives at both the source and the sink would also require quark propagators inverted from different origins, making the calculation computationally expensive.

Because no local operators have particles of spin 2 as their ground state, they require an extended operator at both the source and the sink. This approach is impractical for simulations of spin two particles using Wilson fermions. However the use of covariant derivatives might improve the signal for spin 1 P-wave mesons.

A first step in finding operators involving covariant derivatives which couple to P-wave mesons is to investigate the transformation properties of such operators under the hypercubic group. Most of the irreducible basis functions for the product of up to three covariant derivatives, have been reported in papers on the calculation of the pions distribution function on the lattice by Martinelli

and Sachrajda[39] [26]. However there is an easy way to construct an operator which should have a good overlap with P-wave spin 1 mesons, without using much group theory machinery. Consider the following even parity extended covariant operator:

$$(E_\mu f)(x) = \frac{U_\mu(x)f(x+\mu) + U_\mu^\dagger f(x-\mu)}{2} \tag{1.69}$$

A possible way to improve the signals for P-wave mesons with spin less than two would be to use one of the local operators in table 1.2 at the origin, and an operator with the equivalent gamma matrix Γ at the point x extended by using the E_μ operator in the following way:

$$\sum_i \overline{\psi}(x) E_i \Gamma \psi(x) \tag{1.70}$$

The advantage of using equation 1.70 to create a P-wave meson is that the

$$\sum_i E_i \tag{1.71}$$

operator is invariant under the hypercubic group. The operator in 1.70 will couple to the same particles as the equivalent local operator. Unfortunately the scheme described above has not been investigated numerically, however some results about P-wave mesons will be reported in chapter 5.

1.5.4 Group theory behind the lattice Baryon operators.

The material in this section is background for the construction of operators at finite momentum. The only baryon operator I will report numerical results for in chapter 5 is the nucleon.

The starting point for obtaining a specific baryon operator is a colour singlet 3 quark operator carrying flavour and spinor indices, which can be decomposed with respect to the direct product of the SU(N_f) flavour symmetry with the covering group of the hypercubic group. Normally the tensor could be decomposed by symmetrising with respect to the flavour and spinor indices independently. However in this case because the quark operators are indistinguishable, the two symmetrisations of the two types of index are not independent of each other. For the purposes of calculation the effect of flavour, the colour and the anticommuting nature of the fields cancel out, leaving an object with three Dirac spinor indices, which has certain symmetry properties under the permutation of the indices, and

on which standard group theory techniques can be applied to obtain irreducible spinors

Therefore operators are chosen which are irreducible under the flavour symmetry by using the standard youngs symmetrisers. The following operator will create an isospin 3/2 particle:

$$\Delta_{ijk} = \epsilon^{abc} u_i^a u_j^b u_k^c \tag{1.72}$$

and the following two operators will create isospin 1/2 particles:

$$Q_{ijk} = \frac{\epsilon^{abc}}{2}(u_i^a d_j^b u_k^c - u_j^a d_i^b u_k^c) \tag{1.73}$$

$$P_{ijk} = \frac{\epsilon^{abc}}{2}(u_i^a u_j^b d_k^c - u_k^a u_j^b d_i^c) \tag{1.74}$$

To find out how the spinors in each of the three subspaces transformed under the hypercubic group, I used the following character formulae (although presumably the calculation could have been done in the continuum):

$$n_\alpha = \frac{1}{\mid G \mid} \sum_{g \epsilon G} \chi(g)^{\alpha *} \chi(g) \tag{1.75}$$

with the character tables of the irreducible representations in the paper by Mandula and collaborators [40]. In equation 1.75 n_α is the number of times the α irreducible representation occurs in the representation with characters $\chi(g)$. The number of elements in the group is $\mid G \mid$.

In the following, the character for Dirac quarks on the lattice is $\chi_D(g)$. The isospin 1/2 character is:

$$\chi(g)_{I=1/2} = \frac{\chi_D^3(g) - \chi_D(g^3)}{3} \tag{1.76}$$

and the isospin 3/2 character is:

$$\chi(g)_{I=3/2} = \frac{\chi_D(g)^3 + 3\chi_D(g)\chi_D(g^2) + 2\chi_D(g^3)}{6} \tag{1.77}$$

The results are that the isospin 3/2 operator transforms like:

$$(1,1/2)\oplus(1/2,1)\oplus(3/2,0)\oplus(0,3/2)$$

and the two isospin 1/2 operators transforms like:

$$(1,1/2)\oplus(1/2,1)\oplus(1/2,0)\oplus(0,1/2)\ \oplus(1/2,0)\oplus(0,1/2)$$

The implications of the above results is that the isospin $\frac{3}{2}$ operator in the rest frame contains two spin $\frac{3}{2}$ representations (Δ^{++}) and one spin $\frac{1}{2}$ representation (Δ^{+}). The isospin $\frac{1}{2}$ operator couples to three spin $\frac{1}{2}$ representations (the proton) and one spin $\frac{3}{2}$ representation ($N^{*\frac{3}{2}}$).

A derivation of the correct combinations of the three quark spinors, to form the spin $\frac{1}{2}$ and $\frac{3}{2}$ baryon operators has been done by Hoek and Smit in [27]. They do the calculation entirely in the continuum. The interesting point for studies of operators at finite momentum is that the $(N^*)^{\frac{3}{2}}$ particle operator comes from the decomposition of the $(1,\frac{1}{2})$ and $(\frac{1}{2},1)$ representations. It is not clear how the correct operator for the $(N^*)^{\frac{3}{2}}$ particle could be obtained at finite momentum.

The only operator that will be used in the numerical work in chapter 5 is the following nucleon operator:

$$\epsilon^{abc}(u^a C\gamma_5 d^b)u^c \tag{1.78}$$

1.5.5 Operators at finite momentum.

In the previous review of creation operators on the lattice, a number of the operators depended explicitly on the particle being in the rest frame. For example the $\overline{\psi}\gamma_\mu\gamma_5\psi$ operator is irreducible under the full hypercubic group, but in the rest frame it breaks down into $\overline{\psi}\gamma_0\gamma_5\psi$ which describes the pion and into $\overline{\psi}\gamma_i\gamma_5\psi$ which couples to the a1 particle. It is not clear how a similar split occurs at finite momentum. There is a similar problem with the $(N^*)^{\frac{3}{2}}$ and Δ^+ baryon operators.

It is difficult to form a physical picture of particles at finite momentum on the lattice, because the quantisation of momentum caused by the lattice, runs counter to our normal continuum intuition. Good choices of operators which couple strongly to particles with finite momentum is crucial to the extraction of many quantities of phenomenological interest from the lattice. In this section I will try and demonstrate some of the problems of obtaining such operators on the lattice.

The operator which creates a particle at a finite momentum is unlikely to be the same as the operator which creates the same particle at rest because of the effect of the lattice analogue of the Lorentz transformation. In the continuum, it

is easy to construct the Lorentz transformation:

$$\Lambda_{\mu\nu} = \begin{pmatrix} \gamma & v\gamma & 0 & 0 \\ v\gamma & \gamma & 0 & 0 \\ 0 & 0 & 1 & 0 \\ 0 & 0 & 0 & 1 \end{pmatrix} \tag{1.79}$$

where γ is defined as:

$$\gamma = \frac{1}{\sqrt{1-v^2}} \tag{1.80}$$

between the rest frame of an operator like $\overline{\psi}\gamma_\mu\psi$, to the Lorentz frame travelling with velocity v along the x axis to produce the operator at finite momentum $\Lambda_{\mu\nu}\overline{\psi}\gamma_\mu\psi$. On the lattice, because spatial momentum is quantised, it is not so clear how to construct the analogue of the $\Lambda\mu\nu$ matrix.

For a composite particle such as the rho, it is not obvious even in the continuum, that simple free field theory ideas will produce the correct Lorentz transformed operator. Physical ideas gleaned from the quark model [43] also suggest that new operators are required for particles at finite momentum. The SU(6) symmetry successfully classifies the lowest lying hadrons into irreducible representations; and also produces various quantities, which by clever parameterisations can be used to predict decay amplitudes, and mass splittings. However the symmetry gets some decay amplitudes completely wrong. The SU(2) subgroup of SU(6) which corresponds to the nonrelativistic spin of the particles does not allow transitions between particles with different spin quantum numbers.

This forbids the following two decays:

$$\Delta_{S=\frac{3}{2}} \rightarrow N_{S=\frac{1}{2}} \otimes \pi_{S=0} \tag{1.81}$$

$$\rho_{S=1} \rightarrow \pi_{S=0} \otimes \pi_{S=0} \tag{1.82}$$

both of which are the dominant decays.

The postulated reason for the failure of the SU(6) predictions was that SU(6) is a rest frame symmetry, but the above two decays both involve particles in motion. By combining an SU(2) subgroup whose generators commuted with the boost operators in the x direction, with the standard SU(3) generators, the $SU(6)_w$ group was postulated as a potential candidate for describing collinear decay processors. Although the $SU(6)_w$ symmetry group was moderatively successful in practice, for describing some decay processes, it is not clear how to adapt these ideas for use in numerical hadron spectrum calculations.

Some derivations [44] [45] of the hadron operators seem to solve the problem of projecting out the correct operator at finite momentum. Consider the following projection of the $(N^*)^{\frac{1}{2}}$ particle from the three quark operator with the correct flavour symmetry. By Lorentz invariance the $\eta_\mu^\alpha = (uC\gamma_\mu d)u$ (which contains the spin $\frac{1}{2}$ and spin $\frac{3}{2}$ fields) operator must have the following form:

$$\eta_\mu^\alpha = \Delta_\mu^\alpha + p_\mu v_1^\alpha + \gamma_\mu^{\alpha\beta} v_2^\beta \tag{1.83}$$

where v_1^α and v_2^β are arbitrary spinors, which are determined from the constraints on the spin $\frac{3}{2}$ (Δ_μ^α) field:

$$\gamma_\mu \Delta_\mu = 0 \tag{1.84}$$

$$p_\mu \Delta_\mu = 0 \tag{1.85}$$

required so that the Δ_μ field satisfies the Rarita Schwinger equation. The resulting expression for the Δ_μ fields is

$$\Delta_\mu = \eta_\mu - \frac{p_\mu}{3p^2}(4p.\eta - \not{p}\not{\eta}) - \frac{\gamma_\mu}{3p^2}(p^2\not{\eta} - \not{p}p.\eta) \tag{1.86}$$

This appears to produce an operator which will create a particle with finite momentum. However the appearance of p_μ shows that equation 1.86 is a continuum expression whose validity on the lattice must be questioned. Computationally equation 1.86 is not very useful, because for a two point correlator the field is required in position space. The use of equation 1.86 entails the added burden of fourier transforming.

In this section I have tried to suggest various possible ways of obtaining operators for particles at finite momentum, using particle physics inspired ideas. This has not been very successful in producing either operators or insight. In the next two sections I will try and investigate the problem of obtaining operators at finite momentum, using ideas in solid state physics.

1.5.6 The cubic space group

The full space-time symmetry group for the Lagrangian is the space group of the hypercubic lattice; the semi-direct product of the translational group with the point symmetry group. This is a subgroup of the continuum four dimensional Euclidean group [87]. Operators which create particles must transform irreducibly under the relevant symmetry group, so the space group must be involved in the

correct choice of operators at finite momentum. In solid state physics, space groups are used to help solve the schrödinger equation for electrons moving in crystals; it would be useful if similar ideas could be used in lattice gauge theory. However the origin of the utility of space groups in solid state physics is the (idealised) periodic potential caused by the regular arrangement of atoms in the crystal. This contrasts with the lattice introduced for the nonperturbative solution of field theory, which has no physical origin. So it is not entirely clear that space groups can usefully be used to understand operators on the lattice at finite momentum.

In the rest of the section I will introduce space groups. In the next section I will try and apply the representation theory of space groups to lattice gauge theory.

An element of the space group is defined its operation on a lattice point $\underline{x}$:

$$(\Lambda, \underline{t})\underline{x} = \Lambda\underline{x} + \underline{t} \tag{1.87}$$

where Λ belongs to the point symmetry group and $\underline{t}$ is a translational between two lattice points. In the continuum Minkowski space the analogous symmetry group would be the Poincare group.

The translation group depends on the type of boundary conditions. In this initial study I will use periodic boundary conditions, because this will allow the use of the representation theory of finite groups, and also because the UKQCD collaboration's numerical work uses periodic boundary condition in the spatial directions for the quark and gluon fields. In the continuum limit the boundary conditions should not matter.

Although the invariance group of the Lagrangian is the four dimensional space group, when two point correlation functions are considered only the three dimensional symmetry group remains. From now on I will only consider the three dimensional cubic space group.

1.5.7 A re-examination of the time sliced propagator

I will now motivate the relevance of the representation theory of space groups to lattice gauge theory, by rewriting the time sliced propagator in a way to make its group theoretical nature obvious.

To perform any group theory calculations requires at the very least the characters of the group you are interested in. As a warm up exercise, I will first

consider the characters of the translational group. Although their derivation can be found in many text books on solid state physics, a review of the material here is instructive.

The action of the group operator T in the space is defined by:

$$T(\underline{x})F(\underline{y}) = f(\underline{x} + \underline{y}) \tag{1.88}$$

The translations in space form the direct product of the three one dimensional translations in the x,y and z directions. This means that the characters of the translational group can be obtained by multiplying the characters of the one dimensional translations in the three independent directions, implying I only need to derive the characters for one dimensional translations. The characters $\chi_n(x)$ of the nth irreducible representation are easily derived by using the boundary conditions on the lattice of length L, producing the following constraint:

$$\chi_n(x)^L = 1 \tag{1.89}$$

where n is integer. This is solved to give:

$$\chi_n(x) = e^{\frac{2\pi x n}{L}\hat{\imath}} \tag{1.90}$$

If I set $p = \frac{2\pi n}{L}$, then equation 1.90 is just a fancy way of saying that the spatial momentum is quantised. Using the characters in equation 1.90 and the definition of the translational operator in equation 1.88, I can rewrite the time sliced propagator in equation 1.56 as:

$$\sum_{\underline{x}} e^{-i\underline{x}\underline{p}} G(\underline{x}) = \sum_{\underline{x}} \chi_n(\underline{x})^* T(\underline{x}) G(\underline{0}) \tag{1.91}$$

which up to normalisations can be identified with the standard group theory projection operator for the translational group.

A good group theory text book which discusses the character projection operator is the one by Miller [5]. The character projection operator is defined as:

$$P^\alpha = \frac{n^\alpha}{\mid G \mid} \sum_{g \epsilon G} \chi(g)^{\alpha *} T(g) \tag{1.92}$$

for a group G. T(g) is the operator associated with the element g, α labels an irreducible representation with a dimension n^α, and $\mid G \mid$ is the number of elements in the group. P^α projects out the vectors in the space that the T(g) representation

transforms in, which transform like the α representation. P^α has the following essential projection operator properties:

$$\begin{aligned} P^\alpha P^\beta &= 0 \\ P^\alpha P^\alpha &= P^\alpha \end{aligned} \tag{1.93}$$

for two distinct irreducible representations α and β.

At this point it must be remembered that the true symmetry group is the cubic space group, defined by the operations in equation 1.87, which will have characters different to those of the translational group. This suggests that some progress could be made in understanding the choice of operators a finite momentum, if the characters of the space group are used in the timesliced propagator instead of naively weighting the sum over the lattice sites with the e^{ipx} factor.

Unfortunately the fairly involved mathematics required to extract the characters of the cubic group have prevented any further detailed investigation [87]. My derivation of equation of 1.91 can only be described as loose; a more convincing proof requires the use of the underlying path integral. Hopefully equation 1.91 will eventually be used to shed some light on finite momentum studies of lattice gauge theory.

2

The clover action and the reflection positivity condition.

2.1 Introduction.

In this Chapter I will present my attempts to prove that the clover fermion action satisfies the reflection positivity condition. Unfortunately I have failed to solve this problem; however this record of my attempts at a proof may provide clues to the best way to proceed in the construction of such a proof, as well as providing some insight into the clover action.

There are a number of conditions that must be proved about a lattice field theory based upon the path integral formalism in order to prove the existence of an underlying quantum theory based on a Hilbert space [23] [22]. One of the most important conditions to be proved is the reflection positivity condition. If this is shown to be true, there is a standard procedure for defining a scalar product for the quantum theory's Hilbert space using the expectation values defined by the path integral. The condition also gives information about the analytical continuation from the four dimensional statistical mechanics theory in Euclidean space, back to the Minkowski theory.

For numerical simulation the most important aspect of the reflection positivity axiom is that it allows the construction of a self adjoint positive transfer matrix. The mass spectrum of the theory is related to the log of the eigenvalues of the transfer matrix. In numerical lattice hadron spectrum calculations the masses of the particles are extracted by looking at the exponential decay of two point functions with time. If any eigenvalues of the transfer matrix are negative or

complex, then two point correlators will not decay as pure exponentials but will also contain oscillatory parts, making the extraction of masses more difficult.

I would like to emphasise the importance of the reflection positivity condition to the extraction of experimental numbers from lattice gauge theory. Consider a standard derivation of Lagrangian lattice gauge theory from a Hamiltonian based theory, such as the one done by Creutz [38]. Although a transfer matrix is produced, no information at all is provided about its spectral properties, until of course the theory is fully solved. However, if a field theory satisfies the reflection positivity condition, important information is obtained about the mass spectrum, before any detailed calculations are done.

Recently two groups have reported problems with the extraction of masses from QCD simulations, which they attribute to the failure of the reflection positivity for the action they were using. Parisi and collaborators [37] report problems with the Green's function of P-wave mesons, at a beta value of 5.7, which they suggest is due to the failure of the reflection positivity for the two-link improved fermion action they were simulating. Lepage and Thacker [57] argue that the oscillations in the effective masses, obtained from their heavy quark simulations using a nonrelativistic action, were due to problems with reflection positivity.

The next section will explain the mathematical definition of reflection positivity and describe my attempts to prove the condition using the same methods that were successfully applied to the Wilson action by Osterwalder and Seiler. Then I will try and adapt the proof of the reflection positivity condition for the Wilson action, due to Menotti and Pelissetto, to the clover action. To try and gain some insight into the formal mathematics, and to understand the differences in the exact theorems proved for the Wilson action, I will then consider Wilson fermions in free field theory. The final section will be on the possible implications for numerical simulations, if the clover action does not satisfy the reflection positivity condition.

2.2 The first attempt at a proof.

This attempt at a proof, is based on the ideas in a paper by Osterwalder and Seiler[22]. I will work in temporal gauge where all the matrices in the time direction are set equal to the unit matrix. I need to define a^+ as the set of fields defined by:

$$\{\psi(x), \overline{\psi}(x), U_\mu(x);\ x^0, x^0 + \mu^0 > 0\ \}$$

and also introduce a corresponding definition for a^- The antilinear mapping θ : $a^+ \rightarrow a^-$ is fully defined in [22], but a more convenient definition for my purposes is it s effect on an arbitrary gauge-invariant fermion bilinear, which is:

$$\theta(\overline{\psi}(x)\Gamma f(U_\mu(x))\psi(x)) = \overline{\psi}(\theta x)\gamma_0\Gamma^\dagger\gamma_0 f(U_{\theta\mu}(\theta x))^\dagger\psi(\theta x) \tag{2.1}$$

where $\theta x = (-x_0, x_1, x_2, x_3)$ and Γ is an arbitrary gamma matrix, and f is a function of the gauge fields, which could be a plaquette for example.

The authors of [22] define lattice points in the following way:

$$\mathrm{x} = (x_0 + \tfrac{1}{2}, x_1 + \tfrac{1}{2}, x_2 + \tfrac{1}{2}, x_3 + \tfrac{1}{2})$$

where x_0, x_1, x_2, x_3 are all integers. The above definition of the lattice is symmetric with respect to the coordinate axis, but does not have any points on the axis. In this section I will also use their lattice, but the consequence of this is that a positive transfer matrix can only be defined for an even number of steps.

A theory satisfies the reflection positivity condition if the following result is true:

$$\langle\theta\Im\Im\rangle \geq 0 \tag{2.2}$$

where $\Im$ is a function of the fields belonging to a^+ and the expectation value is the standard one for lattice QCD:

$$\langle A\rangle = \frac{1}{Z}\int \mathcal{D}U\mathcal{D}\psi\mathcal{D}\overline{\psi}e^{-S_{YM}-S_F}A \tag{2.3}$$

where Z normalises the expectation value. If 2.2 is true then the transfer matrix T_2 can be defined as the operation which shifts the fields belonging to a^+, by two lattice spacings in the time direction. A scalar product can be constructed using 2.2, which can be used to show that the transfer matrix is self adjoint. Osterwalder and Seiler also prove the norm of the transfer matrix is less than one, which allows the construction of a Hamiltonian H, via $T_2 = e^{-2H}$.

I now need to define $\mathcal{P}$ as the set of functions which can be written in the form $(\Im A)A$, with A being a function of the fields belonging to a^+. Osterwalder and Seiler show that if $X \in \mathcal{P}$ then:

$$\int \mathcal{D}U\mathcal{D}\psi\mathcal{D}\overline{\psi}X \geq 0 \tag{2.4}$$

They also prove the useful result that if $A \in \mathcal{P}$ and $B \in \mathcal{P}$, then $AB \in \mathcal{P}$. This reduces the problem of proving equation 2.2 to showing that the $e^{-S_{YM}-S_F}$ factor belongs to $\mathcal{P}$.

As the Wilson action has already been shown to belong to $\mathcal{P}$, then to try and prove reflection positivity, for the clover action, I only need to show that the exponential of the clover term:

$$e^{-\sum \overline{\psi}(x)\sigma_{\mu\nu}\sum(U_{\square}-U_{\square}^{\dagger})_{\mu\nu}\psi(x)} \tag{2.5}$$

belongs to $\mathcal{P}$

As a first step, I will try and show that equation 2.5 can be written in the form $(\Theta A)A$, which corresponds to showing that Θ maps every term in the sum comprising the clover part of the action into another term in the sum.

I will first consider an arbitrary clover term in the expansion which lies in the plane defined by two spatial directions. The θ operator acting on this term gives:

$$\theta(\overline{\psi}(x)\sigma_{ij}\sum(U_{\square}-U_{\square}^{\dagger})_{ij}\psi(x)) = \overline{\psi}(\theta x)\gamma_0\sigma_{ij}^{\dagger}\gamma_0\sum(U_{\square}-U_{\square}^{\dagger})_{ij}^{\dagger}\psi(\theta x) \tag{2.6}$$

which is just another term in the expansion. The θ operator has no effect upon the orientation of the field strength.

Now consider a clover term which extends in the time direction. The effect of the θ operator is as follows:

$$\theta(\overline{\psi}(x)\sigma_{0j}\sum(U_{\square}-U_{\square}^{\dagger})_{0j}\psi(x)) = -\overline{\psi}(\theta x)\gamma_0\sigma_{0j}^{\dagger}\gamma_0\sum(U_{\square}-U_{\square}^{\dagger})_{0j}^{\dagger}\psi(\theta x) \tag{2.7}$$

For this case the effect of the θ operator on the orientation of the field strength is crucial. From figure 2.2 it can be seen that the θ operator reverses the orientation of the field strength tensor, producing the extra minus sign. A careful consideration of the clover terms extending across the $x^0 = 0$ plane does not produce any extra problems.

So far I have demonstrated that equation 2.5 can be written in the form of $(\Theta A)A$; if the field strength tensor had been defined using only a single plaquette, then this could not have been done. Unfortunately I have been unable to show that $A \in a^+$, which is the cause of my failure to find a proof. The problem terms are the ones with the plaquettes overlapping the t=0 hyperplane; these can be written in the required form of $(\Theta A)A$, but without $A \in a^+$.

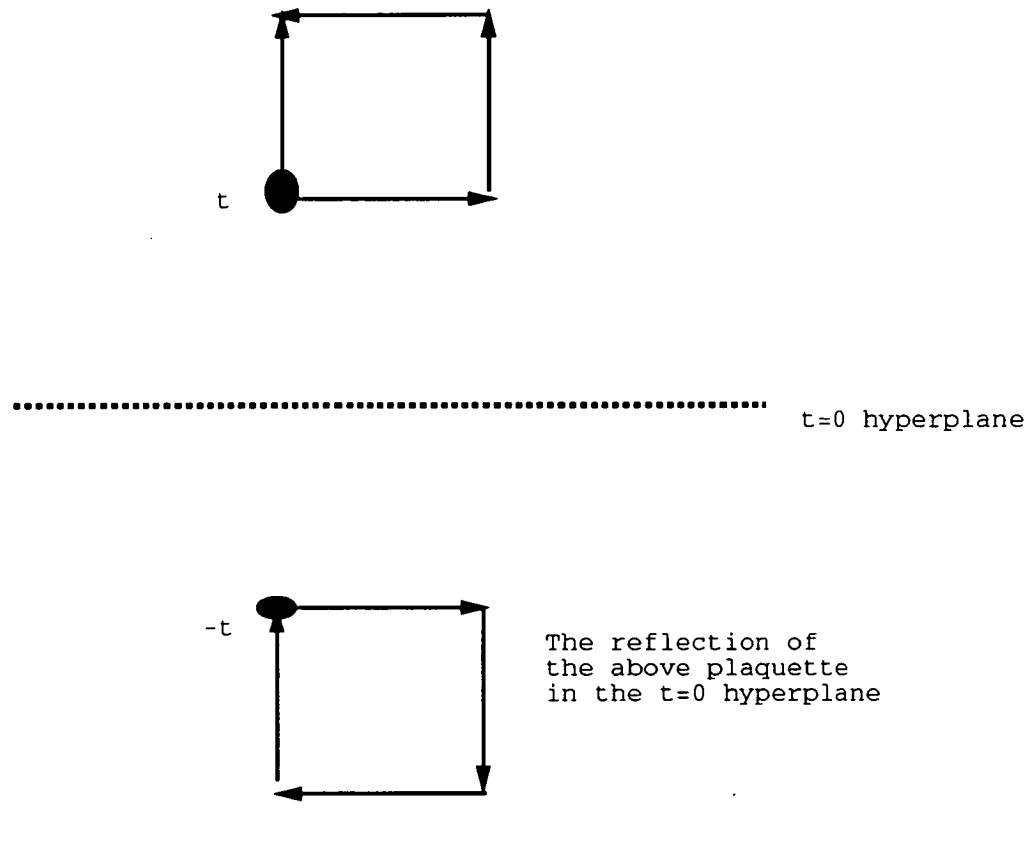

Figure 2.1: The reflection of a plaquette in the t=0 plane.

2.3 The second attempt at a proof.

Lüscher explicitly constructed a transfer matrix for all translations in time for the Wilson action. He was able to show that for the Wilson action with r=1 and the hopping parameter less than $\frac{1}{6}$ the transfer matrix had only real positive eigenvalues.

Unfortunately Lüschers proof was too complicated for me to generalise to the clover action. However Menotti and Pelissetto [34] have an alternative elegant proof of Lüschers result, and it was their method I tried to use. They prove equation 2.2 by integrating out all the fields which do not lie on, or connect to the t = 0 hyperplane. The resulting functional integral over the t = 0 fields is shown to be positive. I will now show why Menotti and Pelissetto's proof will not work for the clover action. I will concentrate on the fermion part of the action, because the treatment of the pure gauge part is the same as in the original paper.

In this section I will revert to working on a hypercubic lattice with the fields sitting on the origin. First define V_4^+ as the fields $\psi(n), \overline{\psi}(n)$ with $n_4 > 0$ and all $U(n)$ with either $n_4 > 0$ or $n_4 + \mu > 0$, there is a similar definition of fields V_4^-. The set of fields $\psi(n), \overline{\psi}(n)$ and $U(n)$ with $n_4 = 0$ and $n_4 + \mu = 0$ are denoted by V_3^0 This splits up of the action into three pieces:

$$S_F = S_F^+ + S_F^0 + S_F^- \tag{2.8}$$

where S_F^0 depends only on V_3^0, S_F^+ depends on V_4^+ and V_3^0, and S_F^- depends on V_4^- and V_3^0. It is useful to introduce Lüscher's half spinor notation [23]:

$$\psi(n) = \begin{pmatrix} x(n) \\ y^\dagger(n) \end{pmatrix}, \overline{\psi}(n) = \begin{pmatrix} x^\dagger(n) \\ -y(n) \end{pmatrix} \tag{2.9}$$

$$\gamma_j = i \begin{pmatrix} 0 & \sigma_j \\ -\sigma_j & 0 \end{pmatrix}, \gamma_4 = \begin{pmatrix} 1 & 0 \\ 0 & -1 \end{pmatrix} \tag{2.10}$$

for the V_3^0 fermi fields. Using similar ideas to the last section and after a careful consideration of the invariance of the V_3^0 fields under the θ operation the following two results are obtained:

$$S_F^+ = \mathcal{J}(U, \psi, \overline{\psi}, x^\dagger(\underline{n}, 0), y^\dagger(\underline{n}, 0), x(\underline{n}, 0), y(\underline{n}, 0)) \tag{2.11}$$

$$S_F^- = \hat{\mathcal{J}}^*(\theta U, \theta\psi, \theta\overline{\psi}, x(\underline{n}, 0), y(\underline{n}, 0), x^\dagger(\underline{n}, 0), y^\dagger(\underline{n}, 0)) \tag{2.12}$$

The $*$ operation is the standard complex conjugation operation and $\hat{}$ means reverse the order of the Grassmann fields.

The functional integral in equation 2.2 is performed over the V_4^+ and V_4^- fields yielding:

$$\begin{aligned} &\int \prod_{\underline{n},j} dU_j(\underline{n},0) d\bar{\psi}(\underline{n},0) d\psi(\underline{n},0) e^{S_G^0 + S_F^0} \\ &\mathcal{G}(U(\underline{n},0), x^\dagger(\underline{n},0), y^\dagger(\underline{n},0), x(\underline{n},0), y(\underline{n},0)) \\ &\hat{\mathcal{G}}^*(U(\underline{n},0), x(\underline{n},0), y(\underline{n},0), x^\dagger(\underline{n},0), y^\dagger(\underline{n},0)) \end{aligned} \tag{2.13}$$

It is at this point that it can be seen that the proof goes wrong for the clover action. In the Wilson case, the equivalent of function $\mathcal{G}$ has only $x^\dagger$ and $y^\dagger$ as Grassmann arguments, and the $\hat{\mathcal{G}}^*$ part of the functional integral for the Wilson action has only x and y as spinor arguments. The significance of this is that the fermion part of the functional integral for the Wilson action, can be written in the form:

$$\begin{aligned} &\int \prod_{\underline{n}} dx(\underline{n},0) dx^\dagger(\underline{n},0) dy(\underline{n},0) dy^\dagger(\underline{n},0) e^{-x^\dagger B x - y^\dagger B^t y} \\ &\mathcal{F}(U(\underline{n},0), x^\dagger(\underline{n},0), y^\dagger(\underline{n},0)) \\ &\hat{\mathcal{F}}^*(U(\underline{n},0), x(\underline{n},0), y(\underline{n},0)) \end{aligned} \tag{2.14}$$

If the obvious change of variables in the functional integral is done, to obtain the $x^\dagger x + y^\dagger y$ in the exponential, the resulting expression can be recognised as the standard scalar product on the Grassmann algebra [35], which shows that $P(U) > 0$, which proves 2.2. The restriction of $\kappa < \frac{1}{6}$ for the Wilson action, comes from the requirement that the matrix B is positive definite.

Unfortunately for the clover action, I cannot see any way of showing that that 2.13 is positive. Conversely I cannot see any way of showing that 2.13 should be negative, so the reflection positivity condition for reflections in the t = 0 hyper plane for the clover action remains an open question. I discuss equations 2.13 and 2.14 in appendix C.

2.4 Numerical work.

2.4.1 Introduction.

I will now look at the Wilson action in free field theory, to try and see some evidence for the violations of positivity, as this might give an estimate for the order of magnitude of these kind of effects for the clover action. This study provides

some insight into the Osterwalder-Seiler proof of positivity, only providing a well defined transfer matrix for an even number of translations.

2.4.2 The quark propagator in free field theory.

To look for violations of the physical positivity, the eigenvalues of the transfer matrix must be calculated or equivalently the mass of a particle in the theory must be obtained. An easy if somewhat unphysical choice (because of quark confinement) is the energy of the quark at different values of spatial momenta. This analysis will also be useful in understanding the energy dispersion relation obtained from a numerical simulation of quenched QCD in chapter 5. This analysis was first done in [19]; here I will try and generalise their work slightly to look at the finite quark mass case.

The standard field theoretical way to look for the energy of a particle is to look for the poles in its propagator. For the lattice scalar field, the propagator is simple enough to obtain the energy directly. However the more complicated structure of fermion propagators (especially improved ones), requires the use of a more systematic technique to obtain E(p). The method in [19] serves the purpose and also has the advantage of being close to the numerical lattice methods.

I will now briefly review the method. Working on a lattice of infinite volume, the connection between the quark propagator $S(p_0, \underline{p})$ in momentum space and its time sliced propagator $G(t, \underline{p})$ is:

$$G(t, \underline{p}) = \int_0^{2\pi} dp_0 e^{-ip_0 t} S(p_0, \underline{p}) \tag{2.15}$$

The integral can be evaluated by using contour integration and the transformation $z = e^{ip_0}$ to give:

$$G(t, \underline{p}) = \oint_C dz \frac{z^{-t}}{iz} \hat{S} \tag{2.16}$$

where the contour C is the unit circle in the complex plane. The connection between the exponential decay of the two-point correlator in numerical simulation and equation 2.16 can clearly be seen. The energy values E_i are extracted from the poles in the integrand z_i which lie within the unit circle, by using $E_i = -\log z_i$. The denominator can be written as a polynomial in z, the roots of which for anything more complicated than the Wilson action propagator, have to be found numerically.

In their studies of the massless Wilson lattice propagator Sheikholeslami and Wohlert found that in general that there were two branches to the energy dispersion relation, one in general lying above the other. For the special case of the Wilson r parameter set equal to 1, there is only one real energy for all momentum values, a result consistent with Lüschers reflection positivity work on the full theory. When r is less one the unphysical energy solution becomes positive and both for the cases of very large or very small r the second energy begins to have a low energy effect. It is interesting to contrast this behaviour with that predicted by the positivity proof of Osterwalder and Schrader, which predicts a well defined transfer matrix for even separations and as a corollary of this, no complex masses.

I repeated the above analysis for the free field Wilson propagator:

$$S(p)^{-1} = \sum_{\lambda} i\gamma_{\lambda} \sin p_{\lambda} + m + 2r \sum_{\lambda} \sin^2 \frac{p_{\lambda}}{2} \tag{2.17}$$

except that I have kept the quark mass nonzero. The unphysical energy has the following small energy and mass expansion:

$$\begin{aligned} E &= \log \frac{(r+1)}{(r-1)} + m - \frac{1}{2}rm^2 + \frac{1}{2}r^2m^3 - \frac{1}{6}m^3 \\ &+ \frac{(6r^3 + 6r - 6r^2m - 3m - 3r^4m)p^2}{24r^2} + O(a^4) \end{aligned} \tag{2.18}$$

which is complex when r is less than one. The physical energy dispersion relation for the Wilson free field propagator with r =1 is:

$$\begin{aligned} E^2 &= m^2 - m^3 + \frac{11}{12}m^4 - \frac{5}{6}m^5 \\ &+ (1 - \frac{2}{3}m^2 + \frac{7}{6}m^3)p^2 \\ &+ (-\frac{1}{3} + \frac{m}{4})((p^2)^2 + \sum_i p_i^4) + O(a^6) \end{aligned} \tag{2.19}$$

in the small mass and momentum limit, which agrees with the result in [19] when m = 0. For improvement it is interesting to note that the only O(a) correction to the continuum relation is a term of the form m^3; there is no mp^2 term.

2.4.3 The pion propagator in free field theory.

Although the last section provided some insight into the reflection positivity question, it was based on the free quark propagator, which is an unphysical object because it is not gauge invariant. The non-observation of individual quarks means

that problems with the quarks energy dispersion relation, or oscillations in its timesliced propagator do not necessarily provide any information about the physical spectrum of the lattice calculation.

For the above reasons, it is interesting to look at hadron correlators in free field theory, to try and and see the effects of the positivity violations. Because all the gauge fields are set equal to the unit matrix, the calculation can be carried out efficiently in momentum space, using the methods of chapter 5.

In figure 2.4.3, I have plotted the free field pion propagator with various values of the hopping parameters, for the Wilson action, using boundary conditions which were periodic in space and antiperiodic in time. The curves for kappa equal to one and two (both of which are above Lüschers bound of $\frac{1}{6}$), clearly show some kind of sickness compared to the ones for more sensible kappa values, at small times. It is difficult to blame the failure of reflection positivity for this behaviour, because if the energy state was complex then the correlator should have oscillations at all times. Because kappa values of this magnitude are unphysical and correspond to having negative masses in the free field theory case, problems with the pion propagator are not unexpected. The kink in the pion propagator for kappa equal to one and two, could just be due to excited states.

2.5 Conclusions.

In this Chapter I have tried and failed to show that the clover fermion action satisfies the reflection positivity condition. Conversely I have been unable to provide an argument to show that it violates the condition. In free field theory the clover term vanishes, and the Wilson and clover action's propagators are the same. Because the propagator of the Wilson action with r equal to one has the nice feature of having only one real energy solution, then this is also true for the clover action. This is a piece of evidence that supports the hypothesis that the clover action obeys the reflection positivity axiom. However a proof for the interacting theory is still required.

In temporal gauge the clover term only connects nearest-neighbour timeslices. This suggests that a well defined transfer matrix can be constructed. The problems I encountered with trying to prove the reflection positivity condition were due to the clover term being too symmetrical. A clover term centred in the t=0 hyperplane extends into both the $t > 0$ and $t < 0$ spaces, which makes the split up of

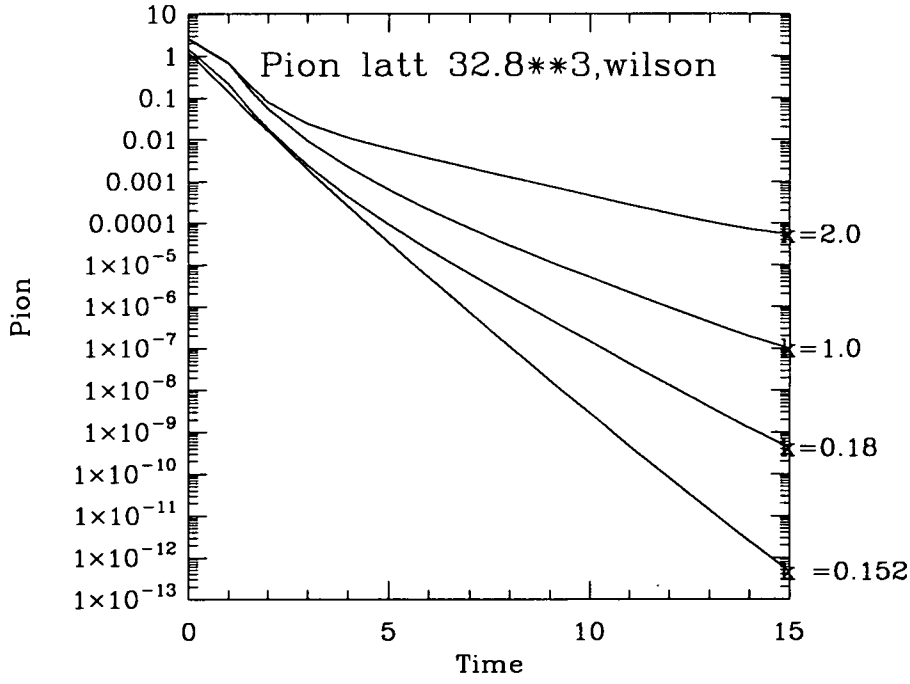

Figure 2.2: The pion propagator for the Wilson action in free field theory.

the functional integral into positive and negative time parts difficult. Unfortunately this is the key requirement in the proof of the reflection positivity bound in equation 2.2.

The construction of a transfer matrix or the proof of the reflection positivity bound will always be a problem with improved QCD lattice actions, because these actions typically involve terms that stretch over more than one time slice. The authors of [58] claim to have proved reflection positivity for a class of two link improved fermion actions, although this class includes the action that Parisi and collaborators had problems simulating, which they argued was due to reflection positivity violations.

The failure of the reflection positivity bound for an improved action should not cause too many problems, because the improved fermion actions are equal to the Wilson action with the addition of irrelevant operators. As the continuum limit is taken positivity should be restored, although there could still be problems with simulations.

Lüscher and Weisz developed a formalism to obtain a transfer matrix for improved pure lattice gauge theories, which have Lagrangians which contain terms that extend over two lattice sites [36]. The basis of their work is that the quantum field theory can be based on a wave function defined on a double layer of equal time hyperplanes. They guess a transfer matrix and obtain qualitative information about its eigenvalues, from which they conclude that two point correlators will always decay exponentially with time, but may have an oscillatory amplitude, due to the possibility of complex energies.

They also argue that for energies below some maximum, a new Hilbert space can be defined which has the property of strict positivity. It is an interesting question to try and find this maximum energy bound, because in the current studies of heavy quark systems, masses are extracted which are the same order of magnitude as the inverse of the lattice spacing. The method they suggest for estimating the maximum energy bound is to look for unphysical poles in the particle propagator in free field theory. Unfortunately for the clover action with r =1, there are no unphysical poles in the fermion propagator, so no estimate can be made.

3

The clover action at strong coupling.

3.1 Introduction.

In this chapter I will study the meson spectrum of the clover action with an arbitrary clover coefficient analytically, by using a strong coupling expansion. Because the meson masses will be known functions of the kappa value and the clover coefficient, this will provide some insight into the best choice of the clover coefficient, and help in comparing the numerical results of simulations which use slightly different forms of the clover action. I will try and find a good choice for the clover coefficient nonperturbatively, by using it to try and obtain a more rapid approach for the pion's energy dispersion relation to the continuum result of $E^2 = p^2 + m^2$.

The main problem is that the improvement idea is intrinsically a weak coupling concept. This is obvious from the fact that the coefficients of the irrelevant operators are series in the coupling constant g, which become undefined in the $g \rightarrow \infty$ limit. However the mass spectrum from the strong coupling expansion is not too bad [13]; the meson spectrum is approximately correct within 10% of experiment, so insight might be gained about continuum behaviour from this work.

The next section will explain the formalism of the strong coupling hopping parameter expansion used, as well as the extra combinatorial problems associated with having the clover term. After that I will present the meson spectrum for the clover action as a function of the clover term coefficient. The energy dispersion

relation for the pion at strong coupling will also be derived. This chapter will be rounded off by a discussion of how the calculation could be extended to the next order in the expansion.

Improved actions have been studied at strong coupling by a number of authors [6] [7], although no one as far as I am aware has studied the clover action.

3.2 Description of the expansion.

The starting point of this work is the calculation of arbitrary meson propagators by expanding the exponential of the lattice action in the inverse of the coupling constant squared and in the hopping parameter. By using the standard rules of group integration, expressions for the propagators can be built up as polynomials in κ and $\frac{1}{g^2}$. This is the analogue of the high temperature expansions used in statistical mechanics, which have been used in the lattice field since the beginning of the subject [8] [9]. The series in κ and $\frac{1}{g^2}$ have to be extrapolated beyond its radius of convergence using Padé ratios or other such pieces of magic.

Here I will follow a slightly different route, based on the ideas in [10] [12], and add another approximation to the g large and κ small approximation, namely a large N approximation. The exact expansion will be a simultaneous one in $\frac{1}{N}$ and $\frac{1}{Ng^2}$ around the $N \to \infty$ and $Ng^2 \to \infty$ limit. The large N approximation will simplify the number of surviving graphs so that the expansion in the hopping parameter can be summed up at every order in $\frac{1}{N}$ and $\frac{1}{Ng^2}$. To simplify the combinatorics I will work to the lowest order in the above expansion and also directly use the quenched approximation. As realistic large lattice QCD simulations are currently done using the quenched theory, I make no apologies for using it.

Working within the quenched approximation, I have to calculate the following meson propagator:

$$\langle 0 \mid \overline{\psi}^1_\beta(n)\psi^2_\delta(n)\overline{\psi}^2_\lambda(0)\psi^1_\alpha(0) \mid 0 \rangle = -\frac{\int \mathcal{D}U M_2(n,0)^{-1}_{\delta\lambda} M_1(0,n)^{-1}_{\alpha\beta} e^{-S_G}}{\int \mathcal{D}U e^{-S_G}} \qquad (3.1)$$

where S_G is the standard pure gauge action and M is the fermion matrix for the clover action defined in equation 1.36, and there is a hidden colour trace. The free indices in equation 3.1 are spinor indices, later in the calculation I will do a Fierz transformation to obtain the standard rho and pion propagators. I will only consider mesons made out of two flavours of quarks, imaginatively called 1 and 2.

At the Ng=∞ order in the expansion the pure gauge action has no effect on the quark dynamics. The meson bound states are produced by the integration of the gauge fields. The general rule for doing the integrations is that only SU(N) singlets are not zero. The standard expressions for the integrals of gauge fields are well known, for example:

$$\int \mathcal{D}U U_{ij} U^{-1}_{kl} = \frac{1}{N}\delta_{il}\delta_{jk} \tag{3.2}$$

In the large N limit expressions such as 3.2 are suppressed, the dominant terms will be ones with integrands which are proportional to the trace of the unit matrix in the gauge field space. In pictures, the surviving graphs are lines of the two fermion flavours bound together.

The kappa in front of the clover term in equation 1.36, breaks the direct correspondence between the number of quark links in the strong coupling graph, and the power of κ at the front of the analytical expression. Although this means that the direct use of random walk ideas cannot be used to sum up the hopping (and stopping!) expansion; the underlying theory of generating functions can do the summation.

I will now heuristically sketch the method used to sum up the hopping parameter expansion; a much more complete treatment is contained in appendix A. If the fermion matrix is rewritten symbolically as

$$M = 1 - \kappa D \tag{3.3}$$

then the integrand in equation 3.1 can be rewritten in the following way

$$M_1^{-1} \otimes M_2^{-1} = (1 - \kappa_1 D)^{-1} \otimes (1 - \kappa_2 D)^{-1} \tag{3.4}$$

where κ_1 and κ_2 are the kappa values of the two flavours of quarks. After expanding in κ, the following result is easy to derive

$$\frac{1}{1-\kappa_1 D}\frac{1}{1-\kappa_2 D} = \sum_{n=0}^{\infty}\sum_{m=0}^{n} D^{n-m} \otimes D^m \kappa_1^{n-m}\kappa_2^m \tag{3.5}$$

Consider one of the several independent surviving contributions to the expansion in equation 3.5. In the $N \to \infty$ limit, the resulting expression will be proportional to N times some gamma matrices. The fact that the integration over the gauge fields only produces a constant factor means that a general term in equation 3.5

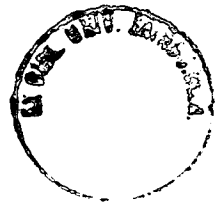

can be split up into a product of the smaller nonvanishing contributions. This suggests that a combinatorial generating function which produces all combinations of a small subset of the surviving graphs is required. The function:

$$D = \frac{1}{1-(S)t} \tag{3.6}$$

serves the purpose; the spinor indices have been suppressed, t is an arbitrary parameter which is set equal to 1 to sum the series, and S is the sum of the nonvanishing component diagrams. The above arguments are all generalisations of the use of random walk ideas and are firmed up in appendix A.

I will now discuss the small component diagrams in the expansion. The $D \otimes D$ terms have surviving graphs from two quark hopping from one site to the next. There are also surviving graphs from the gauge invariant part of the square of two clover terms. The $D^2 \otimes 1$ and $1 \otimes D^2$ terms also contribute to the generating function, because of the square of two clover terms. The $D^4 \otimes D$ and $D \otimes D^4$ terms produce extra graphs not included in those previously discussed, from quarks hopping around a single clover term. Although these graphs are of order (κ^5) compared to the previous set of graphs which are of order (κ^2), I have included them for consistency.

The above graphs produce a generating function of the form:

$$\begin{aligned} D^{-1}_{\alpha\beta,\delta\gamma} &= \delta_{\alpha\beta}\delta_{\delta\gamma}(1-a_1) \\ &- 4\kappa_1\kappa_2 \sum_{\mu} \left[(P^-_\mu)_{\alpha\beta}(P^+_\mu)_{\delta\gamma} e^{ip_\mu} + (P^+_\mu)_{\alpha\beta}(P^-_\mu)_{\delta\gamma} e^{-ip_\mu} \right] \\ &+ a_2 \sum_{\mu\nu} (\sigma_{\mu\nu})_{\alpha\beta}(\sigma_{\mu\nu})_{\delta\gamma} \end{aligned} \tag{3.7}$$

where $P^\pm_\mu = \frac{1}{2}(1 \pm \gamma_\mu)$ and the two constants a_1 and a_2 are defined as:

$$a_1 = \frac{3c^2}{8}(\kappa_1^2 + \kappa_2^2) \tag{3.8}$$

$$a_2 = \frac{c^2\kappa_1\kappa_2}{32} - \frac{c\kappa_1\kappa_2^4}{16} - \frac{c\kappa_1^4\kappa_2}{16} \tag{3.9}$$

The c variable is defined in equation 1.34, such that when c =0 the Wilson action is obtained and when c = 1 the original clover action is produced.

The final expression for the general meson propagator is:

$$G_{\alpha\beta,\delta\gamma}(n) = -N \int_p e^{ipn} D^{-1}_{\alpha\beta,\delta\gamma}(p) \tag{3.10}$$

The factor of N comes from the trace over colour, and can be absorbed in the fermion wave function renormalisation. I now follow the treatment of Kawamoto [10] and do a Fierz transformation on the propagator.

$$D_{\alpha\beta,\delta\gamma}(n) = \sum_{AB} D_{AB}(\Gamma_A)_{\alpha\gamma}(\Gamma_B)_{\beta\delta} \tag{3.11}$$

where Γ_A is one of the sixteen independent products of gamma matrices, which are normalised according to:

$$\text{trace}(\Gamma_A\Gamma_B) = \delta_{AB} \tag{3.12}$$

The connection between the standard meson operators and the general meson propagator obtained above is made by using:

$$\langle 0 \mid T\overline{\psi_n}\Gamma_X\psi_n\overline{\psi_0}\Gamma_Y\psi_0 \mid 0\rangle = \int_p e^{ipn}G_{XY} \tag{3.13}$$

where G_{XY} is defined by:

$$\sum_B D_{AB}G_{BC} = \delta_{AC} \tag{3.14}$$

The energy of the particle is obtained by looking for the zero eigenvalue in D_{AB}, when the four momentum is given by $p_\mu = (\underline{p}, iE)$.

3.3 Results.

In the pseudoscalar and axial vector sector, the coefficient matrix D_{PA} takes the form:

$$D_{PA} = \begin{pmatrix} 1 - 4\kappa_1\kappa_2\sum_\mu \cos p_\mu - 12a_2 - a_1 & 4\kappa_1\kappa_2 \sin p_\rho \\ -4\kappa_1\kappa_2 \sin p_\sigma & \delta_{\rho\sigma}(1 - 4\kappa_1\kappa_2 \cos p_\rho - a_1) \end{pmatrix} \tag{3.15}$$

Using the formalism in the previous section, the mass of the pseudoscalar particle for degenerate quarks is:

$$\cosh M_{PS} = 1 - \frac{(3\,\kappa^2c^2 - 4 + 16\,\kappa^2)(9\,\kappa^2c^2 - 12\,\kappa^5c + 128\,\kappa^2 - 8)}{16\,\kappa^2\,(15\,\kappa^2c^2 - 16 - 12\,\kappa^5c + 96\,\kappa^2)} \tag{3.16}$$

Kappa critical at strong coupling is obtained by requiring the mass of the pion to be zero, the approximate result being:

$$\kappa_c = \sqrt{\frac{1}{\frac{9}{8}c^2 + 16}} \tag{3.17}$$

	clover coefficient		
	c =0	c = 1	c = 1.4
$\kappa_{u,d}$	0.2493	0.2411	0.2339
κ_s	0.2345	0.2264	0.2193
$\kappa_{c\,HKSM}$	0.0836	0.076	0.071
$\frac{1}{a}$ MeV	876	835	800

Table 3.1: The hopping parameters and lattice spacing at strong coupling.

which is, as usual for strong coupling too large; Hamber and Wu [6] also found a small decrease in κ_c from the Wilson value of $\frac{1}{4}$, in their studies of a two link improved action.

For the vector particle, the coefficient matrix is:

$$D_{VT} = \begin{pmatrix} \delta_{\rho\sigma}(1 - a_1 - 4\kappa_1\kappa_2 \sum_{\mu\neq\rho} \cos p_\mu) & \frac{-4\kappa_1\kappa_2}{\sqrt{2}}(\delta_{\rho\delta} \sin p_\lambda - \delta_{\rho\lambda} \sin p_\delta) \\ \frac{4\kappa_1\kappa_2}{\sqrt{2}}(\delta_{\sigma\beta} \sin p_\alpha - \delta_{\sigma\alpha} \sin p_\beta) & \frac{1}{2}(\delta_{\alpha\gamma}\delta_{\beta\delta} - \delta_{\alpha\delta}\delta_{\beta\gamma})f \end{pmatrix} \tag{3.18}$$

where I have defined f as:

$$f = (1 - a_1 + 4a_2 - 4\kappa_1\kappa_2 cosp_\beta - 4\kappa_1\kappa_2 cosp_\alpha) \tag{3.19}$$

The final expression for the mass of the vector meson is:

$$\cosh M_V = 1 - \frac{(3\,c^2\kappa^2 - 4 + 48\,\kappa^2)(5\,c^2\kappa^2 + 4\,c\kappa^5 + 64\,\kappa^2 - 8)}{16\,\kappa^2\,(11\,c^2\kappa^2 + 96\,\kappa^2 - 16 + 4\,c\kappa^5)} \tag{3.20}$$

In the c=0 case, the above masses agree with the results originally derived by Wilson [9].

I will now present results for the meson mass spectrum, using the above general formulae for the vector and pseudoscalar particle masses. I have done this exercise for the three values for the clover coefficient used in numerical simulation: c=0, c=1, and c =1.4, although I have not used the fermion field rotations used by the UKQCD collaboration (see equation 1.49).

I first obtained the $\kappa_{u,d}$ hopping parameters by using the experimental value for the ratio of the pion and rho masses. Knowing this I obtained the lattice spacing using the experimental value of the rho mass. The hopping parameters for the strange and charm masses were obtained by using the masses of the kaon

and the J/ψ particles. This information allowed me to predict the masses in table 3.2.

The slight numerical discrepancy between my results and the ones in [13] for the Wilson action, occurs because there the lattice spacing was obtained by using the value of the rho mass at kappa critical ($\frac{1}{4}$).

It is difficult to give any error due to the truncation of the expansion at the lowest order; for the Wilson action the next order in the expansion only changed the results by 2%, however this correction was in the opposite direction to that required to improve agreement with experiment, so the results for this calculation should be viewed with some caution.

The results show that the value of the clover coefficient has only a small effect on the masses, with the trend being a slight drift towards the experimental value with increasing values of c. There are significant differences between the hopping parameters and the lattice spacings (in table 3.1) required to make the predictions, demonstrating that the clover term is not irrelevant at strong coupling.

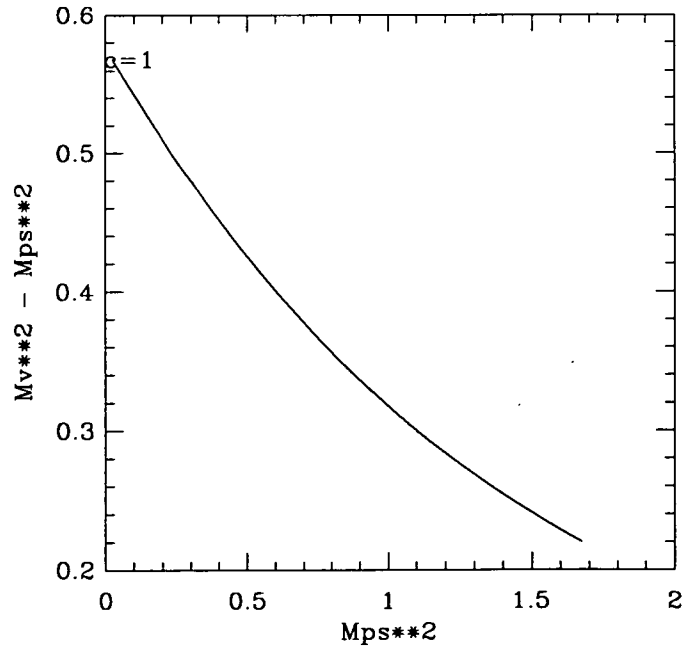

Figure 3.1: The vector pseudoscalar mass splitting for c = 1, the masses are in GeV.

In figure 3.1, I have plotted $M_V^2 - M_{PS}^2$ as a function of M_{PS}^2, experimentally this should be roughly constant. For $\beta \geq 6.0$, it has been found numerically that

	Mass in MeV			
	c = 0	c = 1	c = 1.4	experiment
$M_{K^\star}$	861	861	860	892
M_D	2042	2035	2030	1869
$M_{D^\star}$	2058	2053	2048	2010
M_{D_s}	2106	2099	2093	1969
$M_{D_s^\star}$	2120	2115	2110	2110
M_{η_c}	3096	3095	3094	2980

Table 3.2: The meson masses predicted from the strong coupling expansions.

$M_V^2 - M_{PS}^2$ is roughly constant for low pion masses [46], but begins to decrease as the quark masses enter the heavy quark region. The results from simulation also show that the clover action (with c= or c=1.4) predictions for the hyperfine splitting in the charmonium system is closer to the experimental result, than the Wilson action value is. My results at strong coupling show a decrease in $M_V^2 - M_P^2$ with increasing quark mass, with a curve which is the clover coefficient as it varies between 0 and 1.4, and there is no region of the curve where it is flat.

Using the Maple computer algebra package [75] I obtained the energy of the pion as a function of κ,c and one component of momentum, the result being too complicated to reproduce here. In figure 3.2, I have plotted the deviation of the energy dispersion relation from the continuum result as a function of momentum, for two values of the clover coefficient. The main result is that the Lorentz dispersion relation is rapidly broken even for very small values of momentum, with the Wilson action (perhaps surprisingly) having the smallest deviation. The only real conclusion is that the higher terms need to be calculated in the expansion. A previous strong coupling study [54] of the energy dispersion relation for the scalar glueball in four dimensional SU(2) lattice gauge theory, did not find any evidence for the restoration of the Lorentz energy dispersion relation, although this too could have been because the calculation had not been carried out to high enough order.

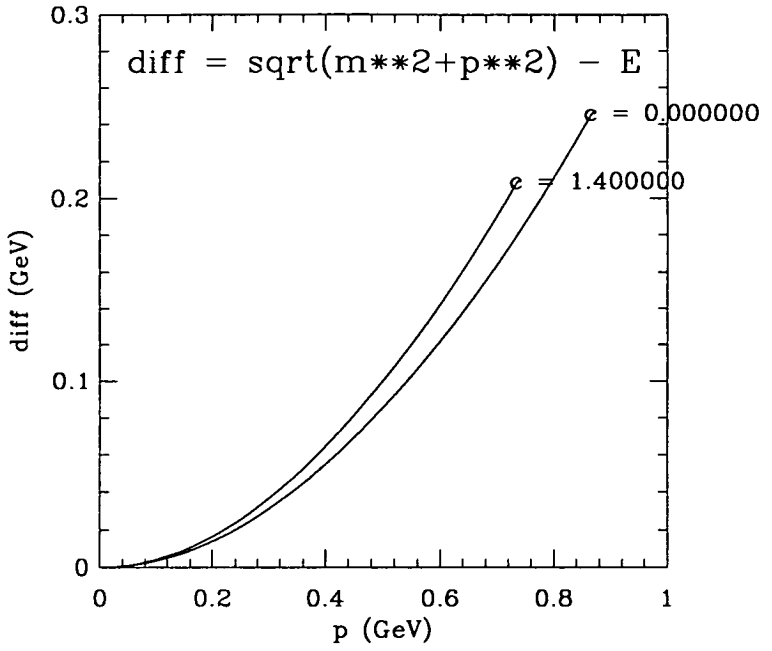

Figure 3.2: The deviation of energy dispersion relation from the continuum result for the pion, with kappa = 0.2.

3.4 Higher orders in the strong coupling expansion.

There is an intuitive reason for why the combinatorics of the strong coupling expansion for the clover action are complicated. There are nice geometrical pictures of strong coupling expansions; the expansion of the pure gauge action is an expansion in area, and the hopping parameter expansion for the Wilson fermion action is an expansion in one dimensional links. However the clover term complicates the picture as now the fermion action contains area like terms. The next order in the expansion for the Wilson action contains plaquette terms from the pure gauge action, being neutralised by the fermions hopping around them. The plaquette term in the clover action will make the combinatorics much more complex, although there is no physical reason why it could not be done.

The disappointing results for the energy dispersion relation obtained from this calculation, should be compared against the results from numerical simulation at weaker coupling, where for the lowest momenta the continuum result holds. This

offers the prospect of a higher-order strong coupling expansion seeing the possible improvement of the energy dispersion relation, with a certain value of the clover coefficient. The consistency of having a single adjustable parameter to improve the spectrum could be checked by comparing its effect on the energy dispersion relation of different particles such as the proton or the pion.

I note here that the useful technique of using effective hadron Lagrangians [11] to do these calculations, naively does not work here, because the clover term does not behave like a source for the gauge fields as the standard fermion gauge interaction terms do. This is a pity, because the effective Lagrangian approach provided a valuable check on the combinatorics of the strong coupling mass spectrum for the Wilson fermion action, and also because it was used in [55] to calculate the decay constants. If the method could have been used for the clover action, then qualitative information could have been obtained about the phenomenologically important f_D decay constant.

4

A calculation of the O(a) corrections to the vacuum polarisation diagram on the lattice.

4.1 Introduction.

So far the clover fermion action has only been studied numerically for the quenched theory. However quenched QCD is only a pragmatic approximation to the full theory, studied because full dynamical QCD simulations are so expensive computationally. It is important to find out whether the clover action is improved for full QCD, because dynamical calculations are carried out on smaller lattices, with large sea quark masses, and with large lattice spacings. These are exactly the conditions where an improved action might produce significantly better physics results.

Dynamical simulations require a lot of computer time, and any algorithmic advantage should be utilised to produce better simulations. The clover fermion action is an ideal candidate for an improved action to be used in simulations of full QCD, because it has only nearest-neighbour interactions, allowing the use of clever methods of speeding up the quark propagator inversions. However it is not clear that the clover action is actually an improved action for dynamical simulations, because as discussed in Chapter 1, it contains O(a) corrections at tree

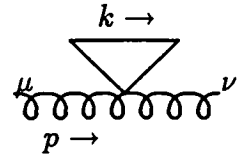

Figure 4.1: The tadpole vacuum polarisation diagram.

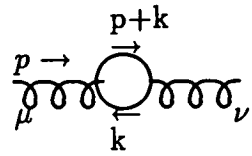

Figure 4.2: The vacuum polarisation diagram.

level. The field rotations in equation 1.49, which coupled with the clover action, produce a partition function with no O(a) corrections, only enter the functional integral coupled to external sources, so they have no effect on the evolution of the gauge configurations.

A crucial test of whether the clover action will be improved for dynamical simulations is to calculate a Feynman diagram containing fermion loops on the lattice, to look for O(a) terms, the natural choice of the diagram being the fermion contribution to the vacuum polarisation. In this Chapter, I will demonstrate that there are no O(a) corrections to the gluon vacuum polarisation diagrams in figures 4.1 and 4.2, for the clover action.

The calculation of lattice artifact corrections to Feynman diagrams is rather subtle, so the first part of this Chapter will discuss the meaning of improvement in weak coupling perturbation theory, and compare the procedure I used to other perturbative techniques. After that the lattice Slavnov-Taylor identities will be used to try and obtain some information about the lattice artifacts. Finally the methods and the results of the calculation will be presented.

4.2 O(a) effects in lattice perturbation theory.

The expansion of a lattice diagram as the continuum limit is taken, is crucial to the understanding of improvement in the context of weak coupling perturbation theory. Symanzik [20] suggested that a lattice diagram D would have the following asymptotic form as the lattice spacing was taken to zero:

$$D_{a\to 0} \sim a^{-\omega} \sum_{n=0}^{\infty} \sum_{m=0}^{l} c_{nm} a^n (log a)^m \tag{4.1}$$

where l is the number of loops in the diagram and ω is its naive degree of divergence. Symanzik originally proved the result for one loop diagrams in lattice Φ^4 theory, but he gave arguments for its general truth based upon his earlier work using the Pauli-Villars regulator method [30] . Lüscher and Weisz later gave a rigorous proof of equation 4.1 for lattices of finite volume [28].

For one loop lattice diagrams, equation 4.1 implies that the $a \log a$ terms will be the ones with the slowest convergence to the continuum limit; improvement in weak coupling perturbation theory corresponds to removal of these terms. In this work it turned out to be convenient to use dimensional regularisation, which means that equation 4.1 is modified [60], by using the traditional field theory rule of thumb:

$$\frac{1}{4-d} \longleftrightarrow \log(\Lambda) + \text{finite} \tag{4.2}$$

where Λ is the ultraviolet cut off, which is of the order of $\frac{1}{a}$ on the lattice, and d is the dimension of space-time.

4.3 Comparison with perturbative matching.

In this section, I want to emphasise the difference between the perturbative matching of operators evaluated on the lattice to continuum regularisation schemes[62], with the perturbative removal of O(a) effects.

As pointed out in chapter 1, matrix elements evaluated numerically, are in the lattice regularisation scheme. To make contact with experiment, a perturbative calculation must be done to convert the lattice matrix element into a continuum regularisation scheme such as $\overline{MS}$. The operator on the lattice evaluated between two states i and f is related to the basic operator by:

$$\langle O^a \rangle_{LATT} = O^0 (1 + \frac{\alpha_s}{4\pi}(-\gamma \log \lambda^2 a^2 + c_{LATT}) \tag{4.3}$$

with O^0 the matrix element of the bare operator, γ the one loop anomalous dimension of the operator, and c_{LATT} a constant. The λ parameter regulates the infrared divergences in the calculation. The corresponding equation for the matrix element in the $\overline{MS}$ scheme at a scale μ is:

$$\langle O^{\mu}\rangle_{\overline{MS}} = O^0(1 + \frac{\alpha_s}{4\pi}(-\gamma \log \frac{\lambda^2}{\mu^2} + c_{\overline{MS}}) \tag{4.4}$$

The above two results can be used to obtain the required connection between the lattice and the $\overline{MS}$ matrix elements:

$$\langle O^{\mu=\frac{1}{a}}\rangle_{\overline{MS}} = \langle O^a\rangle_{LATT}(1 + \frac{\alpha_s}{4\pi}(c_{\overline{MS}} - c_{LATT}) \tag{4.5}$$

For the calculation of O(a) terms in the fermion contribution to the vacuum polarisation diagram, no perturbative connection to the continuum is required. The diagrams will be calculated entirely on the lattice, and the lattice artifact terms extracted; these are terms which do not appear in the equivalent continuum diagram. This information could, if required, be fed back into changing the lattice action, as described in Chapter 1.

4.4 The vacuum polarisation diagram in QED.

In this section, I will compare the asymptotic expansion of a lattice Feynman diagram described by equation 4.1, to expansions of continuum diagrams, which naively look similar. To illustrate the point I will consider the vacuum polarisation diagram in continuum QED.

For QED the diagram in figure 4.2 is the only contribution to the vacuum polarisation of the photon. I will use the results in the book by Itzykson and Zuber [61]. They evaluate the continuum version of figure 4.2 in Minkowski space, using the Pauli-Villars method to regulate the divergences. The final result for the regularised vacuum polarisation diagram is:

$$\omega(k^2, m, \Lambda) = -\frac{2\alpha}{\pi}\int_0^1 d\beta(1-\beta)\{-\log\frac{\Lambda^2}{m^2} + \log[1 - \beta(1-\beta)\frac{k^2}{m^2}]\} \tag{4.6}$$

where Λ is the cut off, m is quark mass, and α is the QED coupling constant.

The finite part of equation 4.6 has an obvious expansion in $\frac{k^2}{m^2}$, which naively looks similar to O(a) corrections to lattice diagrams. I will now reproduce the standard argument to show that the finite parts of the diagram have physical consequences.

The one-loop vacuum polarisation diagram can be summed up into the self energy of the photon propagator, giving the new bare photon propagator:

$$iG_{\mu\nu} = \frac{g_{\mu\nu}}{k^2(1+\overline{\omega}(k^2))} + k_\mu k_\nu \text{terms}. \tag{4.7}$$

In QED the charge of the electron can be defined physically using Coulomb's law, which allows the renormalised photon propagator to be written in the form:

$$iG_{\mu\nu} = \frac{g_{\mu\nu}}{k^2(1+\overline{\omega}(k^2)-\overline{\omega}(0))} + k_\mu k_\nu \text{terms}. \tag{4.8}$$

To see the physical effect of the finite part of the vacuum polarisation diagram, I will now consider its effect on Coulomb's law. After expanding equation 4.8 in $\frac{k^2}{m^2}$, Coulomb's law in momentum space gets modified to:

$$\frac{e^2}{k^2} \rightarrow \frac{e^2}{k^2}(1 - \frac{\alpha}{15\pi}\frac{k^2}{m^2}) \tag{4.9}$$

In configuration space Coulomb's laws is changed to:

$$V(r) = -\frac{Ze^2}{4\pi r} - \frac{\alpha}{15\pi}\frac{Ze^2}{m^2}\delta^3(\underline{r}) \tag{4.10}$$

for an infinitely heavy nucleus of charge -Ze. The delta function produces a small shift in the energy levels of s-wave states for the solution of the hydrogen atom in Dirac's relativistic theory.

The above example has shown that the expansion in $\frac{k^2}{m^2}$ has produced physical effects. However this should already be included in the equivalent lattice diagram, because the Feynman rules on the lattice agree with the continuum as the lattice spacing tends to zero.

4.5 Slavnov-Taylor identities on the lattice.

In the continuum the Slavnov-Taylor identities constrain the structure of the gluon vacuum polarisation diagram. Similar constraints exist on the lattice. However the lower symmetry of the hypercubic lattice compared to the continuum makes them more complicated. I will now discuss whether the Slavnov-Taylor identities on the lattice will help my calculation of the O(a) corrections to the vacuum polarisation diagram.

In the continuum, Lorentz invariance of the theory constrains the tensor structure of the gluon vacuum polarisation tensor in momentum space to have the

form:

$$\Pi^{ab}_{\mu\nu} = (Ap_\mu p_\nu + B\delta_{\mu\nu})\delta^{ab} \tag{4.11}$$

where a and b are colour indices. The Slavnov-Taylor identities can be used to relate the A and B functions. On the lattice the hypercubic symmetry constrains the vacuum polarisation to have the form:

$$\Pi^{ab}_{\mu\nu} = (\delta_{\mu\nu}\sum_{i=0}^{\infty} a_i p_\mu^{2i} + \sum_{i,j=0}^{\infty} b_{ij} p_\mu^{2i+1} p_\nu^{2j+1})\delta^{ab} \tag{4.12}$$

Because I am considering O(a) corrections, I only need to consider the expansion in equation 4.12 up to $O(p^2)$ terms. Kawai and collaborators [29] proposed a general form (up to $O(p^2)$), of the gluon vacuum polarisation tensor:

$$\Pi^{ab}_{\mu\nu} = (c_1\delta_{\mu,\nu} + c_2\delta_{\mu\nu}p_\mu^2 + f_1\delta_{\mu\nu}\sum_\lambda p_\lambda^2 + f_2 p_\mu p_\nu)\delta^{ab} \tag{4.13}$$

where c_1 is a quadratically divergent constant, and c_2, f_1 and f_2 are logarithmically divergent functions of the invariants of the theory. They used equation 4.13 in an identity obtained from the BRS invariance of the lattice action to produce the following relations:

$$c_1 = 0, c_2 = 0, f_1 = -f_2$$

Their final result for the gluon vacuum polarisation tensor, has essentially the same structure as in the continuum:

$$\Pi^{ab}_{\mu\nu} = \left[(\delta_{\mu\nu}\sum_\lambda p_\lambda^2 - p_\mu p_\nu)f_1 + O(p^4)\right]\delta^{ab} \tag{4.14}$$

when only O(a) corrections are considered.

By dimensional analysis, the only possible term that can produce an O(a) lattice artifact, is a correction to the f_1 constant which is proportional the quark mass. Gauge invariance does not give any information about its coefficient, which can only be determined from a weak coupling perturbation theory calculation. The continuum expression for the vacuum polarisation diagram in equation 4.6 does not contain such a term, showing that it is a lattice artifact. The rest of this Chapter will describe the calculation of the O(m) term in the f_1 constant in equation 4.14.

Although I have shown that the lattice analogues of the Slavnov-Taylor identities have not provided any way to estimate the magnitude of the mp^2 term, they

could serve another valuable purpose. In their studies of lattice QED Kenway and de Souza [59] used the expression in equation 4.12, in a Ward identity to obtain relations between the a_i and b_{ij} coefficients. If their arguments could be generalised to QCD, then it could provide a nonperturbative method of improvement, because higher-order lattice artifacts could be summed up in some way.

4.6 Description of the method.

The calculation of Feynman diagrams which contain loops is very difficult on the lattice, because there is much less symmetry compared to the corresponding continuum integral. The fact that the integral is over a finite hyper-cube, means that standard continuum tricks such as Feynman parameters are less straight forward to use. All the standard techniques, which are used on the lattice to calculate integrals, require at some stage taking the $a \rightarrow 0$ limit, which is obviously unacceptable for extraction of O(a) corrections.

Heatlie and collaborators [18] obtained the O(a) corrections for the clover action vertex function and fermion self energy, using the Pauli Villars method, but their method is difficult to understand and they did not complete the calculation by evaluating the $O(ag^2)$ terms.

The vacuum polarisation diagram for a two-link improved action was calculated by Wohlert and Sheikholeslami [19], by calculating the integrals for varying external momentum and fitting the result to a function suggested by asymptotic estimates of the integrand. However they worked at zero quark mass, which is unacceptable when trying to extract O(a) corrections. To use their approach would require fitting the diagram to a function containing both external momentum and quark mass. As log terms are also expected, their technique was not good enough for my purposes.

The technique I used is due to Symanzik [20]which allows a clean calculation of O(a) effects. Symanzik used the method in his studies of improved scalar lattice field theory, and Eguchi and Kawamoto [17]used it to evaluate the one-loop improvement coefficients for a two-link improved action.

The basic idea is very simple; the diagram is expanded in external momentum

and quark mass, about their zero values:

$$I(p,m)_{\mu,\nu} = I(0,0)_{\mu,\nu} + m\frac{\partial I(p,m)_{\mu,\nu}}{\partial m}\mid_{p=0,m=0} + p_\lambda \frac{\partial I(p,m)_{\mu,\nu}}{\partial p_\lambda}\mid_{p=0,m=0} + \cdots \tag{4.15}$$

The coefficients are integrals over the internal momentum only and are regulated by dimensional regularisation. Consider one of the coefficients in the above expansion:

$$C = \int_{-\pi}^{\pi} \frac{d^4k}{(2\pi)^4} F(k) \tag{4.16}$$

Physically, we know that because we are working on a lattice, the UV divergences of the diagrams have been cured. This implies that the problems with the coefficients occur in the infrared region, when $k \to 0$. To regulate these divergences Symanzik used the following useful result:

$$\int_{-\infty}^{\infty} \frac{d^{4+\epsilon}k}{(2\pi)^{4+\epsilon}} \frac{1}{k^n} = 0 \quad \forall n \tag{4.17}$$

from dimensional regularisation [21].

By adding in equation 4.17, with a value of n equal to the leading infrared divergence of the function F, to equation 4.16 the $k \to 0$ divergence can be regulated. The new expression for coefficient is:

$$C = \int_{-\pi}^{\pi} \frac{d^{4+\epsilon}k}{(2\pi)^{4+\epsilon}} (F(k) - \frac{1}{k^n}) - \int_{\text{Outside Brillouin zone}} \frac{d^{4+\epsilon}k}{(2\pi)^{4+\epsilon}} \frac{1}{k^n} \tag{4.18}$$

For n > 4 in equation 4.18 then the outer integral is well defined and can be computed numerically in four dimensions. The interesting case is n=4, where the outer integral produces a pole in ϵ. I will extract the pole by using the following relation:

$$\int_{\text{Outside Brillouin zone}} \frac{d^{4+\epsilon}k}{(2\pi)^{4+\epsilon}} \frac{1}{k^4} = \frac{1}{2}(\frac{1}{2\pi})^2 \frac{1}{-\epsilon} + a_0 + O(\epsilon) \tag{4.19}$$

where a_0 is well-defined constant which can be computed using the rules of dimensional regularisation. In appendix B, I show that a_0 = -0.010744.

4.7 Details of the calculation.

The integral for the Feynman diagram in figure 4.2 is:

$$I(p)^{AB}_{\mu,\nu} = -\int_{-\pi}^{\pi} \frac{d^4k}{(2\pi)^4} \text{trace}(V^A_\mu[k, p+k]S[p+k]V^B_\nu[p+k, k]S[k]) \qquad (4.20)$$

and the integral for the tadpole diagram in figure 4.1 is:

$$I(p)^{2A}_{\mu,\nu} = -\delta_{\mu\nu}\int_{-\pi}^{\pi} \frac{d^4k}{(2\pi)^4} \text{trace}(V^{2A}[k]S[k]) \qquad (4.21)$$

where V^A_μ is the gauge fermion interaction and S is the standard Wilson propagator, and the -1 at the front of the integrals is required because of fermi statistics. The A and B indices are meant to represent the clover (I) or Wilson (W) vertices, which will allow the contributions from the two actions to be distinguished. I shall use the Feynman rules given in [18] and [32]; although gauge fixing is not important to this calculation, I will work in Feynman gauge.

The fermion part of the vacuum polarisation diagram for the Wilson action has been calculated by Kawai and collaborators [29] using massless quarks. However because I need to work at finite quark mass, that work was not very useful to me. To simplify the gamma matrix algebra, I summed over the μ and ν indices. The disadvantage of doing this is that equation 4.14 could not be used to check the calculation. The O(a) correction is now of the form mp^2. Using Symanzik's method, the calculation of the key lattice artifact term mp^2 is independent of the rest of the diagram, so I concentrated on extracting its coefficient from the integral in equation 4.20.

The tadpole from the clover term vanishes when the trace over the gamma matrices is calculated. The tadpole from the Wilson term is independent of the gluon momentum, so does not contribute to the mp^2 term. The Wilson tadpole diagram is required to cancel with the zero external momentum diagram in figure 4.2, so that the gluon is not given a mass, which would break gauge invariance.

I will now describe the calculation of the coefficient of the mp^2 term in equation 4.20. I first evaluated the trace algebra by hand and coded the resulting integrands into the Maple computer algebra package [75]. The integrands were then checked numerically against integrands made from the clover rules using a specific representation of gamma matrices, coded in a separate computer program. The following simplification was found after the trace algebra was calculated

$$\sum_\mu I^{WI}_{\mu\mu} = \sum_\mu I^{IW}_{\mu\mu} \qquad (4.22)$$

The Maple package performed the Taylor expansions to extract the mp_1^2 (p_1 is the first component of the momentum) terms and their leading infrared divergences. The resulting expressions were regulated, if required, and then converted into Fortran routines, which were used in the adaptive Monte Carlo integration routine VEGAS [31], to produce the finite parts of the mp_1^2 terms. I repeated the calculation for the mp_2^2 term and obtained the same results for the pole and finite parts of the diagram, within the statistical errors of the Monte Carlo integration. Another test was to repeat the extraction of the pole parts of the mp_1^2 term in 4.20, after first rescaling the external momentum and the quark mass by one half, to check that the final answer was divided by one eighth.

An important point concerning the use of Maple in this calculation was that the Taylor expansions were evaluated with specifically indexed momentum such as $p_1, p_2, k_1, \ldots$ etc, which basically corresponds to working in four dimensions. The final results for the infrared divergences were reconverted into covariant notation. Strictly speaking this is not allowed in dimensional regularisation, because one of the consequences of a continuous "spatial dimension", is that the vector space has to have an infinite number of dimensions. However unlike in the calculation of trace algebra, no extra factors of ϵ are picked up in the manipulations, so the procedure is legitimate.

4.8 Results.

The coefficients of the mp^2 term in the integral in equation 4.20 are summarised in tables 4.2 and 4.1, where I have factored out the number of fermion flavours f, the group theory factor of $\frac{\delta^{ab}}{2}$, the minus one for the internal fermion loop, the square of the coupling constant, and the trace of the unit Dirac gamma matrix. The results in table 4.2 coupled with equation 4.2 show that the clover action does not produce an $O(ag^2 \log a)$ term (which using $g^2 \sim \frac{1}{\log a}$ is effectively an O(a) term) contribution to the gluon vacuum polarisation diagram. This contrasts with the Wilson action, which does produce an $O(ag^2 \log a)$ correction. The results of this perturbative calculation suggest that the clover action is improved for dynamical fermion simulations.

As a by-product of this calculation the finite parts of the mp^2 terms can be used to estimate the value of the clover coefficient, such that there is no $O(ag^2)$ correction to the vacuum polarisation. The required value of the clover coefficient

Vertex A	Vertex B	Diagram $g^2\frac{-\delta^{ab}}{2}$ f trace(1)
Pauli	Pauli	-0.010781 ± 0.000082
Pauli	Wilson	-0.019275 ± 0.000072
Wilson	Pauli	-0.019275 ± 0.000072
Wilson	Wilson	0.03750 ± 0.00022
Total	Total	-0.01183 ± 0.00026

Table 4.1: Finite parts of the m.p_1^2 terms in the expansion of the clover vacuum polarisation, inside the Brillouin zone.

Vertex A	Vertex B	Diagram $g^2\frac{-\delta^{ab}}{2}$ f trace(1)
Pauli	Pauli	0
Pauli	Wilson	$-\frac{3}{2}(a_0+\frac{1}{2}(\frac{1}{2\pi})^2\frac{1}{-\epsilon})$
Wilson	Pauli	$-\frac{3}{2}(a_0+\frac{1}{2}(\frac{1}{2\pi})^2\frac{1}{-\epsilon})$
Wilson	Wilson	$+3(a_0+\frac{1}{2}(\frac{1}{2\pi})^2\frac{1}{-\epsilon})$
Total	Total	0

Table 4.2: Pole parts and the finite terms outside the Brillouin zone for the m.p_1^2 terms in the expansion of the clover vacuum polarisation.

c, can be obtained by solving the following quadratic equation:

$$0.010781c^2 + 0.03855c - 0.03750 = 0 \tag{4.23}$$

The result is c = -4.371 and c = 0.796, which contrasts badly with the one loop improvement condition of Wohlert [32] of:

$$c = 1 + 0.26590(7)g^2 \tag{4.24}$$

and the mean field value obtained by the Fermilab group of 1.4 [48]. It is probably only legitimate to compare Wohlert's result to mine, because the Fermilab group claim to have taken into account higher order effects in their calculation, which I do not claim to have done. The discrepancy between Wohlert's result and mine is probably due to the use of different improvement conditions, obvious from the fact that Wohlert's result depends on the coupling constant while mine does not. The $O(ag^2)$ corrections to the vacuum polarisation diagram due to fermion loops should really be eliminated by the adjustment of the parameters in the pure gauge action.

The clover action is only on-shell improved, because it contains O(a) terms at tree level. The claim is, that it has no O(a) corrections to physical masses. Wohlert used twisted boundary conditions in his work so that he could calculate an on-shell quantity in weak coupling perturbation theory, and chose the value of the c coefficient to remove the $O(ag^2)$ corrections from it. Because the clover action has O(a) terms in its Feynman rules, it is probably inconsistent with the concept of on-shell improvement to chose a value for c, so that the $O(ag^2)$ terms are removed from an individual Feynman diagram.

5

Hadron spectrum calculations

In this Chapter I will report the results from a number of different hadron spectrum calculations on the lattice. The next section will contain the results of a calculation of the mass spectrum of P-wave mesons from numerical simulations. The second section will include a calculation of the QCD coupling constant. The final section will contain some analysis of particles at finite momentum on the lattice, including: the energy dispersion relation for various particles and a calculation of the pion decay constant from the spatial components of the axial current.

The methods and details of the numerical simulations are briefly reviewed in Chapter 1.

5.1 P-wave mesons on the lattice.

Most quenched lattice simulations concentrate on measuring the properties of a few particles selected from the hordes known experimentally. The familiar old friends of the lattice community are the pion, proton, and the rho (and the equivalent heavy particles); which the quark model describes as S-wave states. At this stage in the attempt to fully solve QCD numerically, it is appropriate to study a small subset of particles to try and study the systematics of the computations. But it is nice to take a sneak look ahead to see lattice gauge theory fulfil its destiny of predicting all of QCD, by looking at a slightly different set of particles.

The particles I will study on the lattice will be P-wave mesons. Specifically I will look at the a_0, a_1, and the b_1 mesons at light quark mass; and the χ_{c0}, χ_{c1}, and h_c P-wave mesons in the charmonium spectrum. Apart from purely spectroscopic

issues concerning these particles, there are other interesting questions to ask; for example there is some debate over whether the a_0 particle is a genuine $q\overline{q}$ state or some kind of bound state of two kaons [74]. However, in this work I will concentrate on extracting the masses and mass splittings.

There is a theoretical argument [33] [88] to show that the signal for P-wave mesons will be noisier than S-wave states. Consider a correlation function:

$$c(t) = \langle 0 \mid O^{\dagger}(t)O(0) \mid 0 \rangle \tag{5.1}$$

where I have suppressed any dependence on position. As $t \rightarrow \infty$ the excited states die away and the correlation function behaves like:

$$c(t) \sim \mid \langle 0 \mid O \mid M \rangle \mid^2 e^{-E_M t} \tag{5.2}$$

where M labels the particle with the lowest mass with the same quantum numbers as the operator O. The fluctuations in the correlator are measured by:

$$\sigma^2 = \frac{1}{N}(\langle 0 \mid (O(t)^{\dagger}O(0))^2 \mid 0 \rangle - C(t)^2) \tag{5.3}$$

The first term in equation 5.3 will dominate because the lightest state in that channel is the two pion state. The final result is an asymptotic formula for the signal to noise ratio:

$$\frac{c(t)}{\sigma} \sim e^{-(E_M - M_\pi)t} \tag{5.4}$$

where m_π is the pion mass. Because P-wave mesons have typically larger masses than their S-wave counterparts, equation 5.4 shows that their signal will fall off more rapidly into the noise.

A number of lattice gauge theory simulations have extracted the masses of P-wave mesons, some more successfully than others. The APE collaboration claim to see some signal for the a1, b1 and a0 particles, using the operators in table 1.2 at a β value of 5.7 [15]. However at $\beta = 6.0$, they only claimed to have a signal for the a1 particle, in their simulations of Wilson fermions.

DeGrand and Hecht [33] use a method based upon the quark model ideas, to extract both P-wave baryon and meson masses. They construct quark wavefunctions with the correct dumb-bell-like shape and combine them with nonrelativistic spinors (constructed from the upper two components of a dirac spinor), using the same ideas as in the quark model. Their approach requires the use of gauge fixing. It is difficult to produce a clean separation of spin and spatial wave functions in lattice calculations, which are essentially based upon relativistic considerations.

The Fermilab group [48] have also extracted heavy quark P-wave masses from a simulation of the mean field improved clover action. To enhance their signals they used suitably chosen wavefunctions, with the standard fermion bilinears. They successfully extracted the mass splitting between the h_c and χ_{c0} particles, and obtained a value for the 1P-1S splitting.

Lepage and Thacker [57] numerically obtained the masses of P-wave mesons comprising charm and beauty quarks in a simulation of nonrelativistic QCD. Davies and Thacker [76] obtained the mass splittings between S-wave and P-wave mesons in a simulation of Upsilon spectroscopy, using a nonrelativistic QCD action.

5.1.1 The 1P-1S mass splitting.

The mass splitting between the S-wave and P-wave mesons is an extremely important quantity for heavy quark lattice simulations. In this section I will explain why this is true.

Experimentally, the splitting between the P and S wave mesons is approximately the same for both the ψ and Υ families of mesons, suggesting that it is insensitive to the mass of the heavy quark. This behaviour is also predicted by potential model calculations [47]. This is good for lattice simulations because the $M_{1P} - M_{1S}$ splitting should be accurately predicted without the need for any complicated tuning of kappa values.

Lepage and Thacker obtained a consistent value for the s-p splitting for the beauty and charm meson systems, from a simulation of nonrelativistic QCD. Davies and Thacker also obtained a consistent value for the spin averaged s-p spitting in a simulation of nonrelativistic QCD at $\beta = 6.0$, using two quark masses with the same order of magnitude as the b quark mass. Using a mean field improved clover fermion action, the Fermilab group went one step further and used the value of the $M_{1P} - M_{1S}$ splitting to obtain the lattice spacing in their simulations (using an unspecified kappa value), because of their faith in this quantity.

The Fermilab lattice group [49] define the 1P-1S splitting in the charmonium system by:

$$M_{1P} - M_{1S} = M_{h_c} - \frac{3M_\psi + M_{\eta_c}}{4} \tag{5.5}$$

To motivate equation 5.5, I will follow Lepage's [47] suggestion, and use potential model ideas. In the heavy quark region, the large mass of the quarks

makes the dynamics essentially nonrelativistic. This allows the calculation of a large number of properties of the charmonium and upsilon mesons, based upon using the Schrödinger equation with a suitable potential (a Coulomb plus linear term being the simplest).

In a simple potential model calculation of the charmonium spectrum, the spin-spin interaction is put in perturbatively; the mass of the S-wave meson would be:

$$M = M_0 + \mathcal{A}\langle \underline{S_1}.\underline{S_2} \rangle \tag{5.6}$$

where M_0 is the eigenvalue of the Schrödinger equation for the given potential used, and $\mathcal{A}$ is the expectation value of the rest of the hyperfine operator once the two quark spin operators S_1 and S_2 have been factored out. It is important to remember that although the spin-spin interaction is suggested by analogy with the QED based dynamics in positronium, it is intrinsically a QCD effect, because the phenomenology of these splittings in hadron physics requires the trace of two SU(3) generators in the $\mathcal{A}$ term 1.3. Using equation 5.6 and the standard rules of the combination of angular momentum the following formulae can be obtained for S-wave mesons:

$$\frac{M_{S_1^1} + 3M_{S_1^3}}{4} = M_0 \tag{5.7}$$

which partially motivates equation 5.5.

The use of equation 5.5 should cancel out some O(a) effects in the S-wave mesons. The concept of on-shell improvement for the clover action suggests that all O(a) effects can be eliminated from the lattice action by a suitable choice of the coefficient of the clover term. Because the clover term is a QCD like magnetic moment, the effect of its coefficient is likely to show up in spin-spin splittings, which therefore will be sensitive to O(a) artifacts. This suggests that the J/ψ - η_c mass splittings will be sensitive to O(a) effects, a picture which has been confirmed in the numerical simulations of the Fermilab [48] and UKQCD groups [46]. The 1P-1S splitting should be less sensitive to O(a) effects and to the choice of the Wilson or clover action.

5.1.2 Numerical Results.

The operators used for all the P-wave mesons studied are in table 1.2. I will first deal (fairly rapidly) with the results from simulation for the a0, a1, and b1 particles. I looked at the P-wave channels for a simulation of the rotated clover

action at $\beta = 6.2$ on a $24^3 \times 48$ lattice using 18 gauge configurations. Results for the pion, rho, nucleon, and delta from the same simulation have been reported in [16]. At kappa equal to 0.14144 there was a very poor signal for the a1 and no signal for the a0 or b1. There was no signal for any of the a0, a1, or b1 at the kappa value of 0.14280.

I will now report initial results for the 1P-1S wave splitting in charmonium obtained from a quenched simulation, using the rotated clover action. The data was from 16 configurations. The β value was 6.2 and the lattice size $24^3 \times 48$. Other details of the simulation are described in chapter 1. The heavy quark propagators were generated using smeared sources and local sinks. The smearing used was gauge invariant Jacobi [73] using 50 iterations with a kappa scalar of 0.25, which corresponds to a smearing radius of four. Four kappa values were used: 0.133, 0.129, 0.125, and 0.121.

I chose the fit region 7, 9, and 11 (and the points on the opposite side of the lattice), because there was a plateau in the effective mass. The effective masses were generally fairly noisy. In figure 5.1 I have plotted the 1P-1S wave splitting as a function of the square of the pseudoscalar particle mass; the data used to make the plot is in table 5.1.

The first impression from figure 5.1 is that the 1P-1S splitting does depend on the quark mass. However this could be slightly misleading. If the lowest quark mass point (with a mass below the charm value) is ignored, the remaining three points are roughly constant within statistical error. Although I have tried to chose a good fit region for all four kappa values, the $\frac{\chi^2}{dof}$ in table 5.1 for the two higher kappa values look suspiciously small. It will be interesting to see how the results change as the statistics increase.

5.1.3 P-wave mesons from local operators.

I will now report results from simulation for heavy quark P-wave mesons obtained from purely local operators on the lattice. The main surprise is that a good signal is obtained. This seems to completely contradict the intuition provided from the nonrelativistic quark model.

The numerical results were obtained from a $\beta = 6.2$ quenched simulation on a $24^3 \times 48$ lattice, using 18 propagators, for both the clover and Wilson actions. The quark propagators were generated using local sources and sinks. The kappa

Particle	κ	$\frac{\chi^2}{dof}$	mass (In lattice units)
Pseudoscalar	0.133	0.81/4	$0.8499\ ^{+34}_{-38}$
Pseudoscalar	0.129	1.73/4	$1.060\ ^{+3}_{-4}$
Pseudoscalar	0.125	4.03/4	$1.256\ ^{+3}_{-3}$
Pseudoscalar	0.121	7.34/4	$1.441\ ^{+4}_{-3}$
vector	0.133	1.94/4	$0.8744\ ^{+44}_{-47}$
vector	0.129	2.69/4	$1.079\ ^{+4}_{-4}$
vector	0.125	4.8/4	$1.271\ ^{+4}_{-4}$
vector	0.121	7.97/4	$1.454\ ^{+4}_{-4}$
h_c	0.133	1.81/4	$1.021\ ^{+13}_{-8}$
h_c	0.129	2.84/4	$1.220\ ^{+14}_{-8}$
h_c	0.125	3.45/4	$1.411\ ^{+14}_{-9}$
h_c	0.121	4.05/4	$1.594\ ^{+13}_{-10}$

Table 5.1: Spectrum results for the 1P-1S mass splitting calculation.

κ	1P-1S splitting (In lattice units)
0.133	$0.1531\ ^{+119}_{-74}$
0.129	$0.1463\ ^{+120}_{-72}$
0.125	$0.1440\ ^{+120}_{-82}$
0.121	$0.1429\ ^{+117}_{-94}$

Table 5.2: Spectrum results for the 1P-1S mass splitting calculation.

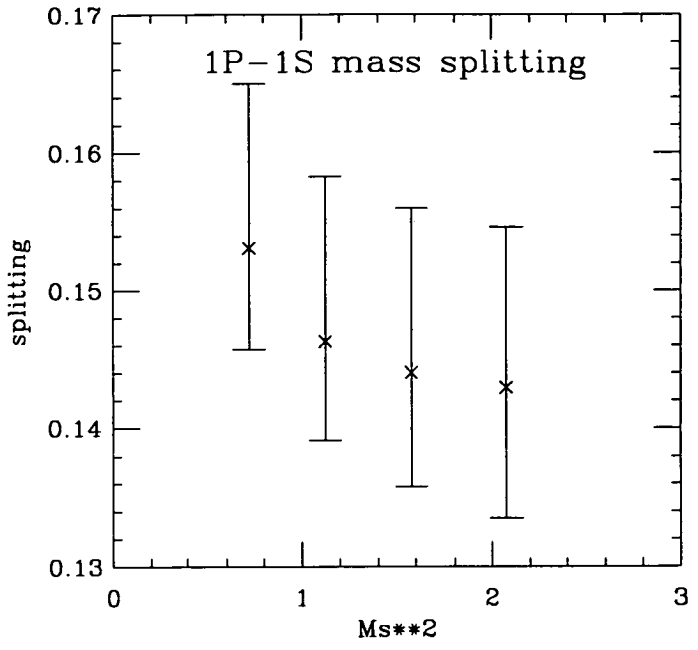

Figure 5.1: The 1P-1S wave splitting plotted against $M_{\eta_c}^2$

value used for the Wilson action simulation was 0.133, and the kappa value for the rotated clover action was 0.129; these values were chosen so that they roughly corresponded to the charm quark mass. Further details of the simulation can be found in [46], where a detailed analysis of the masses and decay constants of the J/ψ and the η_c particles can be found.

To demonstrate that good signals for P-wave mesons are obtained, I have plotted the effective mass for the h_c particle from the clover action simulation in figure 5.2. I used the same fit range for the vector and pseudoscalar particles as in [16]. When I tried the same fit region for the P-wave mesons, the χ^2/dof were unacceptable large ($\sim$ 6 for the χ_{c1} particle). A further investigation of the fit regions revealed a difficulty in obtaining a fit region where simultaneously for all three particles and for both actions, a χ^2/dof of less than two was obtained from every fit. The eventual fit region I chose had low χ^2/dof for all six possible fits. I also looked at the mass splittings, by fitting to the ratios of the two propagators, the results are in tables 5.5 and 5.6.

Because the quark masses used in the simulations are approximately the same as the charm quark mass, I have used the value of the lattice spacing $\frac{1}{a}$

Particle	$\frac{\chi^2}{dof}$	m.a	m (MeV)	Expt mass(MeV)
h_c	0.28/4	$1.263\ ^{+24}_{-27}$	$3448\ ^{+66}_{-74}$	3526
χ_{c0}	1.5/4	$1.237\ ^{+23}_{-21}$	$3377\ ^{+63}_{-57}$	3415
χ_{c1}	0.7/4	$1.262\ ^{+22}_{-23}$	$3445\ ^{+60}_{-63}$	3511
η_c	10/6	$1.066\ ^{+6}_{-4}$	$2910\ ^{+16}_{-11}$	2980
J/ψ	9.8/6	$1.076\ ^{+4}_{-5}$	$2937\ ^{+11}_{-14}$	3096

Table 5.3: The charmonium mass spectrum predicted by the Wilson action with $\kappa = 0.1330$, on 18 configurations. m is the result from the simulation and a is the lattice spacing.

= 2.73(5)GeV obtained from the string tension [16], to convert the results into physical units. The error in the 1P-1S splitting was obtained using the bootstrap method.

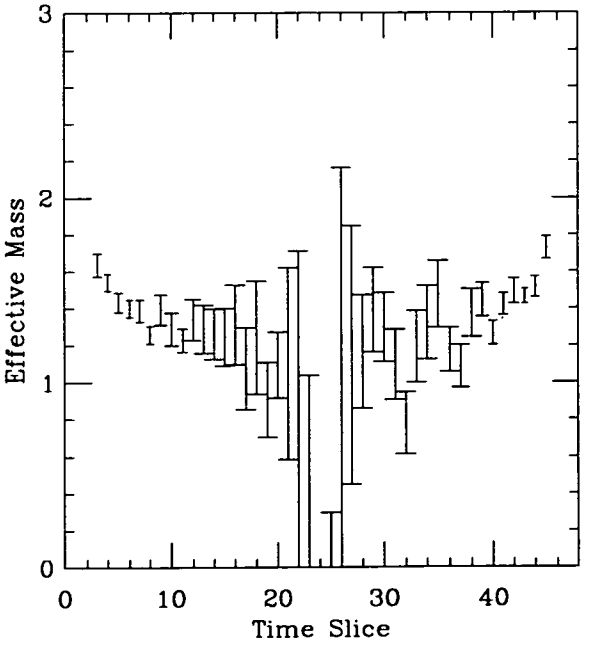

Figure 5.2: The effective mass plot for the h_c particle. The clover action with kappa = 0.129

Particle	$\frac{\chi^2}{dof}$	m.a	m (MeV)	Expt mass (MeV)
h_c	0.8/4	$1.300\ ^{+49}_{-50}$	$3549\ ^{+134}_{-137}$	3526
χ_{c0}	3.9/4	$1.235\ ^{+40}_{-26}$	$3372\ ^{+109}_{-71}$	3415
χ_{c1}	1/4	$1.290\ ^{+30}_{-35}$	$3522\ ^{+82}_{-96}$	3511
η_c	9.7/6	$1.071\ ^{+6}_{-4}$	$2924\ ^{+16}_{-11}$	2980
J/ψ	7.6/6	$1.088\ ^{+5}_{-5}$	$2970\ ^{+14}_{-14}$	3096

Table 5.4: The charmonium mass spectrum predicted by the clover action with $\kappa = 0.1290$, on 18 configurations. m is the result from the simulation and a is the lattice spacing.

The results for the three P-wave meson masses measured for both actions are all consistent with their experimental values, within the large error bars. It is slightly surprising that the lattice predictions for the charmonium spectrum come out so well, when the effects of lattice artifacts are expected to become important with energies $\sim \frac{1}{a}$.

The results for the mass splittings show that only the $M_{h_c} - M_{\chi_{c0}}$ splitting has an error (just) smaller than the differences in masses. For comparison the Fermilab group [48] quote from their simulations:

$$M_{h_c} - M_{\chi_{c0}} = 54 \pm 15 \text{ MeV}$$

It is very interesting to see local operators couple to P-wave channels. The potential model approach has been very successful in understanding the phenomenology of the charmonium spectrum. The requirement that the P-wave state wavefunction is zero at the origin is at the heart of the potential model approach, because it is one of the boundary conditions for the solution of the Schrödinger equation, in a central potential. As pointed out in chapter 1, the local operators used in this study have the same J^{PC} quantum numbers as the P-wave mesons, so perhaps it is not surprising that interesting results can be obtained from these channels. Logically if the nonrelativistic quark model has proved an unreliable guide, then the reason for this success with the P-wave mesons must be due to relativistic effects.

As expected from the fluctuation argument in a previous section the errors

Splitting	$\frac{\chi^2}{dof}$	a.m	m (MeV)	Expt mass(MeV)
$M_{1P} - M_{1S}$		0.216 $^{+48}_{-51}$	590 $^{+131}_{-139}$	459
$M_{h_c} - M_{\chi_{c0}}$	3.5/4	0.065 $^{+54}_{-38}$	177 $^{+147}_{-104}$	111
$M_{h_c} - M_{\chi_{c1}}$	2/4	0.022 $^{+32}_{-32}$	60 $^{+87}_{-87}$	15
$M_{\chi_{c0}} - M_{\chi_{c1}}$	4.5/4	-0.044 $^{+45}_{-24}$	-120 $^{+122}_{-66}$	-96

Table 5.5: clover results for P-wave mass splittings, kappa = 0.1290

Splitting	$\frac{\chi^2}{dof}$	m.a	m(MeV)	Expt mass(MeV)
$M_{1P} - M_{1S}$		0.189 $^{+23}_{-27}$	516 $^{+63}_{-73}$	459
$M_{h_c} - M_{\chi_{c0}}$	2.7/4	0.031 $^{+25}_{-18}$	85 $^{+68}_{-49}$	111
$M_{h_c} - M_{\chi_{c1}}$	2/4	0.010 $^{+12}_{-10}$	27 $^{+32}_{-27}$	15
$M_{\chi_{c0}} - M_{\chi_{c1}}$	3/4	-0.018 $^{+11}_{-9}$	-49 $^{+30}_{-25}$	-96

Table 5.6: Wilson results for P-wave mass splittings, kappa = 0.1350

in the P-wave masses are an order of magnitude larger than the errors in the S-wave meson masses. If the data from the local quark propagators is compared against the previous smeared results, they differ by less than 2σ, which is not statistically significant.

This work has shown that P-wave mesons in the charmonium system can easily be studied on the lattice, with essentially the same effort as their more favoured S-wave cousins. It would be interesting to see whether the use of extended operators described in section 1.5 will improve the signal.

5.2 Calculation of the coupling from lattice QCD.

In QCD with no quarks or massless quarks, the value of the strong coupling at a given energy scale can be used to calculate the coupling at all energies. The value of $\alpha(\mu)$ at one scale (μ) must be determined experimentally. A great deal of theory is required for the extraction of $\alpha(\mu)$; a large part of the uncertainty in its current

value comes from theoretical problems. Most experimental determinations of $\alpha(\mu)$ are obtained at high energy, where the asymptotic freedom of QCD implies that perturbation theory can be used in its extraction. For example, results from the LEP accelerator are being used to calculate the value of $\alpha(\mu = M_z)$ at the mass of the Z particle.

A knowledge of the magnitude of $\alpha(\mu)$ is crucial to whether perturbation theory is a valid tool (or how many orders in the expansion are required) for a calculation of a given experimental process at a particular energy [89]. QCD is hard to solve and thus it is difficult to verify or falsify it. The consistent extraction of $\alpha(\mu)$ from many different experiments at different energies scales is an extremely good test of its validity.

Lattice gauge simulations offer the prospect of the calculation of $\alpha(\mu)$ at low energies in a nonperturbative way which is complimentary to the standard methods. In principle the calculation of $\alpha(\frac{\pi}{a})$ from the lattice is simple; a simulation is performed at a given value of the coupling to produce a quantity (such as m_π or f_π), from which a value for the lattice spacing can be obtained. Perturbation theory is then used to relate the lattice and continuum couplings at a scale of $\frac{\pi}{a}$.

A central problem of the lattice calculation is the correct extraction of the lattice spacing, which requires the calculation of a believable quantity, unaffected by lattice artifacts or finite size effects. The QCD spectrum using light quarks (u,d or s) is difficult to use, because there are not many theoretical tools which can be used to estimate the effects of the quenched approximation, or uncertainties due to the extrapolation of the numerical results to physical quark masses. However for heavy quark systems such as charmonium, the dynamics are governed mainly by nonrelativistic effects and not by the complicated breaking of chiral symmetry that governs the light hadron spectrum; the hope is that any systematic errors in the calculation can be accounted for. The most important systematic error is the effect of the quenched approximation; at large quark mass it is claimed by Lepage [47] that the results can reliably be corrected for this.

5.2.1 Description of the method.

I will basically use the method described by the Fermilab group [49]. Throughout this section I will work with zero flavours of quarks; in the next section the results will be "unquenched". The perturbative connection between the coupling on the

lattice and in the continuum $\overline{MS}$ scheme $g_{\overline{MS}}(\frac{\pi}{a})$ is given by [77] [78]:

$$\frac{1}{g_{\overline{MS}}(\frac{\pi}{a})} = \frac{1}{g_0^2}(1 - \frac{1}{3}g_0^2) + 0.025 \tag{5.8}$$

The current prejudice is that a mean field based relation gives a more accurate relation between the two coupling constants, because it takes into account the effects of tadpole graphs. This gives a slightly different relation between the two coupling constants [49]:

$$\frac{1}{g_{\overline{MS}}(\frac{\pi}{a})} = \frac{1}{g_0^2}\langle \mathrm{trace} U_p \rangle + 0.025 \tag{5.9}$$

where $\langle \mathrm{trace} U_p \rangle$ is the mean plaquette which can be obtained from numerical simulation. At $\beta = 6.2$ the value measured from the UKQCD simulations was 0.6136 (with an error smaller than the last decimal place).

To obtain the lattice spacing, a suitable choice of experimental number must be extracted from the numerical simulation. One obvious choice is the 1P-1S mass splitting, which I have previously argued should not be contaminated by O(a) effects. The expected quark mass independence of the 1P-1S splitting removes the need for messy extrapolations or interpolations between the quark masses used in the simulation to the physical charm quark mass. Another good choice is the value of the lattice spacing obtained from the string tension; although this quantity is obtained via an indirect experimental measurement, the current consensus is that it produces an accurate value for the lattice spacing with small error bars. The use of the above measures of the lattice spacing will produce a value of $\alpha(\mu)$ for the clover, Wilson, and pure gauge actions. The difference between the three numbers will be a measure of the systematic error due to lattice artifacts.

The value of $\alpha(\mu) = \frac{g^2}{4\pi}$ depends on both the regularisation scheme and the scale; to compare the results of different experiments some standard must be adopted. I will use the one in the particle data book, which uses $\alpha(\mu)$ at a scale of 5 GeV in the $\overline{MS}$ scheme as the benchmark. I have used the values of the 1P-1S splitting in tables 5.5 and 5.6, obtained from the simulations using local operators. The value of the lattice spacing obtained from the string tension comes from [16], and comes from the same eighteen configurations that were used in the P-wave simulations.

The integration constant of the renormalisation group equation is the Λ parameter, which is another way of pinning down the running coupling constant. Λ

is defined as:

$$\Lambda = \mu \exp(-\int^{g(\mu)} \frac{dg}{\beta(g)}) \tag{5.10}$$

which is independent of the scale. Although Λ is the typical energy scale of the QCD dynamics, the above definition is problematic. As pointed out by Lüscher and collaborators in [72], the extraction of Λ requires the use of:

$$\Lambda = \lim_{|\mu| \to \infty} | \mu | (b_0 g^2(\mu))^{-\frac{b_1}{b_0^2}} e^{-\frac{1}{b_0 g^2(\mu)}} \tag{5.11}$$

where b_0 and b_1 are one and two loop coefficients of the Callan Symanzik equation. Unfortunately the $\mu \to \infty$ limit is approached logarithmically with energy, which makes the definition 5.10 difficult to use as a way of fixing the QCD coupling constant.

Pragmatically I will use the two loop definition of Λ. The solution of the renormalisation group equation for the coupling constant for QCD with n_f flavours of massless quarks is:

$$\alpha(\mu) = \frac{12\pi}{(33 - 2n_f)\log(\frac{\mu^2}{\Lambda^2})} \times \left[1 - \frac{6(153 - 19n_f)}{(33 - 2n_f)^2} \frac{\log(\log(\frac{\mu^2}{\Lambda^2}))}{\log(\frac{\mu^2}{\Lambda^2})} \right] \tag{5.12}$$

with corrections which are:

$$O(\frac{\log^2(\log(\frac{\mu^2}{\Lambda^2}))}{\log^3(\frac{\mu^2}{\Lambda^2})}) \tag{5.13}$$

I assumed that equation 5.12 had no corrections and obtained Λ, by inverting it numerically. The value of $\alpha(\mu)$ at a scale of 5GeV was obtained by using the Λ in equation 5.12. Using the numbers in the Fermilab paper, I obtained their final result for $\alpha(\mu)$ (I did not try to reproduce their error), using the procedure previously outlined. To obtain the errors on calculated quantities I used naive error analysis, which essentially means using formulae obtained by differentiation, although an extension of the bootstrap procedure used to obtain the mass splittings could have been used for the zero quark results. The conversion of the answer to the four quark real world required the use of a theoretical error, which has to be combined with the statistical error in some sensible way. Since the theoretical error dominates the error in the final value of $\alpha(\mu)$, the use of standard error analysis seemed adequate.

5.2.2 "Unquenching" the calculation.

The method in the last section allowed the calculation of the coupling constant or equivalently $\Lambda_{\overline{MS}}$ in a theory free of fermions. To make contact with experiment, the results must be corrected to obtain the answer for QCD with four flavours of quarks, in the region corresponding to the 5 GeV convention of the particle data book.

Lepage [47] has various physical arguments to suggest that the quenched approximation has little effect on the charmonium spectrum. The decays of excited $\bar{c}c$ states into D mesons are thought to be mediated by the light quark's vacuum polarisation. The decay widths are of the order of 50 to 100 MeV, which Lepage argues, implies that the shift in the charmonium meson masses due to light quark vacuum polarisation effects are of this magnitude. This has been partially confirmed by the results from two recent quenched simulations [46] [48] at around the charm mass, which show around a 50 MeV discrepancy between experiment and simulation for the $m_{J/\psi} - m_{\eta_c}$ mass splitting. However this splitting is sensitive to O(a) effects and it is not clear how much of the discrepancy between experiment and simulation is due to the quenched approximation. Comparing the expected discrepancy of around 100 MeV between the quenched and full theory to the masses of ground state $\bar{c}c$ mesons ($\sim$ 3 GeV), produces the hope that some sort of perturbative analysis could be done on a quenched result to obtain a full QCD prediction. The heavy mass of the charm quark makes the creation of a $\bar{c}c$ pair unlikely, suggesting a small effect on the mass spectrum due to internal heavy quark diagrams.

The method used to unquench the calculation must explicitly take into account the effect of the running coupling. I will use the results obtained in the Fermilab paper [49], which uses a perturbative arguments based on the integration of the renormalisation group equation.

In the perturbative approach, they argue that the coupling constant for the quenched and dynamical theories can be made to agree at roughly the binding energy in the ground state of the charmonium system, which is approximately 400 MeV. The coupling is then evolved up to 5 GeV to obtain the shift in the coupling by using:

$$\Delta g^{-2} = \int_{\mu_1}^{\mu_2} d\log q^2 (\beta_0^{n_f} - \beta_0^0 + (\beta_0^{n_f} - \beta_0^0) g^2 + \cdots) \tag{5.14}$$

where:

$$\begin{aligned} \beta_0^{n_f} &= (11 - \frac{2n_f}{3})\frac{1}{16\pi^2} \\ \beta_1^{n_f} &= (102 - \frac{38n_f}{3})\frac{1}{(16\pi^2)^2} \end{aligned} \tag{5.15}$$

The energy scales μ_1 and μ_2 are big enough so that perturbation theory is valid and the order g^4 corrections are negligible. If I had used an observable for a particle made out of light quarks to obtain the lattice spacing, then the lowest energy scale would have been in a region where perturbation theory is not valid and equation 5.14 could not have been used to correct the results.

The Fermilab group quote the following shift as the change in coupling between the full and quenched theory at 5GeV.

$$\Delta g^{-2}(\mu = 5GeV) = -0.110 \pm 0.030$$

I used their correction to add four fermions to my calculation.

5.2.3 Results.

The lattice calculation of the coupling constant at the standard scale of 5 GeV (or $\Lambda_{\overline{MS}}$) requires a reasonably large amount of theoretical manipulation to obtain a number for the simulations. For this reason I have expanded the analysis so that the effect of each adjustment can clearly be seen. Tables 5.7 and 5.8 show the results using standard perturbation theory and mean field theory ideas respectively. As a comparison I have included a compendium of results from different lattice simulations taken from [47].

The final result of this calculation is a value for $\alpha(\mu)$ for four fermion flavours at a scale of 5GeV; the values obtained by using mean field theory improved perturbation theory is consistent with other lattice calculations and only moderately inconsistent with the latest result from LEP. The use of mean field perturbation theory, rather than "normal" perturbation theory produces a shift of roughly twice the order of magnitude of the statistical error. The effect of the "unquenching" produces shifts in the results by a factor of roughly three times the statistical error; both the mean field theory shift and the unquenching shift are in the same direction.

The final error in the $\alpha(\mu)$ figure is dominated by the uncertainty in the conversion between the four and zero quark coupling constants. This is particularly

	Action		
	Rotated clover	Wilson	Pure gauge
$\frac{1}{a}$ GeV	2.13(51)	2.43(34)	2.73(5)
$\Lambda^{(0)}$ GeV	0.113(27)	0.129(18)	0.1459(26)
$\Lambda^{(4)}$ GeV	0.060(24)	0.071(19)	0.084(22)
$\alpha(\mu = 5GeV)$	0.139(11)	0.144(8)	0.1495(85)

Table 5.7: The QCD coupling results from this simulation, using weak coupling perturbation theory

	Action		
	Rotated clover	Wilson	Pure gauge
$\frac{1}{a}$ GeV	2.13(50)	2.43(34)	2.73(5)
$\Lambda^{(0)}$ GeV	0.175(41)	0.199(28)	0.224(4)
$\Lambda^{(4)}$ GeV	0.107(44)	0.128(42)	0.150(39)
$\alpha(\mu = 5GeV)$	0.158(15)	0.165(13)	0.171(11)

Table 5.8: The QCD coupling results from this simulation, using mean field theory.

evident in the comparison between the lattice spacing obtained from the string tension and that obtained from the 1P-1S splitting, where the error in the string tension is an order of magnitude less than in the mass splitting case, but the errors on the final results for $\alpha(\mu)$ are comparable. It is interesting to note that all the errors in lattice results from different groups are approximately the same, suggesting that an improved value for $\alpha(\mu)$ can only come from a better understanding of the relation between the quenched and the unquenched theories.

$\alpha_{\overline{MS}}(\mu = 5GeV)$	β	Description
0.174 $\pm$ 0.012	5.7 - 6.1	Charm (Fermilab group)
0.171 $\pm$ 0.012	6.0	Bottom (NRQCD group)
0.169 $\pm$ 0.016	5.7	Bottom (NRQCD group)
0.173 $\pm$ 0.012	5.7	Bottom (NRQCD group)
0.216 $\pm$ 0.012	-	Extrapolation from LEP

Table 5.9: Lattice determinations of the QCD coupling , and a value from LEP, taken from [47]

5.2.4 Criticism of the method.

Although the final answer for $\alpha(\mu)$ was consistent with other work, the method required the occasional suspension of belief in some of the theoretical manipulations.

It is easy to criticise the conversion of the quenched zero quark coupling constant result to the four quark value of the real world. This flaw in the method will eventually be removed by the use of dynamical simulations. While we are waiting for the improvements in algorithms and computing power to make this possible, it would be useful to think of more convincing ways of unquenching the calculation.

The hopping parameter expansion offers the prospect of quantifying the shift in coupling due to the neglect of the fermion determinant. The following argument [1] derives the coupling shift. If the fermion determinant is written in the form:

$$\det M = e^{\text{trace}\log M} \tag{5.16}$$

and if the fermion matrix M is symbolically written is:

$$1 - \kappa D \tag{5.17}$$

expanding in κ the fermion determinant can be written in the form of an effective pure gauge action:

$$S_{eff} = \sum_{j=1}^{\infty} \frac{\kappa^j}{j} \text{trace}(D^j) \tag{5.18}$$

Only even values of j survive the above sum and the first nonvanishing component is at j = 4, which corresponds to the sum of the plaquettes over all the sites on the lattice, which is basically the Wilson pure gauge action. The $O(\kappa^6)$ term corresponds to various Wilson loops made out of six links. The first term allows the estimation of the shift in the pure gauge coupling, which for Wilson's fermion action is:

$$\Delta\beta_{Wilson} = 48 n_f \kappa^4 \tag{5.19}$$

for n_f flavours of quark.

The use of this formula requires that the higher order corrections in kappa can be neglected, so it is unreliable to estimate the effect of light quark internal diagrams. However it could prove valuable in the estimation of the shift due to the fermion determinant of the charm quark. A numerical simulation of full QCD

at β of 5.3 on a 8^4 lattice has shown that equation 5.19 fails for values of the hopping parameter between 0.156 and 0.167 [64].

The requirement to use mean field theory to convert the coupling on the lattice into the $\overline{MS}$ continuum value is also a problem. In high energy calculations of $\alpha(\mu)$, one of the difficulties in extracting a result is knowing the effect of truncating the perturbative expansion [89]. This is exactly the same problem for the lattice calculation, complicated by nonperturbative effects. The theoretical uncertainty should be reduced by using a physical definition for the coupling. A start in this direction has already been made by Michael in [71] for pure gauge theory, and Lüscher and collaborators in [72] for the O(3) sigma model.

5.3 The Hadron spectrum at finite momentum..

In field theory, because of the translational invariance of the typical Lagrangian in particle physics, it is customary to work in momentum space. There are a number of quantities that can only be calculated at finite momentum, such as various phenomenologically important form factors. It is therefore interesting to study hadron operators on the lattice at finite momentum.

One of the basic quantities that can be extracted from a lattice simulation with operators at finite momentum is the energy of the particle as a function of momentum. Although the lattice breaks the translational invariance of the theory, in the continuum limit the effect of the lattice should disappear. The deviation of a particle's energy as a function of momentum, from the continuum energy dispersion relation, is a measure of the restoration of the continuum space-time symmetries. For form factors, the numerical lattice energy dispersion relation is required to know when the results are reliable continuum predictions. It is also an interesting test of improvement to compare the energy dispersion relation for the Wilson and clover actions, because violations of the continuum result could be due to O(a) effects.

In the rest of this Chapter, I will present initial results from a numerical study of lattice operators at finite momentum using the clover action. The next section will contain a brief description of the program which computed the two-point correlators at finite momentum, and the ways in which it was validated. Next I will present results for the energy dispersion relation for the pseudo-scalar meson, vector meson, and the proton. The final section will contain a calculation of the

pion decay constant from the vector components of the axial current, which can only be done at non-zero momentum.

The notation I will use for spatial momentum on the standard UKQCD $24^3 \times 48$ lattice is (n_1, n_2, n_3), which is code for a momentum of:

$$\underline{p} = \frac{2\pi}{24}(n_1, n_2, n_3) \tag{5.20}$$

5.3.1 Details of the program.

I will now discuss various aspects of the computer program which ties together quark propagators to form two-point hadron correlators, with special emphasis on the problems that occur when the operators are at finite momentum. A previous study of the pion at finite momentum, using Wilson fermions at $\beta = 6.0$ revealed problems with the pion signal (on a spatially coarse lattice) with a momentum of $\frac{2\pi}{10}$, which motivates a study of the numerical aspects of the calculation to try and get useful results. I will focus on the calculation of the meson propagators at finite momentum, because as pointed out in section 1.5 there are theoretical problems with choosing the correct operators which create baryons at finite momentum. It was felt that the proton was sufficiently well understood to be simulated at finite momentum, so I added a routine into the program to do this task.

The program I will now briefly describe is essentially an implementation of equation 1.56. The program has to calculate the timesliced propagator:

$$\begin{aligned}\sum_{\underline{x}} \langle \overline{\psi}_1 \Gamma_{sink} \psi_2(t, \underline{x}) \overline{\psi}_2 \Gamma_{source} \psi_1(0, \underline{0}) e^{i\underline{p}.\underline{x}} \rangle = \\ - \sum_{\underline{x}} \mathrm{trace} \Gamma_{sink} Q_2(t, \underline{x}; 0, \underline{0}) \Gamma_{source} \gamma_5 Q_1^{\dagger}(t, \underline{x}; 0, \underline{0}) \gamma_5\end{aligned} \tag{5.21}$$

where Γ_{source} and Γ_{sink} are gamma matrices, and Q_i is a quark propagator, with the value of i labelling the flavour. The trace in equation 5.21 is over the spin and colour indices.

The program which calculates the meson propagators in equation 5.21, basically loads in time-sliced-sized chunks of the two quark propagators from disk, does the spin and colour traces, and finally sums the result over the spatial lattice. The cause for concern about the numerical accuracy of working at nonzero momentum, arises from the extra fluctuations in sign caused by the $e^{i\underline{p}.\underline{x}}$ factors, which could cause cancellation problems as the sum over the spatial lattice is taken. Naive ideas of trying to separately accumulate the positive and negative

real parts of the time sliced propagator in the sum, can be rejected on grounds of efficiency. The best that can be done is to accumulate the sum over the spatial lattice in double precision, even though for memory reasons the quark propagators are stored as single precision numbers.

Naively there is a big difference between the calculation of a timesliced meson propagator at finite momentum and normal lattice gauge theory calculations, where due to translational invariance, the actual position in the lattice is unimportant. The only significant thing for a given field's evolution is the state of its neighbours. The calculation of the phase factors requires the knowledge of the actual spatial position in the lattice of a specific point. However the operation of multiplying by a phase factor is still a local operation (important for implementation on parallel machines), so it was conveniently coded up by filling up a table of phase factors, at the start of the calculation, whose spatial position was labelled in the same way as the quark propagators.

To save on memory and to reduce the number of costly trigonometric operations, only the phase factors for the three lowest values of the momentum in three independent directions were stored as tables; phase factors for higher values of momentum were obtained by multiplication. Because some of the meson correlators are either even or odd under momentum inversion, this was built into the program by taking sin or cos transforms, instead of straight Fourier transforms.

5.3.2 Validation of the code

Once a computer program has been written to do a simulation of some physical process, it first must be tested. In sophisticated computer jargon this is known as bug hunting.

5.3.3 Free field calculations of hadron correlators.

The independent calculation of the hadron correlators in free field theory, provided an important test on the production propagator inversion and spectrum codes, and was also used in the investigations of reflection positivity in chapter2. The basic ideas and equations are described by Carpenter and Baillie [42]. I generalised their method to work with non-degenerate meson correlators at finite momentum and also did an equivalent calculation for the clover pion correlator. The authors of reference [42] were interested in the investigation of finite size effects in the

non-interacting theory, so they worked with a continuous time variable. However for code validation purposes it is important to work with a discrete time lattice, so as to mirror the production codes.

I will first discuss the free field calculation for the Wilson action. If S(k) is the free field quark propagator in momentum space, which is commonly used in perturbative calculations, then the time sliced quark propagator is defined as:

$$S_{L_4}(t,\underline{k}) = \frac{1}{L_4}\sum_{k_4} e^{ik_4 t} S(k) \tag{5.22}$$

The expression for the propagator for a possibly non-degenerate meson at finite spatial momentum $\underline{p}$ can be written as:

$$\sum_{\underline{x}} \langle \overline{\psi}_1 \Gamma_{sink} \psi_2(t,\underline{x}) \overline{\psi}_2 \Gamma_{source} \psi_1(0,\underline{0}) e^{i\underline{p}.\underline{x}} \rangle =$$
$$\frac{1}{L^3}\sum_{\underline{k}} \mathrm{trace} \Gamma_{sink} S_2(t,\underline{k}) \Gamma_{source} \gamma_5 S_1^{\dagger}(t,\underline{k}+\underline{p}) \gamma_5 \tag{5.23}$$

where the momentum sums run over:

$$k_\mu = \frac{2\pi(n_\mu + \delta_\mu)}{L_\mu}, n_\mu = 0,\ldots,L_\mu - 1 \tag{5.24}$$

with $\delta_\mu = 0$ or $\frac{1}{2}$ for periodic or anti-periodic conditions respectively. The sin and cos transforms were tested by choosing Γ_{sink} and Γ_{source} so that the function was even or odd under spatial momentum inversion. The propagator for nondegenerate mesons was obtained by using different quark masses in the S_1 and S_2 quark propagators.

The above techniques were implemented in a program which was used to help debug the 1992 version of the production spectrum code run on the 64 node i860 Meiko Computing Surface and the CM200 Connection Machine, in Edinburgh. I also wrote a program which calculated the free field proton propagator at finite momentum, using the ideas of Carpenter and Baillie [42], which was also used to debug the production code.

As a test of the clover action propagator inversion code I wrote a generalised version of the above free field calculation. The main problem is that the fermion propagators for the Wilson and clover actions are identical in free field theory, because the field strength tensor vanishes. To write a piece of code which was sensitive to the clover term required working with a gauge configuration which was simple enough to Fourier transform, but which did not produce a zero clover term.

The easiest choice of configuration was "crossed constant background fields", in which all the gauge fields in a given direction are set equal to the same SU(3) matrix: $U_\mu(x) = U[\mu]$.

There is an added computational burden to this method. For free field theory Wilson fermions, the inversion of the fermion matrix to obtain the quark propagator can be done analytically, using the properties of the Dirac gamma matrices. For the clover fermion matrix in crossed constant background fields the inversion had to be done numerically, for every value of momentum in the summation in equation 5.23. The fermion field rotations in equation 1.49 were implemented for the crossed background field configuration. The rotated clover propagator S_{ROT} was obtained by using:

$$S_{ROT} = R(p) S_{clover} R(p) \tag{5.25}$$

where R(p) was defined by:

$$R(p) = 1 - \frac{1}{4} \sum_{\mu} (e^{ip_\mu} U[\mu] - e^{-ip_\mu} U^\dagger[\mu]) \tag{5.26}$$

and S_{clover} is the clover fermion propagator.

The program was fast enough to produce a pion correlator on an $4^3 \times 8$ lattice, which was used in the validation of the propagator inversion code in 1991. 64 node i860 Meiko Computing surface

5.3.4 The effect of quark propagator convergence on hadron correlators.

Quark propagators in lattice gauge theory simulations are obtained by numerically inverting the fermion matrix. Because the fermion matrix is too big to fit into computer memory, iterative solution techniques suited to its sparse structure are used to do the inversion. The slight problem with iterative techniques is that they do not produce the exact solution (up to rounding errors) after a fixed number of iterations. This means that a decision must be made on the number of iterations to be used or the convergence criteria, so that the solution produced is close enough to the exact one.

At the beginning of the UKQCD project, exhaustive tests were carried out to find which algorithm produced quark propagators with the minimum amount of computer time. Investigations were also carried out into the convergence of the algorithms using a variety of different error functions based essentially on single called residuals

quark propagators and on the pion propagator[51]. However, for operational reasons no tests were carried out to determine the effect of the convergence of the quark propagators on hadron correlators.

Because of the possible cancellation involved in their calculation, hadron correlators at finite momentum could be sensitive to the quark propagator convergence. In this section I will try and test for this.

To do the test I used a modified production propagator inversion program on the Edinburgh CM200 , which had been changed so that it dumped only a subset of the timeslices for its current spin colour component, every 120 iterations for five restarts. The red-black preconditioned minimal residual algorithm was used with an over-relaxation parameter of 1.1. The test was done for a Wilson propagator on a $\beta = 6.2$ gauge configuration with a lattice volume of $24^3 \times 48$. The time slices used were: 8, 16, 20, and 24, because they spanned the fit region used in the extraction of masses from hadron correlators.

I analysed the rho, proton, pion and b1 particle correlators at the two momentum values (1,1,1) and (3,0,0). The result was that after 360 iterations all the correlators had converged . Sample graphs for the proton and the first component of the rho are shown in figures 5.5 and 5.4, and the corresponding residual is in figure 5.3.

This allows me to come to the happy conclusion that there are no problems with hadron correlators at finite momentum, due to the convergence criteria of the quark propagator. If the finite momentum correlators had been found not to converge, it would have been difficult to do anything about it (notwith standing the large number of propagators already calculated), because there is a minimum convergence bound below which rounding errors start to produce problems. The test in this section should be viewed as a consistency check on the quark propagator and hadron spectrum codes.

5.3.5 Details of the simulation.

The final sections of this thesis contain initial results from a quenched simulation of QCD. For convenience I will collect together here the relevant details. The β value was 6.2 and the lattice size was $24^3 \times 48$, sixteen gauge configurations were used. Some of the results are from quark propagators with local or smeared sinks and sources (I will indicate which). The smearing used gauge invariant Jacobi

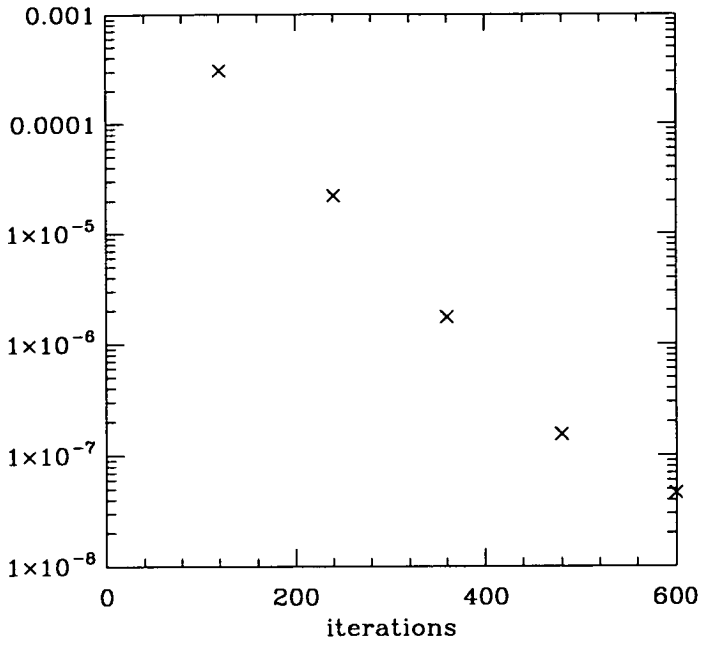

Figure 5.3: The residue of the quark propagator

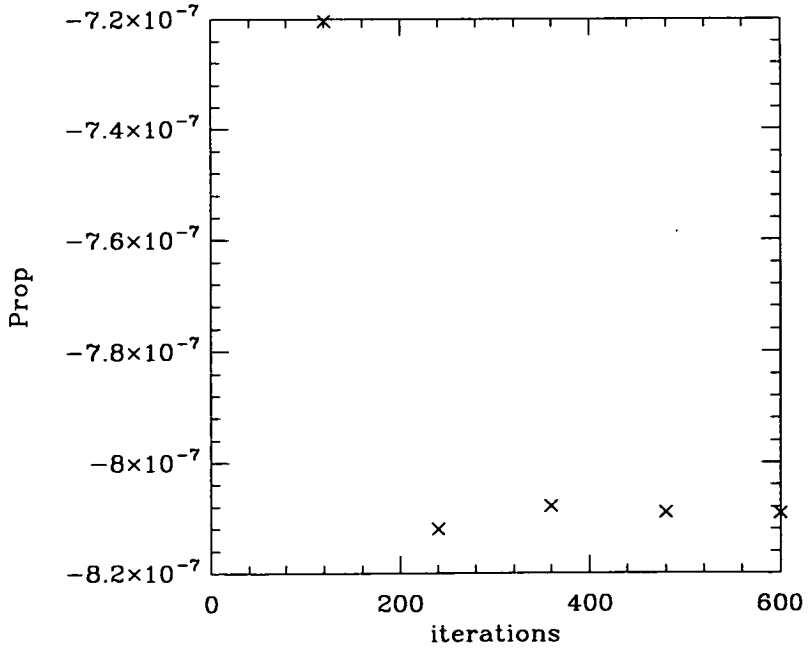

Figure 5.4: The rho propagator at p=(1,1,1) at time slice 20

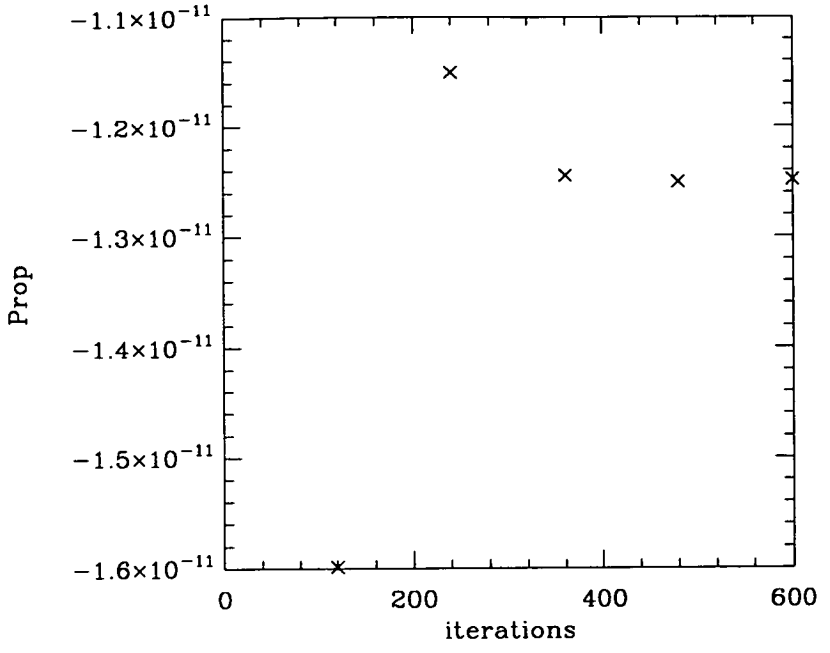

Figure 5.5: The proton propagator at p=(1,1,1) at time slice 24

smearing, 50 iterations with $\kappa_{scalar} = 0.25$. This corresponds to a smearing radius of 4 [73].

5.3.6 Effective mass plots.

Previous lattice hadron spectrum calculations have revealed problems with obtaining signals for particles at finite momentum. As a starting point of the analysis I will consider effective mass plots, which give a good indication of when there is a signal for various particles and help in choosing fitting ranges.

I will first consider the particles made out of the quarks with "small" masses, the actual kappa values being 0.14144 and 0.14262. The general rule seemed to be that the signal for the lighter quark mass particles was much noiser than for the heavier quark particles. For the pion, rho and proton the effective mass plots had reasonable plateaus between timeslices 12 and 18, for momentum with a magnitude less than $\sqrt{3}$. For the proton and the rho at the momentum of (1,1,1), it looked as though higher statistics would produce a usable signal.

The signal for the pion seemed more noisy than for the rho and the proton at all momenta. After a momentum of $\sqrt{2}$ there was no trace of a signal.

I also looked at the a0, a1, and b1 particles at various values of momentum. The signal for the particles at zero momentum was poor for light quark masses, or not there at all, and it did not improve as the magnitude of the momentum was increased.

I looked at the data with smeared sources and smeared sinks at a kappa value of 0.133. Here the effective mass plots did not show a loss of signal, as was the case for the light quark masses, however they did get very noisy.

The general conclusion from looking at the effective mass plots is that the signal for all particles with momentum greater than $\sqrt{2}$ should not be believed. The following figures are effective mass plots for the pion, proton and the rho.

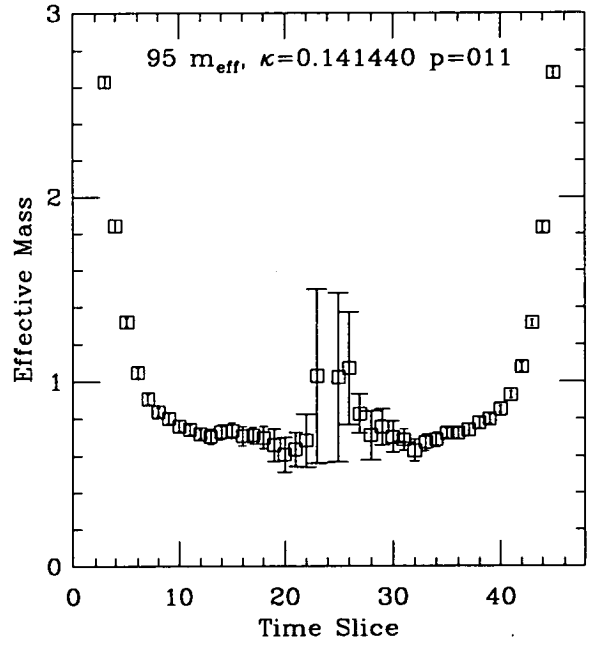

Figure 5.6: The effective mass plot for the proton, $\kappa = 0.141440$, p=(0,1,1)

5.3.7 The energy dispersion relation from numerical simulation.

The energy dispersion relations are shown in the following figures. The type of quark sources used and the kappa values are shown in the captions. The fit region for the local-local data was 12,14,16 and the fit region for the smeared-smeared data was 7,9,11. Although in the previous section on effective masses, I

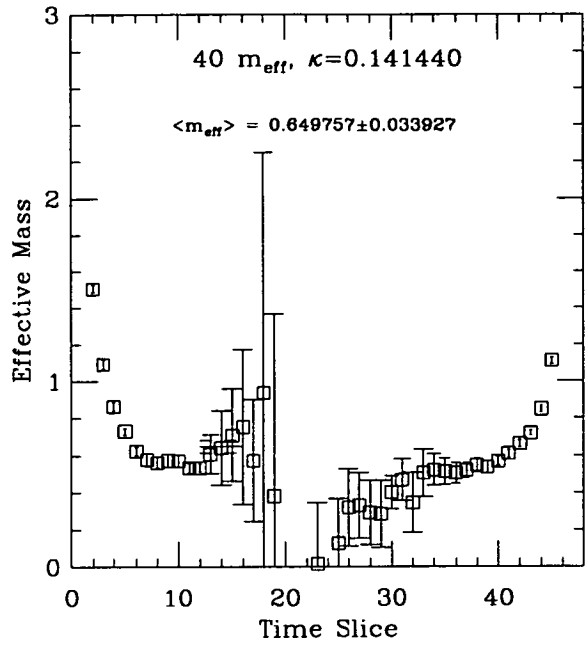

Figure 5.7: The effective mass plot for the pion, $\kappa = 0.14144$, p=(0,1,1)

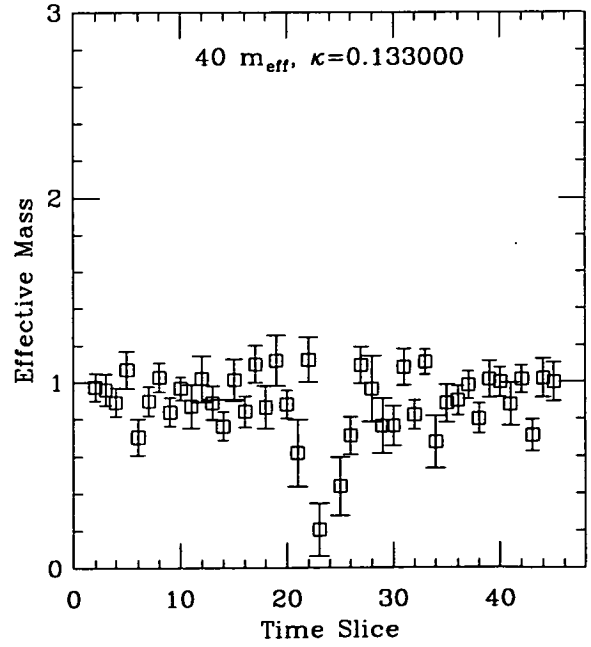

Figure 5.8: The effective mass plot for the pseudoscalar meson, $\kappa = 0.133$,p=(0,1,1)

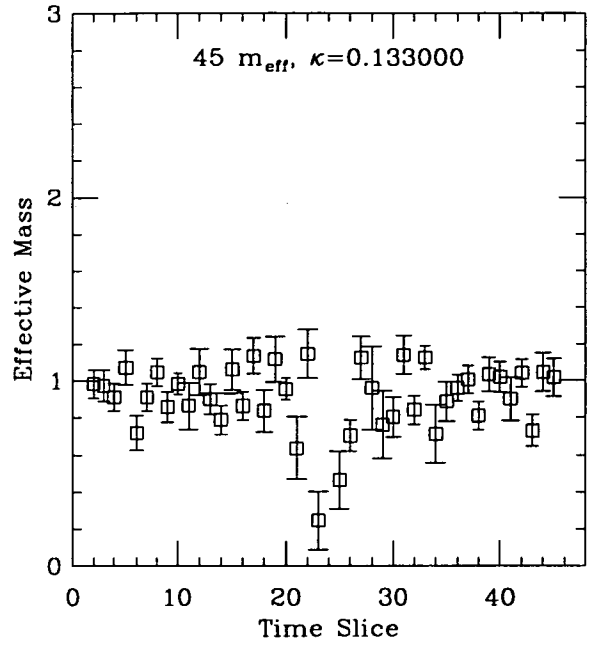

Figure 5.9: The effective mass plot for the vector meson, $\kappa = 0.133$, p=(0,1,1)

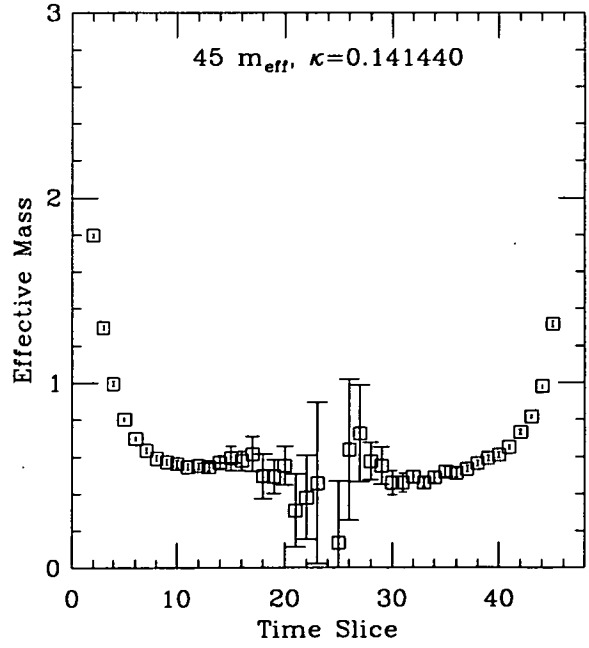

Figure 5.10: The effective mass plot for the rho, $\kappa = 0.14144$, p=(0,1,1)

stated that no particles had good plateau regions with momentum above $\sqrt{2}$ in magnitude, I was unable to resist some of the low $\frac{\chi^2}{dof}$ for some of the fits at higher momentum values. The results here should show the possibilities of a higher statistics calculation. The continuous curves in the figures are the continuum energy dispersion relations.

The general conclusions from the energy dispersion relationships is that the agreement between the numerical results, and the continuum curve is good within the large error bars. At the momentum where the relation breaks down there are problems with obtaining signals for the particles.

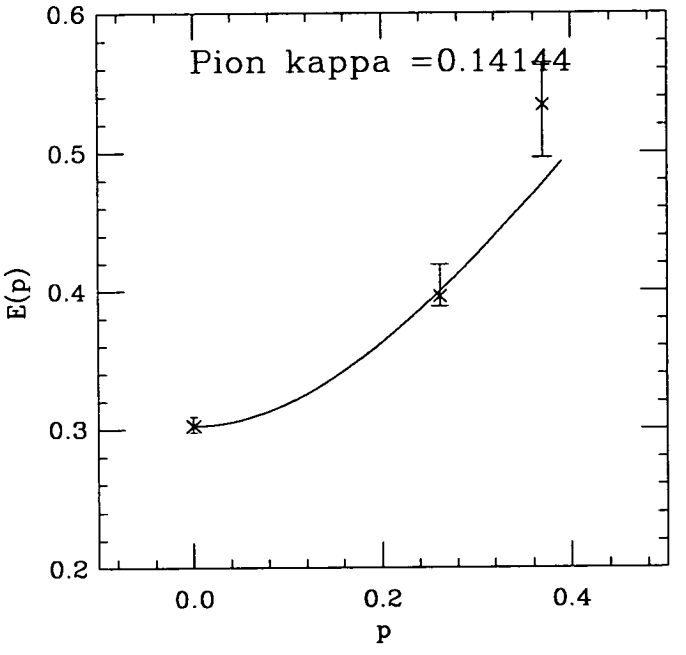

Figure 5.11: The energy dispersion relation for the pion, $\kappa = 0.14144$, local sources and sinks.

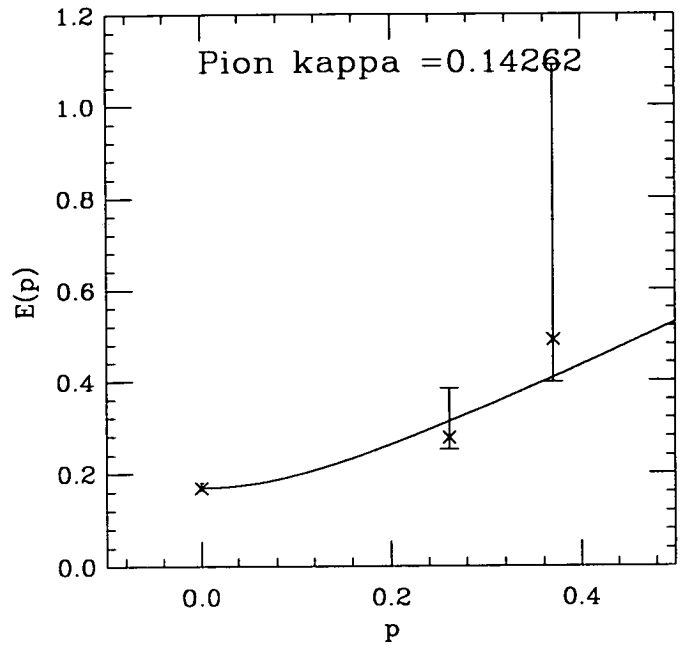

Figure 5.12: The energy dispersion relation for the pion, $\kappa = 0.14262$, local sources and sinks.

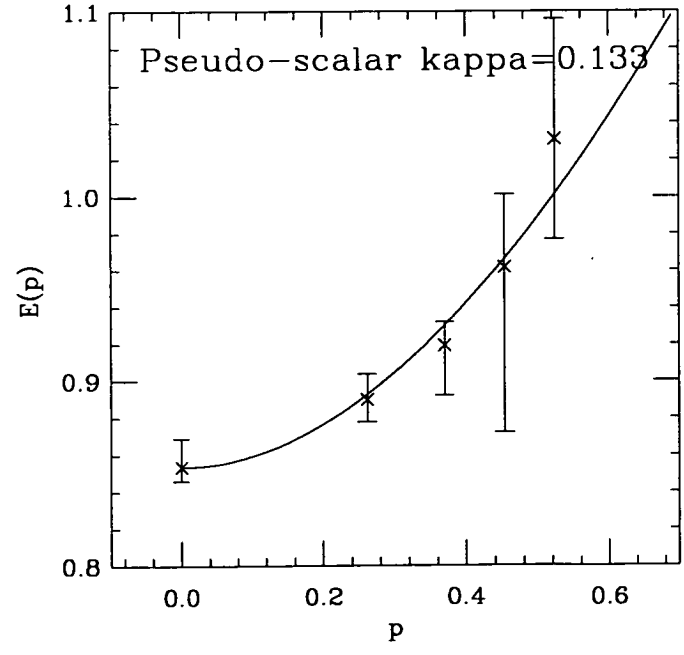

Figure 5.13: The energy dispersion relation for the pion, $\kappa = 0.133$, smeared sources and sinks.

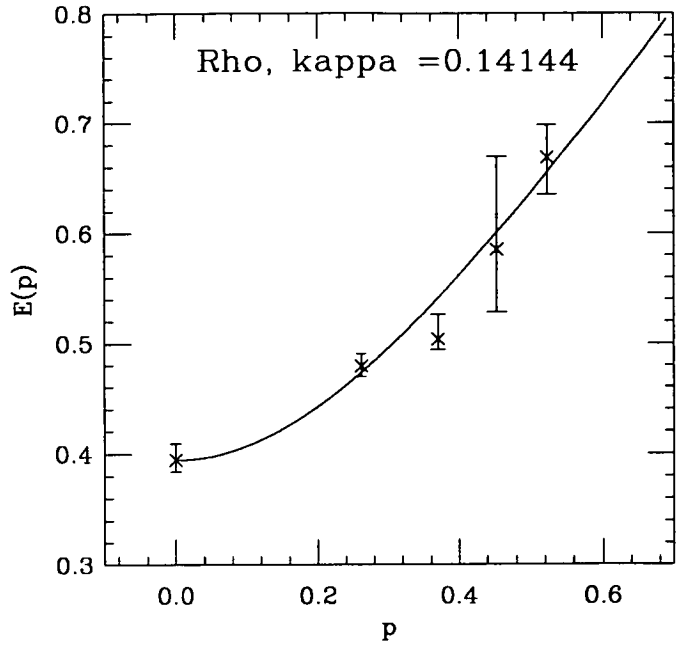

Figure 5.14: The energy dispersion relation for the rho, $\kappa = 0.14144$, local sources and sinks.

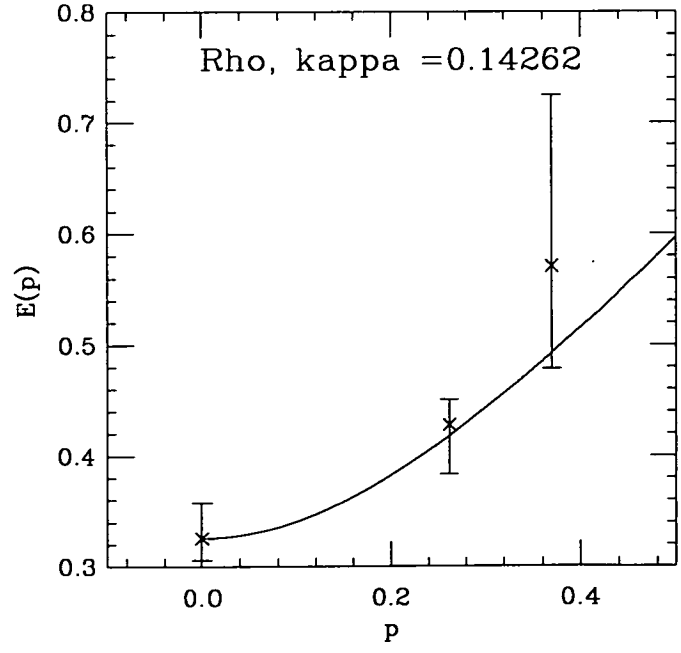

Figure 5.15: The energy dispersion relation for the rho, κ =0.14262, local sources and sinks.

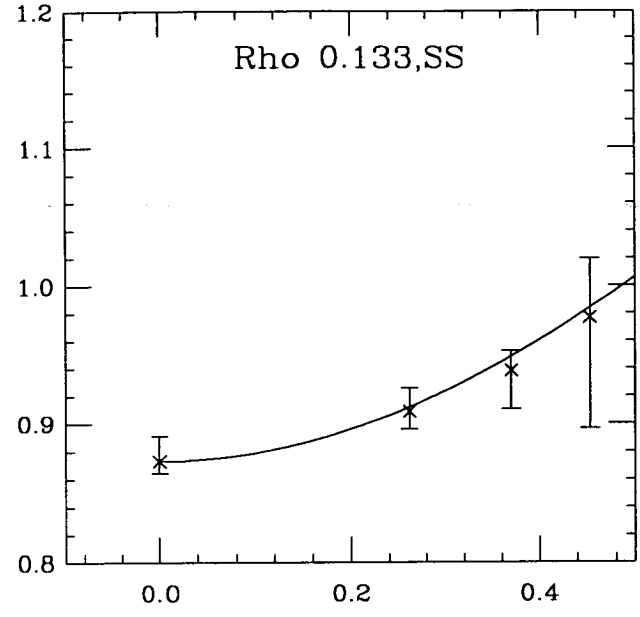

Figure 5.16: The energy dispersion relation for the rho, κ =0.133, smeared sources and sinks.

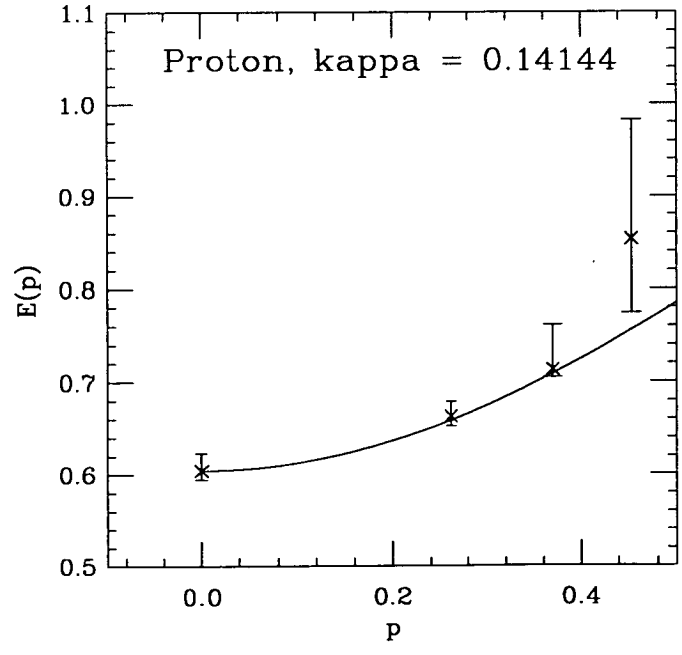

Figure 5.17: The energy dispersion relation for the proton, κ =0.14144, local sources and sinks.

Momentum	$\frac{\chi^2}{dof}$	Energy
000	4.15/4	$0.8535\ ^{+153}_{-\ 76}$
100	3.24/4	$0.8900\ ^{+139}_{-119}$
110	2.4/4	$0.9195\ ^{+128}_{-272}$
111	2.02/4	$0.9619\ ^{+395}_{-895}$
200	3.64/4	$1.031\ ^{+\ 65}_{-\ 54}$

Table 5.10: The energy of the pseudoscalar particle as a function of momentum with κ = 0.133, smeared sources and sinks were used.

Momentum	$\frac{\chi^2}{dof}$	Energy
000	4.16/4	$0.8731\ ^{+180}_{-\ 85}$
100	3.44/4	$0.9086\ ^{+168}_{-129}$
110	2.86/4	$0.9380\ ^{+143}_{-280}$
111	2.3/4	$0.9765\ ^{+429}_{-803}$
200	4.3/4	$1.029\ ^{+\ 47}_{-\ 51}$

Table 5.11: The energy of the vector meson as a function of momentum with $\kappa = 0.133$, smeared sources and sinks were used.

5.3.8 Further work on the energy dispersion relation.

The deviation of the energy of a particle as a function of its momentum is a direct test of the lattice artifacts in the action. Unfortunately the calculation of the Wilson action correlators at finite momentum has not been done. Numerical simulation of the nonlinear sigma model showed that Symanzik's one-loop improved action had a dispersion relation which followed the continuum one to much higher values of momentum than two other lattice nonlinear sigma model actions [52]. So it will be interesting to compare the energy dispersion relations of the clover and Wilson actions. One of the problems with that calculation is that the particle's energies are only available for the lowest values of momentum,

Momentum	$\frac{\chi^2}{dof}$	Energy
000	3.98/4	$0.3259\ ^{+321}_{-198}$
100	0.9/4	$0.4281\ ^{+228}_{-444}$
110	4.47/4	$0.5711\ ^{+1539}_{-921}$

Table 5.12: The energy of the rho $\kappa = 0.14262$, local sources and sinks

Momentum	$\frac{\chi^2}{dof}$	Energy
000	3.92/4	$0.3944\ ^{+146}_{-101}$
100	3.45/4	$0.4792\ ^{+114}_{-93}$
110	13.38/4	$0.5034\ ^{+229}_{-91}$
111	5.89/4	$0.5851\ ^{+846}_{-567}$
200	6.38/4	$0.6689\ ^{+295}_{-336}$

Table 5.13: The energy of the rho as a function of momentum with $\kappa = 0.14144$ local sources and sinks were used.

Momentum	$\frac{\chi^2}{dof}$	Energy
000	1.6/4	$0.6045\ ^{+190}_{-98}$
100	1.75/4	$0.6634\ ^{+157}_{-111}$
110	2.23/4	$0.7131\ ^{+482}_{-82}$
111	3.02/4	$0.8535\ ^{+1296}_{-791}$
200	7/4	$0.9234\ ^{+1591}_{-470}$

Table 5.14: The energy of the proton as a function of momentum with $\kappa = 0.14144$ local sources and sinks were used.

Momentum	$\frac{\chi^2}{dof}$	Energy
000	2.41/4	$0.1691\ ^{+119}_{-52}$
100	0.95/4	$0.2764\ ^{\cdot\ \cdot}_{-241}$
110	4.71/4	$0.4896\ ^{\cdot\ \cdot}_{-919}$

Table 5.15: The energy of the pion as a function of momentum with $\kappa = 0.14262$ local sources and sinks were used.

Momentum	$\frac{\chi^2}{dof}$	Energy
000	3.15/4	$0.3021\ ^{+\ 66}_{-\ 46}$
100	2.61/4	$0.3959\ ^{+232}_{-\ 72}$
110	1.08/4	$0.534\ ^{+\ 30}_{-\ 38}$

Table 5.16: The energy of the pion as a function of momentum with $\kappa = 0.14144$ local sources and sinks were used.

because of the loss of signal at higher momentum. The comparison between the two actions will be facilitated by doing more sophisticated analysis of the data. For example a better test of the energy dispersion relation is to look at the ratio of correlators at zero and finite momentum to obtain E(p)-m, which has smaller errors than the energy obtained from fitting a single correlator.

There is another interesting question that can be studied using the energy dispersion relationship, which is important for the study of heavy quarks on the lattice. There is a prejudice that as the quark mass exceeds one (in lattice units), the results from simulation become unreliable. However Lepage has an argument to show that this might be wrong [47]. To explain his ideas he considers the energy dispersion relation of free lattice Wilson quarks. Using the methods described in section 2.4.2, the energy E of a Wilson quark can be obtained as a function of the momentum p and the quark mass m. To show that in the continuum limit relativity was restored, I taylor-expanded $E(m,p)$ in both m and p to obtain equation 2.[illegible] However in the heavy quark region $m \sim 1$ and this expansion is

invalid. The correct thing to do is to expand the energy only in the momentum:

$$E = m_1 + \frac{p^2}{2m_2} \tag{5.27}$$

where m_1 and m_2 are defined as:

$$m_1 = \log(1+m) \tag{5.28}$$

$$\frac{1}{2m_2} = \frac{2+4m+m^2}{2(1+m)(2m+m^2)} \tag{5.29}$$

Lepage further argues that the m_2 mass is the one which is important for the dynamics, rather than m_1. The m_1 factor produces a constant shift in the energy, and thus does not show up in the mass splittings. It would be interesting to try and fit the energy dispersion relation for heavy quark mesons to equation 5.27, to try and obtain evidence for m_1 not being equal to m_2. This would test Lepage's ideas in the interacting theory, which underpin the use of propagating Wilson quarks for simulating heavy quarks.

5.3.9 Decay constants at finite momentum.

The calculation of decay constants from lattice QCD simulations are vital physical predictions. In this section I will calculate the pion decay constant at finite momentum, and argue that a similar calculation for heavy quarks would test its contamination by lattice artifacts. The f_B decay constant is the most sought after because its value is required for the extraction of elements of the CKM matrix. With propagating Wilson quarks the mass of the bottom quark is too big to produce believable results on current (and probably future) sized lattices. However f_B can be obtained from the simulation of a standard Wilson like action, by working with quarks with masses of the order of charm mass and then using theoretical scaling relations to extrapolate the result up to the b-region.

The decay constant for a pseudo-scalar particle is defined in the following equation:

$$\langle 0 \mid A_\mu(0) \mid B(p) \rangle = f_B p_\mu \tag{5.30}$$

where A_μ is the axial current $\overline{q_1}\gamma_\mu\gamma_5 q_2$ and B(p) is a pseudoscalar particle with momentum p.

Typically in lattice calculations the decay constant is obtained by using the zeroth component of equation 5.30. However at nonzero momentum the decay

constant could be extracted from the spatial components of the axial vector current. This is particularly important at large quark masses, where the effect of lattice artifacts could make the results unreliable.

Richards and collaborators [53] obtained values for the pion decay constant f_π, by using the spatial components of the axial vector, in a dynamical simulation of Wilson fermions at $\beta = 5.6$ and $\beta = 5.7$ on 12^4 and 16^4 lattices. The kappa values used in the simulation were 0.160 and 0.157. They used gauge invariant smearing. Their results for f_π obtained for the lowest value of momentum were consistent with the values obtained from the rest frame; the statistical errors were also a similar order of magnitude. The values of f_π were also obtained for the second lowest momentum, on the lattices they worked on.

As a warm up exercise, I will try and obtain consistent values for f_π at finite momentum, using local operators at the source and the sink. To use the spatial parts of equation 5.30 to obtain f_π at finite momentum requires using a different operator at the sink compared to the source. A pion operator is required at one end to project out the pion state, at the other end the axial vector is required to obtain the correct amplitude in equation 5.30. The following off diagonal correlation function was used:

$$C(\underline{p},t) = \sum_{\underline{x}} e^{-i\underline{p}\cdot\underline{x}} \langle 0 \mid A^\dagger_\mu(\underline{x},t) A_0(\underline{0},0) \mid 0 \rangle \tag{5.31}$$

An expression for f_π can be obtained by using the same method as in chapter 1

$$f_\pi = \frac{2E_{A\pi}a_{A\pi}}{p_\mu\sqrt{2E_{\pi\pi}a_{\pi\pi}}} \tag{5.32}$$

where $a_{A\pi}$ is the amplitude of the off diagonal correlator and $E_{A\pi}$ is the energy. The $E_{\pi\pi}$ and $a_{\pi\pi}$ parameters are the corresponding ones from the pion to pion channel, and are required for normalisation.

Table 5.17 contains the values of $\frac{f_\pi}{Z_A}$ obtained from simulations for the different components of the axial current at a momentum of (1,0,0). The pion decay constants are all in the lattice scheme. All the $\frac{\chi^2}{dof}$ for all the channels fitted were less than 1.5, and consistent pion masses were obtained between the different channels. Because of the problems seen with the pion signal with a momentum of (1,1,0). I did not try the same procedure at this higher momentum.

All the values of f_π in table 5.17 are consistent with each other. Although the f_π values obtained at finite momentum are larger than the equivalent rest frame

κ	Operator			
	$\langle \pi \mid A_i \mid 0 \rangle$	$\langle 0 \mid A_i \mid \pi \rangle$	$\langle 0 \mid A_0 \mid \pi \rangle$	$\langle \pi \mid A_0 \mid 0 \rangle$
0.14262	$0.248\ ^{+165}_{-186}$	$0.218\ ^{+161}_{-149}$	$0.061\ ^{+\ 30}_{-\ 31}$	$0.052\ ^{+171}_{-\ 36}$
0.14226	$0.196\ ^{+\ 85}_{-105}$	$0.101\ ^{+\ 34}_{-\ 49}$	$0.063\ ^{+\ 10}_{-\ 20}$	$0.049\ ^{+\ 19}_{-\ 15}$
0.14144	$0.101\ ^{+\ 19}_{-\ 27}$	$0.082\ ^{+\ 18}_{-\ 22}$	$0.073\ ^{+\ \ 7}_{-\ 11}$	$0.058\ ^{+\ \ 9}_{-\ 14}$

Table 5.17: Values of the lattice scheme pion decay constant, in lattice units, obtained from operators with a momentum of (1,0,0).

κ	Operator	
	$\langle 0 \mid A_0 \mid \pi \rangle$	$\langle \pi \mid A_0 \mid 0 \rangle$
0.14262	$0.044\ ^{+\ \ 4}_{-\ 16}$	$0.062\ ^{+\ 13}_{-\ 21}$
0.14226	$0.052\ ^{+\ \ 5}_{-\ 13}$	$0.054\ ^{+\ 13}_{-\ 16}$
0.14144	$0.065\ ^{+\ \ 4}_{-\ \ 9}$	$0.057\ ^{+\ \ 8}_{-\ \ 8}$

Table 5.18: Values of the lattice scheme pion decay constant, in lattice units, obtained from the rest frame.

results in table 5.18, this is not statistically significant. Table 5.17 shows that the zeroth component of the axial current produces a value for f_π with the smallest error.

In this section I have demonstrated that it is possible to obtain f_π from the vector parts of equation 5.30. As is customary for an initial analysis of the data, I have used the most naive method to obtain f_π at finite momentum. The resulting large errors could be reduced by using more sophisticated techniques, for example, one of the methods described in [53]. The use of smeared operators might also help to decrease the errors. It will be interesting to use this method for nondegenerate D like mesons, as a check on the calculation in a regime where the forces of lattice artifacts are opposed to physical predictions.

6

Conclusions.

I will now review the progress and describe further work on the various research projects described in this thesis.

Although in chapter 2 I failed to prove that the clover action satisfies the reflection positivity condition, the fact that the clover action is a nearest-neighbour action, suggests that the condition is true for the clover action. It is still a challenge to construct a proof of the reflection positivity condition and obtain qualitative information about the clover action mass spectrum, before any detailed calculations are done.

The strong coupling study of the clover action in chapter 3 did not produce any insight into improvement. However it would be interesting to calculate the next order in the expansion, to look for differences between the clover and Wilson actions, in the energy dispersion relation and in the evolution of the $M_V^2 - M_{PS}^2$ splitting with quark mass.

In chapter 4, I showed that there are no O(a) corrections to the one loop vacuum polarisation diagram on the lattice. Because the clover action has O(a) terms in its Feynman rules, it is not clear that standard weak coupling perturbation theory is the best technique to investigate lattice artifacts. It might be better to try to use the methods developed by Wohlert [32], which he claimed allowed him to calculate on-shell quantities in perturbation theory. It would be interesting to find out, if a single value of the clover coefficient could remove all one loop O(a) terms from every physical prediction.

The penultimate chapter in this thesis contained results from, numerical simulations, all of which, would have provided a clearer physical picture with higher statistics. It will be interesting to continue the study of P-wave mesons in the

charmonium system. Better lattice operators are required to reduce the errors on the masses and to obtain accurate mass splittings. It is an unsolved problem to find a good computationally cheap method of simulating spin 2 particles, using propagating quarks and no nonrelativistic approximations. It is important to continue to calculate numerically the 1P-1S splitting, to see whether it is independent of quark mass. The finite momentum analysis should be used to try and test Lepage's [47] ideas on the problems with heavy quark simulations, using quark masses which are of the same order of magnitude as the cut off.

Appendix A

Summation of strong coupling propagator graphs.

I will now show the relationship between random walks and effective meson propagators, in the strong coupling limit. This produces a method of summing up a class of graphs in the hopping parameter expansion, which was used in chapter 3. This technique was first used by Kawamoto in a strong coupling study of the Wilson action [10]. The following derivation is on a infinite four dimensional hyper-cubic lattice, with its sites labelled by four integers. For simplicity I will suppress spinor indices.

In the random walk problem the number of possible random walks which starting from the origin end at the site n after L steps is $N_L(n)$. The evolution of $N_L(n)$ is controlled by:

$$N_L(n) = \sum_{m}^{\infty} M(n,m) N_{L-1}(m) \tag{A.1}$$

For a random walk which allows the particle to stop, the matrix M(n,m) equals:

$$M(n,m) = \sum_{\mu} (\delta_{n+\mu,m} + \delta_{n-\mu,m} + c\delta_{n,m}) \tag{A.2}$$

where c is the analogue of the clover coefficient in equation 1.34.

In the random walk problem, the analogue of the strong coupling meson propagator is the total number of paths ending at the site n, after walks with all possible numbers of steps. This is conveniently calculated by using the generating function:

$$N(n,\kappa) = \sum_{L=0}^{\infty} \kappa^L N_L(n) \tag{A.3}$$

The translational invariance of the matrix M means that N(n,κ) can simply be calculated in momentum space. Fourier transforming equation A.1 gives:

$$\hat{N}_L(p) = \sum_{\mu}(e^{ip_\mu} + e^{-ip_\mu} + c)\hat{N}_{L-1}(p) \tag{A.4}$$

This is simply solved for $N_L(p)$ to produce:

$$\hat{N}_L(p) = (\sum_{\mu}(e^{ip_\mu} + e^{-ip_\mu} + c))^L \tag{A.5}$$

The final result for the generating function is:

$$N(n,\kappa) = \int_p \frac{e^{ipn}}{1 - \kappa\sum_\mu(e^{ip_\mu} + e^{-ip_\mu} + c)} \tag{A.6}$$

which has the form of a lattice propagator. In the strong coupling expansion the matrix M is obtained from the low terms in the hopping parameter expansion. Once M has been calculated, an effective meson propagator can immediately be written down using equation A.6. This effectively sums up the contributions from the low order graphs in the hopping parameter expansion to the meson propagator. The mass of the meson is obtained by looking for the pole in its effective propagator.

Appendix B

Derivation of the a_0 constant.

I will now derive a value for the constant a_0 defined in equation 4.19.

In dimensional regularisation the following result holds:

$$\int_{OutsideBrillouinZone} \frac{d^d k}{(2\pi)^d} \frac{1}{(k^2)^2} = -\int_{-\pi}^{\pi} \frac{d^d k}{(2\pi)^d} \frac{1}{(k^2)^2} \tag{B.1}$$

If I define $\hat{k_\mu} = 2 \sin \frac{k_\mu}{2}$ and $\hat{k}^2 = \sum_\mu \hat{k_\mu}^2$ and add and subtract a useful term to equation B.1, the following result is obtained:

$$\int_{OutsideBrillouinZone} \frac{d^d k}{(2\pi)^d} \frac{1}{(k^2)^2} = \int_{-\pi}^{\pi} \frac{d^d k}{(2\pi)^d} \left(\frac{1}{(\hat{k}^2)^2} - \frac{1}{(k^2)^2}\right) - \int_{-\pi}^{\pi} \frac{d^d k}{(2\pi)^d} \frac{1}{(\hat{k}^2)^2} \tag{B.2}$$

The first result is finite and I evaluated it numerically to get the value:

$$0.012537 \pm 0.000013$$

The divergent second term can be found by using the results in an appendix in [63]

$$\int_{-\pi}^{\pi} \frac{d^d k}{(2\pi)^d} \frac{1}{(\hat{k}^2)^2} = \frac{1}{8\pi^2}\left(\frac{1}{d-4} - \log 4\pi + F_0\right) \tag{B.3}$$

where F_0 is a constant equal to 4.369225. Putting all the above equations together leads to a value of a_0 given in Chapter 4.

Appendix C

Grassmannian integrals.

In this appendix I want to flesh out an argument in chapter 2, required in the study of reflection positivity. I will explain why equation 2.14 is positive, but the sign of the expression in equation 2.13 cannot easily be determined. I will adapt the treatment on Grassmann algebras found in the text book by Itzykson and Drouffe [90].

Consider a finite Grassmann algebra with N elements η_i, which satisfy the rule:

$$\eta_i \eta_j + \eta_j \eta_i = 0 \tag{C.1}$$

The Grassmann algebra generated contains expressions like:

$$\begin{aligned} f(\eta) &= f^0 + \sum_i f^i \eta_i + \sum_{i<j} f^{ij} \eta_i \eta_j + \sum_{i<j<k} f^{ijk} \eta_i \eta_j \eta_k + \cdots \\ &= \sum_{0 \le k \le N} \frac{1}{k!} \sum_{\{i\}} f^{i_1 + \cdots + i_k} \eta_{i_1} \cdots \eta_{i_k} \end{aligned} \tag{C.2}$$

where the inner sum is over permutation of integers, and $f^{i_1 \cdots i_k}$ is an antisymmetric tensor. The dimension of the resulting algebra is 2^N. The definition of the scalar product is:

$$\langle g, f \rangle = \sum_{k=0}^{N} \frac{1}{k!} \sum_{\{i\}} \overline{g}^{i_1 + \cdots + i_k} f^{i_1 + \cdots + i_k} \tag{C.3}$$

where the bar stands for complex conjugation.

It is important to introduce a second set of N anticommuting variables $\overline{\eta}_i$. This allows the definition of the antilinear map $f \longrightarrow \overline{f}$ by:

$$\sum_k \sum_{\{i\}} f^{i_1 + \cdots + i_k} \eta_{i_1} \cdots \eta_{i_k} \longrightarrow \sum_k \sum_{\{i\}} \overline{f}^{i_1 + \cdots + i_k} \overline{\eta}_{i_k} \cdots \overline{\eta}_{i_1} \tag{C.4}$$

Using the rules for the integration of Grassmann variables in equation 1.22, the scalar product in equation C.3 can be written in the form:

$$\langle g, f \rangle = \int d\eta_N d\overline{\eta}_N \cdots d\eta_1 d\overline{\eta}_1 e^{-\sum_{i=1}^{N} \eta_i \overline{\eta}_i} \overline{g}(\overline{\eta}) f(\eta) \tag{C.5}$$

For a proof of this see the book by Itzykson and Drouffe [90] Equation C.5 with f = g is essentially the same as equation 2.14 (apart from the change in notation). This is the key result which shows that the Wilson action with r equal to 1 satisfies the reflection positivity condition.

Now I will consider the equivalent result for the clover action. In the notation of this appendix equation 2.13 is:

$$\langle g, f \rangle = \int d\eta_N d\overline{\eta}_N \cdots d\eta_1 d\overline{\eta}_1 e^{-\sum_{i=1}^{N} \eta_i \overline{\eta}_i} f(\eta, \overline{\eta}) \overline{f}(\overline{\eta}, \eta) \tag{C.6}$$

To show that the Grassmann integral in equation C.6 is not positive for all functions f, I will construct a counter example for the special case of N = 2. It is sufficient to work with a function of the form:

$$f(\overline{\eta}, \eta) = a \eta_1 \eta_2 \overline{\eta}_1 \overline{\eta}_2 \tag{C.7}$$

substituting equation C.7 into equation C.6, I obtain:

$$\int d\eta_2 d\overline{\eta}_2 d\eta_1 d\overline{\eta}_1 e^{-\eta_1 \overline{\eta}_1 - \eta_2 \overline{\eta}_2} f(\eta, \overline{\eta}) \overline{f}(\overline{\eta}, \eta) = -(\overline{a} + a) \tag{C.8}$$

with special choices of a, equation C.8 can be negative. This example has shown why it cannot be proved that equation 2.13 is positive.

Bibliography

[1] I.Montvay Numerical calculations of hadron masses in quantum chromodynamics. *Rev.Mod.Phys.*59(1987)263.

[2] R.C.Johnson Angular momentum on a lattice. *Phys.Lett.*114B(1982)147.

[3] Mandula J.E. and Shpiz E. Double valued representations of the four-dimensional cubic lattice rotation group. *Nucl.Phys.*B232(1983)180.

[4] J.E.Mandula Quark-antiquark-gluon exotic fields for lattice QCD. *Phys.Lett.* B135(1984)155.

[5] W.Miller *Symmetry groups and their applications.* Academic press 1972.

[6] H.W.Hamber and C.M.Wu Some predictions for an improved fermion action on the lattice. *Phys.Lett.* 133B(1983)351.

[7] H.Gausterer and C.B.Lang Strong coupling hadron propagators for modified fermion actions. *Phys.Lett.154B* (1985)68.

[8] K.G.Wilson Confinement of quarks. *Phys.Rev.* D10(1974)2445.

[9] K.G.Wilson Quarks and strings on a lattice. *New phenomena in subnuclear physics(Erice 1975)* ed A. Zichichi.

[10] N.Kawamoto Towards the phase structure of euclidean lattice gauge theories with fermions. *Nucl.Phys.* B190(1981)617.

[11] N.Kawamoto and J.Smit Effective Lagrangians and dynamical symmetry breaking in strongly coupled lattice qcd. *Nucl.Phys.* B192(1981)100.

[12] B.DeWit and G't.Hooft Nonconvergence of the $\frac{1}{N}$ expansion for SU(N) gauge fields on a lattice. *Phys.Lett.* 69B(1977)61.

[13] N.Kawamoto ad S.Shigemoto A trial for analytic calculations of the meson spectrum in SU(3) lattice QCD. *Phys.Lett.* 114B(1982)42.

[14] The APE collaboration $\beta = 6.0$ quenched Wilson fermions. *Phys.Lett.*B258(1991)195.

[15] P.Bacilieri at al. The hadronic mass spectrum in quenched lattice QCD: Results at $\beta = 6.0$ and $\beta = 5.7$ *Phys.Lett.* B214(1988)115.

[16] UKQCD Collaboration Quenched Hadrons using Wilson and O(a)-Improved Fermion Actions at $\beta = 6.2$ *Phys.Lett.* B284(1992)

[17] T.Eguchi and N.Kawamoto Improved lattice action for Wilson fermions. *Nucl.Phys.*B237(1984)609.

[18] G. Heatlie et al. The improvement of hadronic matrix elements in lattice QCD. *Nucl.Phys.*B352(1991)266.

[19] B.Sheikholeslami and R. Wohlert Improved continuum limit lattice action for QCD with Wilson fermions. *Nucl.Phys.*B259(1985)572.

[20] K.Symanzik Continuum limit and improved action in lattice theories. *Nucl.Phys.*B226(1983)187.

[21] J.Collins *Renormalization* Cambridge monographs on mathematical physics.

[22] K.Osterwalder and E.Seiler Gauge field theories on a lattice. *Ann. of Phys.* 110(1978)440.

[23] M.Lüscher Construction of a Self-adjoint, Strictly Positive Transfer Matrix for Euclidean Lattice Gauge Theory. *Commun.Math.Phys.*54(1977)283.

[24] K.Osterwalder and R.Schrader Axioms for Euclidean Green's functions II *Commun.Math.Phys.* 42(1975)281.

[25] K.Osterwalder and R.Schrader Axioms for Euclidean Green's functions. *Commun.Math.Phys.* 31(1973)83.

[26] G.Martinelli and C.Sachrajda A lattice calculation of the second moment of the pion's distribution amplitude. *Phys.Lett.*190B(1987)151.

[27] J.Hoek and J.Smit.. On the 1/g**2 corrections to hadron masses. *Nucl.Phys.*B263(1986)129.

[28] M.Lüscher and P. Weisz Efficient numerical techniques for perturbative lattice gauge theory computations. *Nucl.Phys.*B266(1986)309.

[29] H. Kawai, R Nakayama, and K. Seo. Comparison of the lattice Λ parameter with the continuum Λ parameter in massless qcd. *Nucl.Phys.*B189(1981)40.

[30] K.Symanzik. Renormalization Problem in Nonrenormalizable Massless Φ^4 theory. *Commun.Math.Phys.*45(1975)79

[31] G.P.Lepage A new algorithm for adaptive multidimensional integration. *J.of Comp. Phys.*27(1978)192

[32] R.Wohlert Improved continuum limit lattice action for quarks. DESY 97-069, July 1987

[33] T.DeGrand and M.Hecht. Observation of orbitally excited hadrons in simulations of lattice QCD. *Phys.Lett*B275(1992)435

[34] P.Menotti and A.Pelissetto General Proof of Osterwalder-Schrader Positivity for the Wilson action. *Commun.Math.Phys.* 113(1987)369

[35] F.A.Berezin *The method of the second quantization.* Academic press 1966

[36] M.Lüscher and P.Weisz Definition and general properties of the transfer matrix in continuum limit improved lattice gauge theories. *Nucl.Phys.*B240(1984)349

[37] Maria-Paloa Lombardo et al. Lattice QCD Spectroscopy with an Improved Wilson Fermion Action. Rome preprint ROM2f-92-46

[38] M.Creutz Gauge fixing, the transfer matrix, and confinement on a lattice. *Phys.Rev.*D15(1977)1128

[39] G.Martinelli and C.Sachrajda A lattice calculation of the pion's form factor and structure function. *Nucl.Phys.*B306(1988)865

[40] J.Mandula, G. Zweig, and J. Govaerts Representations of the rotation reflection symmetry group of the four-dimensional cubic lattice. *Nucl.Phys.*B228(1983)91

[41] A. Kronfield and D. Photiadis. Phenomenolgy on the lattice: Composite operators in lattice gauge theory. *Phys.Rev.* D31(1985)2939

[42] D.Carpenter and C.Baillie Free fermion propagators and lattice finite-size effects. *Nucl.Phys.*B260(1985)103.

[43] F.E. Close . *An Introduction to Quarks and Partons.* Academic press 1979

[44] David Richards Unpublished notes on hadron operators.

[45] Ken Bowler Unpublished notes on lattice QCD.

[46] UKQCD Collaboration The Hyperfine Splitting in Charmonium: Lattice Computations using the Wilson and Clover Fermion Actions. Edinburgh Preprint 92/510

[47] G.P. Lepage Simulating Heavy Quarks. *Nucl.Phys.B(Proc.Suppl.)*26(1992)45

[48] Aida X.El-Khadra Charmonium with improved Wilson fermions II: The spectrum *Nucl.Phys.B(Proc.Suppl.)* 26(1992) 372

[49] Aida X. El-Khadra, G. Hockney, A Kronfield, and P. Mackenzie. A determination of the Strong Coupling Constant from the Charmonium spectrum. FERMILAB preprint 91/354-T

[50] P.B.Mackenzie Charmonium with improved wilson fermions I: A determination of the strong coupling constant. *Nucl.Phys.B(Proc.Suppl.)* 26(1992) 369

[51] A.Simpson. Algorithms for lattice QCD Edinburgh PhD thesis 1991

[52] S.Meyer and B.Berg. Restoration of Lorentz invariance in the lattice O(3) model with improved actions. *Nucl.Phys.*B240(1984)559

[53] D. Daniel, R. Gupta, and D. Richards. Calculation of the pion's quark distribution amplitude in lattice QCD with dynamical fermions. *Phys.Rev.* D43(1991)3715

[54] N.Kimura and A.Ukawa Energy dispersion momentum dispersion of glueballs and the restoration of Lorentz invariance in lattice gauge theories. *Nucl.Phys.*B205(1982)637

[55] R. Groot, J. Hoek, and J. Smit. Normalization of currents in lattice QCD. *Nucl.Phys.*B237(1984)111

[56] D. Weingarten Monte Carlo evaluation of hadron masses in lattice gauge theory. *Phys.Lett.*109B(1982)57

[57] B.Thacker and P.Lepage Heavy-quark bound states in lattice QCD. *Phys.Rev.*D43(1991)196

[58] H.Gausterer and C.Lang Action Dependence of the Strong Coupling Spectrum in Lattice Gauge Theory. *Z.Phys.*C28(1985)475

[59] R.Kenway and S.de Souza Non-compact lattice QED at large fermion mass. *Nucl.Phys*B354(1991)39

[60] G't Hooft Computation of the quantum effects due to a four-dimensional pseudoparticle. *Phys.Rev.*D14(1976)3432

[61] C.Itzykson and J.Zuber *Quantum Field Theory.* McGraw-Hill 1980

[62] C.T. Sachrajda Lattice perturbation theory. Southampton preprint 89/90-4

[63] S.Caracciolo, P. Menotti, and A. Pelisseto One-loop computation of the energy momentum tensor for lattice gauge theories. *Nucl.Phys.*B375(1992)195

[64] R.Gupta, A.Patel, C.Baillie, G. Guralnik, W.Kilcup, and S.Sharpe. QCD with Dynamical Wilson Fermions. *Phys.Rev.* D40(1989)2072

[65] A.S.Kronfield Lattice QCD. Fermilab-Conf-92/040-T

[66] R.D.Kenway Non-perturbative Calculations in the Standard Model. *Rep.Prog.Phys.*52(1989)1475

[67] M.Lüscher and P.Weisz On-shell Improved Lattice Gauge Theories. *Commun.Math.Phys.*97(1985)59

[68] M.Baake, G. Gemünden, and R Oedingen. Structure and representations of the symmetry group of the four-dimensional cube. *J.Math.Phys.*23(1982)944

[69] L.H.Ryder *Quantum Field Theory* Cambridge University Press 1986

[70] P.Ramond. *Field theory: A modern primer.* Benjamin/Cummings

[71] C.Michael The Running Coupling from Lattice Gauge Theory. *Phys.Lett.*B283(1992)103.

[72] Lüscher , P.Weisz, and U.Wolf. A numerical method to compute the running coupling in asymptotically free theories. *Nucl.Phys.*B359(1991)21.

[73] The UKQCD collaboration. Gauge Invariant Smearing and Matrix Correlators using Wilson Fermions at $\beta = 6.2$ Edinburgh Preprint 92/513

[74] Particle Data Group Review of particle properties *Phys.Rev.*D45 part II (1992) S1

[75] B.W. Char et al. *Maple reference manual.* Waterloo Maple Publishing 1991

[76] C.Davies and B.Thacker Upsilon spectroscopy from lattice QCD. *Nucl.Phys.B(Proc.Suppl.)* 26(1992) 375

[77] A.Hasenfratz and P.Hasenfratz The connection between the Λ parameters of lattice and continuum QCD. *Phys.Lett.* 93B(1980)165

[78] R.Dashen and D.J.Gross Relationship between lattice and continuum definitions of the gauge-theory coupling. *Phys.Rev.*D23(1981)2340

[79] H.B.Nielsen an M.Ninomiya Absence of neutrinos on a lattice. (I). Proof by homotopy theory. *Nucl.Phys.* B195(1982)541

[80] E.Wigner On unitary representations of the inhomogeneous Lorentz group. *Ann.of Math.* 40(1939)149

[81] G.Martinelli, C.T.Sachrajda, and A.Vladikas A study of improvement in lattice QCD. *Nucl.Phys.*B358(1991)212

[82] H.Fritzsch, M.Gell-Mann, and Leutwyler. Advantages of the color octet gluon picture. *Phys.Lett.* 47B(1973)365

[83] M.Lüscher and P.Weisz Computation of the action for on-shell improved lattice gauge theories a weak coupling. *Phys.Lett* 158B(1985)250

[84] G.P.Lepage and P.B.Mackenzie On the Viability of lattice Perturbation Theory preprint FERMILAB-PUB-91/355-T

[85] W.Wetzel Extending improvement to fermions. *Phys.Lett.* 136B(1984)407

[86] Y.V.Novozhilov *Introduction to elementary particle theory.* Pergamon Press.

[87] C.J.Bradley and A.P.Cracknel *The mathematical theory of symmetry in solids.* Oxford University Press

[88] G.P.Lepage. From actions to answers- Proc 1989 Theoretical Advanced Summer Institute in Particle Physics, eds T.DeGrand and T.Toussaint. World Scientific Singapore 1990

[89] G.Altarelli. Experimental tests of perturbative QCD. *Annu.Rev.Nucl.Part.Sci.*39(1989)357

[90] C.Itzykson and J.Drouffe *Statistical field theory Volume 1* Cambridge Monographs on mathematical physics 1991